AMRL-TR-67-212

BIOCHEMICAL DEFENSE MECHANISMS AGAINST PULMONARY IRRITANTS

STEVEN CARSON, PhD

RICHARD E. GOLDHAMER

FOREWORD

This study was co-sponsored by the Biomedical Laboratory of the Aerospace Medical Research Laboratories, Aerospace Medical Division, Wright-Patterson Air Force Base, Ohio 45433, and the Life Sciences Division of the Office of Aerospace Research, Arlington, Virginia 22209. The research was performed in accordance with the Contract No. AF33(615)-5309 in support of Project 7163, "Research on Biomechanisms and Metabolism". Dr. Steven Carson was principal investigator and Richard E. Goldhamer was co-investigator for the Food and Drug Research Laboratories, Inc., Maurice Avenue at 58th Street, Maspeth, New York 11378. Dr. Kenneth C. Back, Chief, Toxicology Branch, Toxic Hazards Division was the contract monitor for the Aerospace Medical Research Laboratories. Research was initiated on 15 July 1966 and completed on 15 July 1967.

This technical report has been reviewed and is approved.

ROBERT H. LANG, LT COL, USAF, MC
Chief, Biomedical Laboratory
Aerospace Medical Research Laboratories

ABSTRACT

Studies have been performed in which mammalian mucociliary apparatus has been characterized under normal conditions following exposure to three irritant gases, i. e., 100 per cent oxygen, ozone (O_2) and nitrogen dioxide (NO_2). Investigations were made in normal and treated animals providing physical, electrophysiological, biochemical, and morphologic data of effects due to exposure. A method for in vitro microscopic observation of viable cilia and adjacent mucus blanket has been described in terms of ciliary beat and movement of particles embedded in the mucus. In vitro volumetric estimation of mucus thickness was compared to electrical resistance measurements in the attempt to provide an in vivo method to determine mucus depth alterations in treated animals. Polarographic studies of oxygen dependent enzymes were carried out on pooled stripped epithelial tissue of untreated animals and comparison made with tissues exposed to ozone and NO_2. Exposure to 100 per cent oxygen caused a significant but self-limiting decrease in mucus velocity and viscosity. Acute exposure to NO_2 (35 and 75 μg per kg) caused marked dose dependent changes in velocity and viscosity. Exposure to 0.5 ppm ozone for a 14 day period resulted in general mucostasis and elevated viscosity levels.

TABLE OF CONTENTS

TABLES

FIGURES

SECTION I

INTRODUCTION

The initial defense mechanism that permits the animal organism to exist in an irritant atmosphere is the mucociliary apparatus. The importance of this "system" in clearing potentially deleterious materials from respiratory tract has been emphasized by a number of authors.

The present program was instituted to provide basic information on the biochemical and physical factors which affect the structure and function of the tissue elements that form the primary basis for physiologic defense during exposure to pulmonary irritants. Work in these Laboratories has demonstrated that the sequence of events, following acute exposure to a pulmonary irritant, is initiated solely by impingement of the irritant on the mucus film lining the upper respiratory airways. The nature of the irritant and the manner of its application in large part determine the qualitative and quantitative nature of the post-exposure reaction. In exposure to gaseous agents, chemical composition is the principal determinant of effect.

To result in effective clearance, a number of critical events must occur following exposure to an environmental irritant of particulate, gaseous, or mixed particulate-gaseous composition. From the data presented by Albert and co-workers (ref 1) on human volunteers, by Laurenzi (ref 2) on mice, and in our report (ref 3) on cats, effective clearance of 70 per cent of inhaled particulate (mono- or polydispersed) occurs via the "mucociliary elevator" moving cephalad, which is then disposed of by swallowing and excretion via the gastrointestinal tract, and to a lesser degree by expectoration.

Approximately 30 per cent of the foreign material administered by a single exposure is more slowly cleared via alveolar macrophage, with transport across interstitial membranes and the lymphatics. Another involves a slow process whereby material moves up against a gravity gradient in terminal bronchioles to the area in which mucociliary transport occurs.

The manner and character of the response, though similar, may vary with acute, subacute, or chronic exposure. Studies have indicated that under continuous 24-hour exposure the reaction of the mucociliary apparatus may differ from that following other types of exposure, since the nature of the homeostatic or accommodative responses may be markedly modified.

The published results of investigations carried out in these Laboratories (reported and summarized in the 1965 Duke Symposium on Cilia (ref 4), and more recently at the New York Academy of Sciences Conference on "Interdisciplinary Investigation of Mucus Production and Transport" (ref 5) support the view that differential levels of response occur in the mucociliary tract, depending on the duration and nature of the irritant

insult. The findings indicated the relative initial independence of mucus flow on ciliary beat as affected by the impingement of gaseous, particulate, or mixed aerosol irritants. Similarly, the data indicated that deleterious responses may be elicited in the ciliated cells underlying the mucus sheath, affecting either the rate or chronicity of beat upon prolonged inhalation insult. However, this effect, once begun, was also associated in every instance with marked changes in mucus flow. The generalization was made that mucostasis may be achieved without detectable impairment of ciliary beat, whereas ciliastasis is always associated with mucostasis (ref 6, 7, 8, 9, 10). In the course of these studies, several new techniques were evolved.

The effects of chronic exposures have been studied using cigarette smoke as the challenging agent. A periodicity in response has been observed which appears to reflect temporary and reversible alterations. The integrity of the ciliated epithelium is affected only after prolonged exposure, and eventual regeneration occurs after adequate rest and removal of the insult. The effects of repeated exposure vary directly with the intensity of the insult and its duration.

Within the limitation of maintenance of the integrity of the whole animal, i.e., resistance to upper respiratory infection, etc., neither the onset, the duration, nor the intensity of response of mucus flow (expressed as velocity in mm per minute) is deleteriously affected. Insofar as the surface events on the mucus layer of the trachea are concerned, the response appears to be self-limiting. This may result from the overall phenomenon of transport, i.e., the time required for cephalad movement of mucus from the deepest area of penetration of the inhaled aerosol. Characteristically, other than highly specific classes of materials, i.e., protein precipitants, acrolein, and various phenolic substances, normalization of flow velocity can be anticipated in 10 minutes. Although cilia do not appear to play a role either in the immediate response nor in the subsequent changes, evidence has been obtained which suggests that the interrelationship of ciliary activity and mucus flow is necessary for normalization of the previously impaired function of the mucociliary apparatus.

Bioelectric characteristics of the mucus film have been investigated in vivo after systemic and inhalatory exposure to various materials. Of particular interest were the apparent differences between in vitro and in vivo systems. These changes may reflect a conservation of energy, indicating the increased capacity of the system to do work, i.e., to increase clearance of inhaled particles. The changes in the electrical nature of the ciliary tissue have been shown to parallel the changes in mucus flow. Thus the total mucociliary function appears to be one of tissue-mucus sheath interaction in which a multiplicity of physiochemical and biochemical mechanisms play a role, involving energy transfer from the beating cilia to the overlying mucus, developing shear forces and affecting "spinbarkeit" and other rheologic properties of the mucus.

Generally, investigators concerned with mucociliary function have failed to properly characterize the differential responses as well as the interrelationship of the two major components involved in the mechanics of respiratory clearance. They have tended to disregard certain critical factors concerned with the capacity of cilia to maintain chronicity.

Notwithstanding previous reports from these Laboratories, based on data from acute studies, in which the changes were described as independent of the tissue, it now appears that in terms of the integrated response, the epithelial component to these reactions is critical. This contribution may be via energy transfer to the mucus, changes in ciliary beat force, or some more complex system, such as the active transport of water or ions across the epithelial surface into the mucus, causing the observed physical changes.

It has been shown that ciliated tissue is affected by the electrical resistance and conductivity of the mucus sheath. That the tissue plays a role in the defensive alteration of mucus flow is indicated by the observation that the ratio of goblet:ciliated epithelial cells varies with chronic exposure to irritants. Rohdin and others have reported that the two types of cells are derived from a single cell type (ref 11). Several hypotheses have been evolved to explain this interaction, some of which are shown here:

1. Laminar mucus flow has been observed after impingement of foreign particles on the surface. The flow rate at the tissue-mucus interface is greater than that of the mucus-air interface and may be differentially affected.

2. This differential flow rate produces an upward pressure/concentration gradient which actively prevents penetration of the insulting material to the tissue surface.

3. The laminar flow pattern is caused by introduction of various ionic species into the lower layer of the mucus from the tissue.

4. The ions are actively transported across the tissue-mucus interface. This requires cellular energy production and possible dissipation via the ciliated epithelium.

5. The change in molecular polarity in the mucus with resultant laminar flow pattern appears to be the first defense against respiratory insult.

Other equally tenable theories have been proposed. All require further biochemical and histological support. It was the purpose of this investigation as herein conducted to develop the data from which a firmer understanding of the cellular and tissue factors involved in mucociliary response, the physical analysis of this response, and the basis for correlating the two, can be adduced.

The emphasis in the proposed study has thus been on the physical, chemical, and biochemical characterization of ciliated epithelium in relation to the mucus flow and/or ciliary beat frequency, employing exposure to irritants, i.e., nitrogen dioxide, ozone, or pure oxygen atmospheres, as the means of differentiating the normal from the irritated status.

SECTION II

PHYSICAL ANALYSES OF MUCUS AND CILIA

MUCOCILIARY APPARATUS

Based on analysis of the events in non-mammalian species (ref 12), a mechanical model for ciliary action of the mucociliary apparatus has been postulated. Although this model cannot completely reproduce the mammalian system, it has formed the basis of a working hypothesis to study the interrelationships between ciliary wave motion, mucus flow, and particle transport. On the surface of ciliated tissue is a mucus layer, interspersed within which are debris and particles. From the many observations made, there is firm agreement that the mucus moves in the direction of the ciliary effective beat and that two layers are involved. The first is the region of turbulent flow adjacent to the cilia and is dependent upon the rhythmicity and motion of the cilia. The second is distal to the cilia and is termed the region of laminar flow. The characteristics of this region are undoubtedly similar to those which exist in the vascular system.

The purpose of the present phase of the investigation was to study the characteristics of the ciliary motion and to correlate it with mucus flow.

Hypothetically, the cilia beat in a regular manner exhibiting characteristic bending movements. The forward stroke of the cilia (in the direction of fluid motion) is considered to be the working stroke while the backward stroke is the relaxation stroke. Since cilia exhibit metachronism, the pattern could be symplectic, antiplectic, or diaplectic. Photographic studies were performed on extirpated tracheal sections obtained from cats. These studies, utilizing time-delay still photography, indicated that the mucus blanket possessed physical configuration. A more intensified effort was therefore directed toward examining the action by means of cinematography. The studies were intended to elucidate:

(a) Measurement of ciliary beat by recording the cilia movement directly rather than by inference from changes in light patterns reflected from the surface of the mucus sheath (as carried out by other workers) (ref 13, 14).

(b) Measurement of ciliary beat by recording the cilia movement via observation of oscillating particles of entrapped debris.

(c) Cinematographic analysis of the periodicity of individual cilia to enable construction of representative diagrams of the sundry positions of the cilia during its motion. This analysis might lend itself to energy studies for both the working and relaxation strokes of the cilia.

(d) Cinematographic analysis of the periodicity of groups of cilia determined by the nature of the metachronal pattern and the relative motions of members of the various groups.

(e) Cinematographic analysis of the surface of the mucus sheath to determine the nature of surface disturbances and to correlate these disturbances with observed ciliary motion.

(f) Cinematographic analysis of the turbulent and laminar flow regions of mucus to delineate the transition area of the two flow patterns, and to determine the velocity of the laminar portion of the stream as a function of position within the mucus stream.

(g) To study the effects of altered environment on the functioning of the mucociliary apparatus described above.

METHODOLOGY

Under surgical anesthesia the ventral midline soft portions of several tracheal cartilage rings are isolated from the trachea and fixed to glass slides by pressure sensitive transparent plastic tape (approximately 15 mm width, 0.051 mm thickness) so that the mucosal surface faces the objective lens of a Nikon S-K microscope. An integrated Koehler Illuminator is used to project the light onto a N.A. 1.30 condenser diaphragm and to project the image of the field diaphragm onto the specimen. A 100X objective lens in combination with a specially equipped supplementary condenser lens (Nikon Model S-K system) is inserted against the illuminating lamp housing to reduce the filament image. The condenser is further equipped with a variable iris in order to adjust the ape ture for oblique illumination.

By individually adjusting each specimen to avoid flare and other injurious effects of reflection, a suitable intensity of light, specimen area and angle of view may be obtained for photographic purposes.

For the study of individual cilia, observations are made of the cut edge of the excised tracheal segment under oil immersion at 1500X magnification wherein the covering mucus blanket and individual cilia are visualized. Simultaneously, motion pictures of mucus flow and cilia motility are taken at 64 frames per second with a 16 mm camera (Keystone K-55) mounted on the microscope and equipped with a f=31.22 mm for 1/8 projection lens, and a 15X magnification microscope eyepiece.

RESULTS

Through cinematography, utilizing a speed of 64 frames per second and a magnification of 1500X, a segment of cilia from an excised cat tracheal tissue was analyzed during a 4.65 second period. During this interval, the average beat rate of the cilia was 12.45 cycles per second, with a range of 10.67 to 14.22 cycles per second. The accompanying table lists the distribution of measurements over the entire period.

Cycles per Second	Percentage of total Measurements Recorded*
14.22	6.9
12.80	65.5
11.63	20.7
10.67	6.9

*Based on 58 individual determinations

From this table it can be seen that this analysis yielded a frequency of 12.80 cycles per second in approximately two-thirds of the recorded measurements. Although the curve is skewed to the left, the data are significant in that these results agree with the frequency of similar motion reported following indirect observations. For additional details refer to Film Strip A, Sequence 5 on page 15.

Observations of adjunct groups of cilia during the above measurement periods suggest that if metachronal wave patterns exist in ciliary beat, these patterns are not diaplectic. However, at present insufficient evidence is available to determine definitively the type of metachronal pattern which does exist.

In addition to the direct measurements used in determining cilia frequency, an alternative indirect technique was also employed. As indicated previously, particulate matter is observed in the mucus layer. Often a particle is trapped in the region of the cilia and thus is caused to oscillate at the rate of the ciliary oscillations. From this series of film sequences, several particles have been observed in this position in different segments of cat tracheal tissue. Utilizing the oscillating movements of the trapped particles, the beat frequency from two different segments of tracheal tissue obtained from two normal cats was estimated to be 12 and 13.47 cycles per second. The data are shown in Film Strip A, Sequences 12 and 16 (pages 18-20). These data compare favorably with those recorded above for direct observation of ciliary beat.

It must be emphasized that the experimental capabilities were limited by the lack of high speed cinematographic equipment during the conduct of the test. Its use would result in better quantitative data since the greater the number of frames per cilia beat cycle that can be visualized, the greater the precision in measurement.

The nature of the flow in the mucus blanket has been studied and in the region adjacent to the cilia, it is clearly turbulent. This turbulence has been visualized (Film Strip A, Sequences 4 and 10, pages 13 and 17). The results of debris motion are summarized in table I below.

TABLE I

PARTICLE VELOCITIES[1]

Particle No	Particle size	Duration of track	Velocity, mm/min		
			min	max	avg
	mm	sec			
1-A4	.0060	.45	1.440	11.880	4.002[2]
2-A4	.0020 to .0030	.45	1.920	17.400	---
1-A10	.0100 to .0170	.36	6.780	7.560	7.200

[1]Maximum velocity resulted from direct impact with oscillating cilia or by turbulence.

[2]Average velocity indeterminate because of directional path of particle.

The circulatory motion of debris seen above beating cilia suggests the turbulent nature of the fluid flow in the region of the tips of the cilia. Furthermore, the turbulence caused particles to be dislodged from larger agglomerations of debris.

In the region above the turbulence, the film data suggest that the mucus flow is laminar. Particles visualized in Film Strip B were carried by a laminar layer of fluid motion beginning no more than 0.005 mm from the top of the cilia. Four particles in Film Strip B, Sequence 4, approximately 0.0060 to 0.0075 mm in diameter, were tracked as they moved with the mucus blanket over the same path at different times during a period lasting approximately 4.3 seconds. The particle velocities of three of the particles differed by less than 5.5 per cent from the mean average velocity of the three particles. The fourth particle differed from the above mean average by 40 per cent, see table II below.

TABLE II

PARTICLE VELOCITIES[1]

Particle No	Particle size	Duration of track	Velocity, mm/min		
			min	max	avg
	mm	sec			
1-B4	.0075	1.37	3.336	4.128	3.558
2-B4	.0075	1.17	3.888	4.374	4.068
3-B4	.0058	1.09	2.526	6.012	4.296
4-B4	.0075	.52	3.666	6.114	4.470

[1]Flow is laminar.

Additional measurements of particle velocity were made in the mucus layer in order to relate particle velocity to particle position in this area. Because of the limited amount of film available for this analysis and because of limitations inherent in the available research equipment it has not been possible to achieve this goal to date. However, considerable experimental data have been accumulated concerning particle velocities without reference to particle position (table III).

TABLE III

PARTICLE VELOCITIES[1]

Particle No	Particle size	Duration of track	Velocity, mm/min		
			min	max	avg
	mm	sec			
1-B3	.0070	.14	---	---	12.072
2-B3	.0188	.19	15.360	18.870	17.100
3-B3	.0088 to .0175	.19	15.510	15.750	15.618
4-B3	.0075 to .0188	.08	---	---	14.820
5-B3	.0138	.19	---	---	10.140

[1]Flow is laminar.

It has previously been reported that lycopodium spores moving on the surface of the mucus are observed to travel at rates of about 12 mm per minute (ref 15, 5) and the velocities shown in table III are similar.

The velocities for the remaining particles (table IV) are of one-half to one order of magnitude less. This difference appears to be due to the fact that the velocity of surface particles has been determined and recorded during in situ investigations, whereas the investigations recorded above were performed in vitro. Since in vitro preparations are more time-consuming than the in situ studies, the former were subject to greater desiccation during preparation thus resulting in an increased viscosity of the mucus sheath with attendant decrease in particle velocities.

TABLE IV

PARTICLE VELOCITIES[1]

Particle No	Particle size	Duration of track	Velocity, mm/min		
			min	max	avg
	mm	sec			
1	.0025 to .0075	1.26	1.656	2.280	2.064
2	.0100	.80	---	---	2.826
3	.0075	1.61	1.128	1.200	1.164
4	.0100	1.23	2.304	3.102	2.838
5	.0025 to .0075	1.45	1.194	1.734	1.356

[1]Flow is laminar.

In Part C the theoretical approaches for studies of the periodicity of individual cilia and for computing the kinetic energy generated during the working and relaxation strokes of the cilia are presented. Fig 1 represents in summary fashion the various positions of individual cilium during the working stroke.

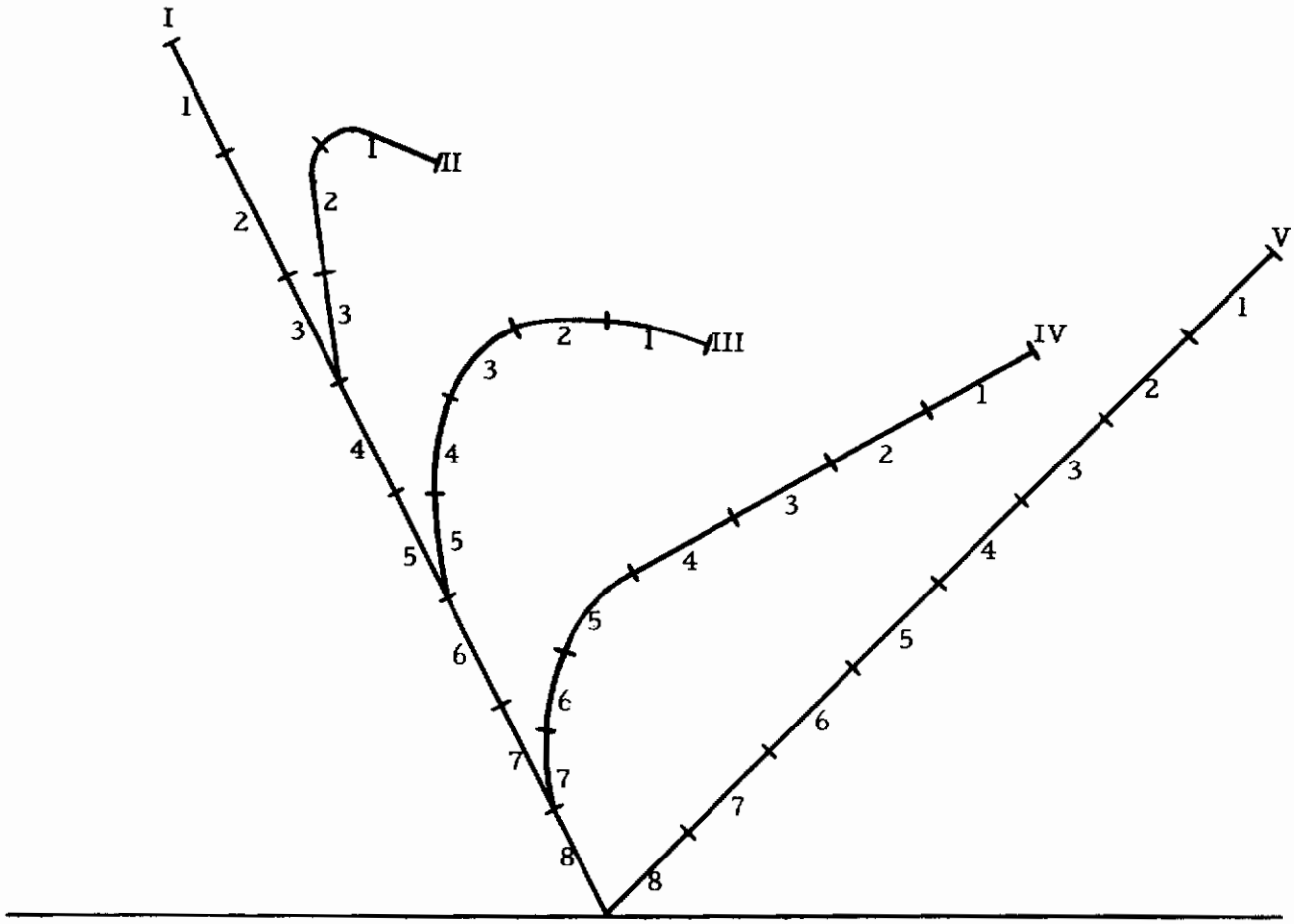

Figure 1
Hypothesized Working Stroke of a Cilium

Assuming that there are five positions of the cilium during the working stroke, and that the elapsed time for the cilium to advance one position is equal to T seconds, with each cilium divided into eight segments of equal mass, then the kinetic energy associated with the movement of the first segment from position 1 to position 2 is given by the equation:

$$E = 1/2\ mV^2_{1-2}$$

where the subscript 1-2 stands for the first segment moving from position 1 to 2 in T seconds. The linear distance moved by the center of gravity of segment 1 in going from position 1 to position 2 can be determined directly from the film. Hence, V_{1-2} can be approximated. Similarly the kinetic energy associated with the movement of segment 2 can also be determined.

Thus the kinetic energy associated with the motion of the entire cilium from position 1 to position 2 is given by the equation:

$$\sum_{n=1}^{8} 1/2\ mV^2_{n-2}$$

In a similar manner the kinetic energy associated with the motion of the entire cilium from position 2 to 3 is given by the equation:

$$\sum_{n=1}^{8} 1/2\ mV^2_{n-3}$$

Consequently, the kinetic energy associated with the motion of the entire cilium from position 1 to position 5 is given by the double sum:

$$\sum_{K=2}^{V} \sum_{n=1}^{8} 1/2\ mV^2_{n-K}$$

The estimate improves as P and R go to infinity and the kinetic energy associated with the working stroke is:

$$\lim_{\substack{P\to\infty \\ R\to\infty}} \sum_{K=2}^{P} \sum_{n=1}^{R} 1/2\ mV^2_{n-K}$$

Similarly the energy associated with the relaxation stroke can also be calculated.

Unfortunately, with the present equipment, it is not possible to obtain the necessary data to perform this analysis.

ANALYSIS FILM STRIP A

CILIA OSCILLATED FREQUENCY - PARTICLE VELOCITIES

Certain of the sequences which are amenable to pictorial representation are depicted on the following pages. Others are merely discussed and the data drawn from them included.

Sequence 1

frame rate - 64 frames per sec

magnification - 1500 x

This sequence illustrates a highly turbulent region located above the tips of the cilia. The direction of flow is from background to foreground, i. e., toward the viewer.

On frame 107, a particle 30×10^{-4} mm in diameter enters from the background in third quadrant moving toward the foreground, coming into focus. Its path is toward the viewer and toward the top of the picture. It leaves the picture at top of the third quadrant on frame 116.

Because the particle is not moving parallel to the focal plane, its velocity cannot easily be determined. If needed, the velocity could be estimated by calibrating the fuzziness of the image as a function of distance from focal plane.

Sequence 4 - Particle No 1

frame rate - 64 frames per sec

magnification - 1500 x

Particle velocity

particle diameter:	0. 0060 mm
overall distance traveled:	0. 0300 mm
distance from top of cilia to bottom of particle:	0 to 0. 0015 mm

Frame No.	Distance Traveled Between Positions	Distance/ Frame	Velocity
	mm	mm	mm/sec
61	0	-	-
70	0.0058	6.37×10^{-4}	2.460
73*	0.0150	30.90×10^{-4}	4.880
77	0.0165	3.75×10^{-4}	1.440
90	0.0300	10.35×10^{-4}	3.960

*Burst of energy apparently provided by group of cilia directly

Average distance per frame calculated using increment in distance divided by increment in frame number. Over entire length of travel: 10.35×10^{-4} mm. Average velocity over entire length of travel: 3.960 mm per min. Cilia height: approximately 0.006 mm measured to top of halo.

Sequence 4 - Particle No. 2

frame rate 64 frames per sec

magnification 1500 x

Particle velocity

particle diameter: 19.95×10^{-4} to 30×10^{-4} mm

Particle enters fourth quadrant from left hand side at frame 95, moves to right a distance 60×10^{-4} mm, completes this move on frame 107.

Average distance per frame: 5×10^{-4} mm

Average velocity: 1.920 mm per minute

Between frames 107 and 108 the particle moves to the right and upwards a distance of 45×10^{-4} mm.

Average distance per frame: 45×10^{-4} mm

Average velocity: 17.400 mm per minute

At completion of this motion, the particle is adjacent to tips of cilia. The particle then moves upward along the tips of the cilia a distance of 90×10^{-4} mm. This motion takes place between frames 108 and 114.

Average distance per frame: 15×10^{-4} mm

Average velocity: 5.760 mm per minute

The particle continues to move upward along the tips of the cilia a distance of 105×10^{-4} mm. This motion takes place between frames 114 and 124.

Average distance per frame: 10.5×10^{-4} mm

Average velocity: 4.02 mm per minute

Sequence 5

frame rate - 64 frames per sec

magnification - 1500 x

Cilia Beat Rate

The group of cilia observed lie in the region just above the 50 mark on the projected scale (see film). The region is 0.005 mm in width and one end is adjacent to the 50 mark (0.005 mm is equivalent to 5 units and projected scale). The top of the cilia group is marked by the halo of reflected light. The bottom by cell material of clearly different aspect.

The numbers below appearing under 'Frame No.' are the frame numbers corresponding to the maximum height or elevation of the halo above the base material. The motion is clearly periodic.

Frame No.	Frames/ Cycle	Cycles/ sec	Frame No.	Frames/ Cycle	Cycles/ sec
102	5	12.8	249	5	12.8
107	5	12.8	254	5	12.8
112	5	12.8	259	5	12.8
117	5	12.8	264	5	12.8
122	5	12.8	269	5 1/2	11.63
127	5	12.8	274 1/2	4 1/2	14.22
132	5	12.8	279	5	12.8
137	5	12.8	284	5 1/2	11.63
142	5	12.8	289 1/2	5 1/2	11.63
147	4 1/2	14.22	295	5 1/2	11.63
151 1/2	4 1/2	14.22	300 1/2	4 1/2	14.22
156	5	12.8	305	5	12.8
161	5	12.8	310	6	10.67
166	5	12.8	316	5	12.8
171	5	12.8	321	5	12.8
176	5	12.8	326	6	12.8
181	5 1/2	11.63	331	5 1/2	11.63
186 1/2	5 1/2	11.63	336 1/2	5 1/2	11.63
192	5	12.8	342	5	12.8
197	5	12.8	347	6	10.67
202	5	12.8	353	5	12.8
202	5	12.8	358	5	12.8
212	5	12.8	363	5	12.8
217	5	12.8	368	5 1/2	11.63
222	5	12.8	373 1/2	5 1/2	11.63
227	5	12.8	379	5	12.8
232	6	10.67	384	5 1/2	11.63
238	5	12.8	389 1/2	5 1/2	11.63
243	6	10.67	395	5	12.8

Distribution of Frames/Cycle	
Frames/Cycle	Per cent of Total
4 1/2	6.9
5	65.5
5 1/2	20.7
6	6.9

The total film strip represents 298 frames for 58 cycles or an average of 5.13 frames per cycle which is equivalent to 12.45 cycles per second. The total test duration is 4.65 seconds.

Observation of adjacent groups of cilia suggests that if metachronal wave patterns exist they are not diaplectic. Many more similar film records will be required to obtain more reliable information on metachronal patterns.

Sequence 10

frame rate - 64 frames per sec

magnification - 600 x

Particle Velocity

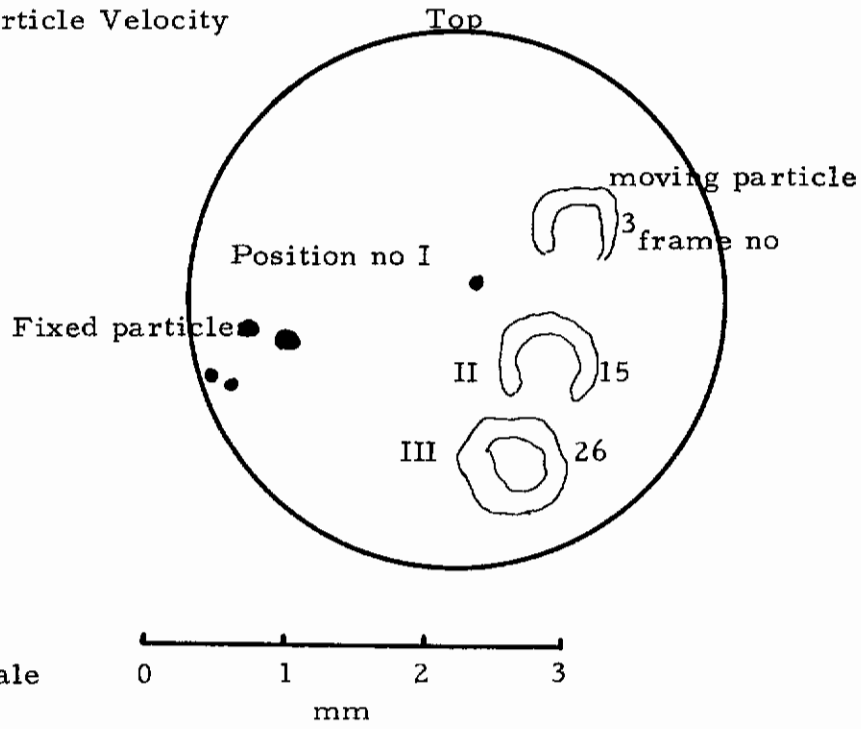

Position No	Frame No	Distance Traveled Between Positions	Distance/ Frame	Velocity
		mm	mm	mm/min
I	3	0.0237	19.80×10^{-4}	7.560
II	15	0.0193	17.55×10^{-4}	6.780

Particle size - .01 to .017 mm in diameter

Sequence 12

frame rate - 64 frames per sec

magnification - 600 x

Particle Oscillation

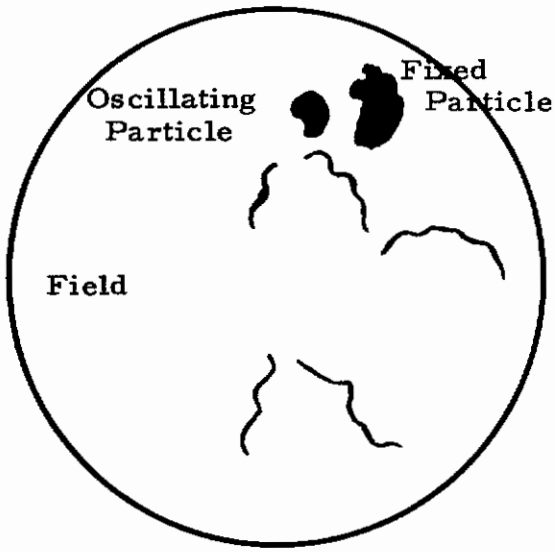

Below is a chart indicating frame numbers occurring when particle is at extremity of oscillation on right side. The frames per cycle are also indicated.

Frame No.	Frames/Cycle	Cycles/Sec
117	6	10.67
123	6	10.67
129	4	16.00
133	5 1/2	11.63
138 1/2	6 1/2	9.85
145	6	10.67
151	4	16.00
155	3 1/2	18.28
158 1/2	5 1/2	11.63
164	6	10.67
170	6	10.67
176	5	12.80

Note that the variation is from 9.85 to 18.28 cycles per second

The position of the oscillating particle at the extremity of the motion is difficult to determine accurately, which has undoubtedly contributed to the large variation. This error can be reduced by noting only the frame numbers at the beginning and at the end, therefore, dividing the error among many cycles of oscillation. Thus, 64 frames are required to oscillate through 12 cycles yielding 5.33 frames per cycle over one second (average rate is 12 cycles per second).

(64 frames above difference between frame numbers 117 and 181 is coincidental)

Average rate of oscillation is in close correspondence with direct measurement of the cilia beat (refer to sequence 5).

Sequence 16

frame rate - 64 frames per sec

magnification - 600 x

Particle Oscillation

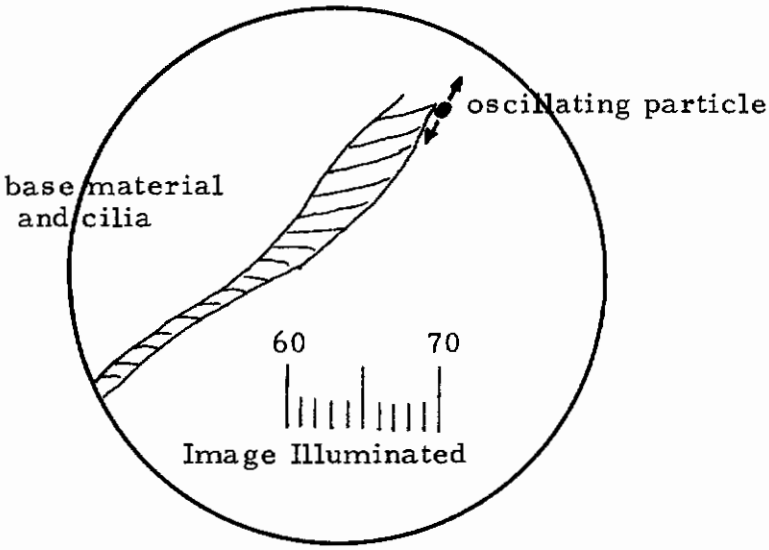

A particle evidently trapped in a region adjacent to the tops of the cilia is clearly seen to be oscillating.

It takes on its lowest position on frame no. 15. Below is a chart of succeeding frame numbers on which it assumes the lowest position, (i.e., one extremity of the oscillation).

Frame Number - Assumes Lowest Extremity
15
20
25
30
34

Hence frames per cycle are 5, 5, 5, and 4. This yields 12.8, 12.8, 12.8, and 16 cycles per second.

Again noting that errors can be significantly reduced by using measurements at the beginning and end, we obtain 19 frame numbers per four cycles or an average of 4.75 frames per cycle or an average rate of 13.47 cycles per second. (Duration of this run is only 0.3 seconds).

Data are consistent with the beat rate measured directly in sequence 5.

ANALYSIS FILM STRIP B

MEASUREMENT OF PARTICLE VELOCITIES

Sequence 1

frame rate - 64 frames per sec
magnification - 600 x

Velocities of five particles

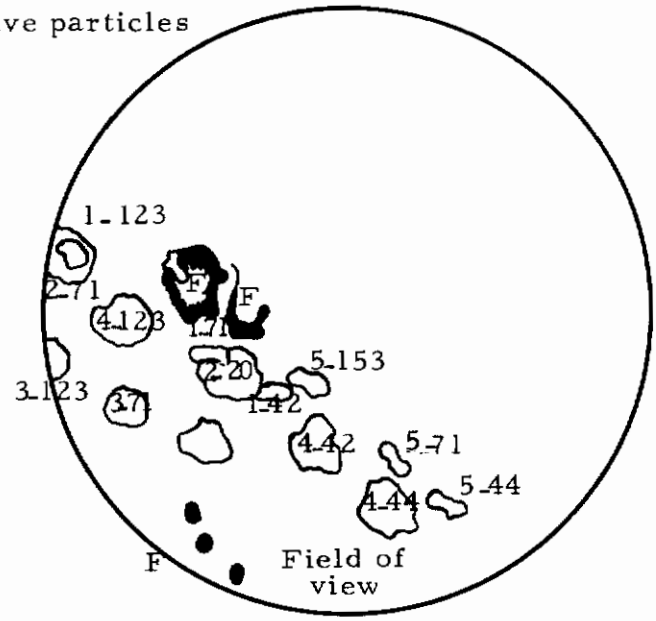

Particle position is documented in the above as a function of the frame number. Particle size can be read directly. Areas marked F were fixed during the motion and represent the frame of reference.

3-20 represents particle 3 at frame 20

scale 1/40 mm = 19 mm

CINEMATOGRAPHIC DETERMINATION OF PARTICLE VELOCITY

SEQUENCE 1

Particle No.	Particle Size	Frame No.	Distance Traveled Between Postions	Δ Frames	Distance/ Frame	Velocity
	mm		mm		mm	mm/min
1	0.0025 to 0.0075	42	0.0125	29	4.31×10^{-4}	1.656
		71	0.0308	52	5.93×10^{-4}	2.280
		123				
2	0.0100	20	0.0375	51	7.36×10^{-4}	2.826
		71				
3	0.0075	20	0.0150	51	2.94×10^{-4}	1.128
		71	0.0162	52	3.12×10^{-4}	1.200
		123				
4	0.0100	44	0.0162	27	6.00×10^{-4}	2.304
		71	0.0420	52	8.08×10^{-4}	3.102
		123				
5	0.0025 to 0.0075	44	0.0122	27	4.52×10^{-4}	1.734
		71	0.0205	66	3.11×10^{-4}	1.194
		137				

Sequence 3

frame rate - 64 frames per sec

magnification - 600 x

Velocities of five particles

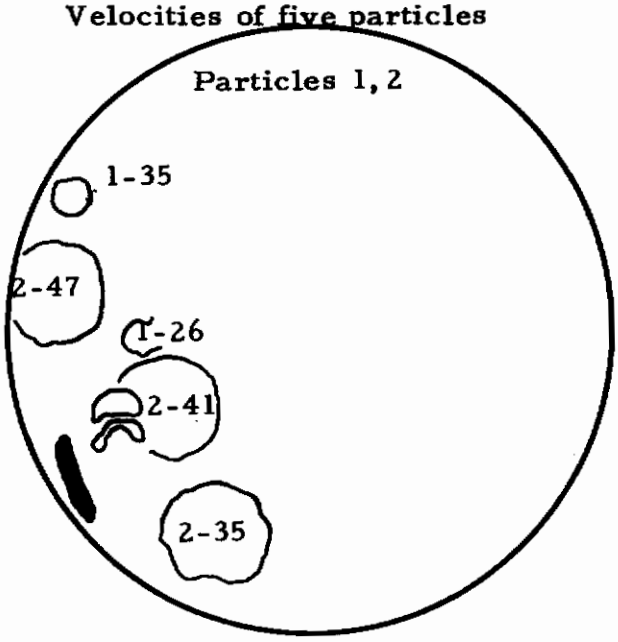

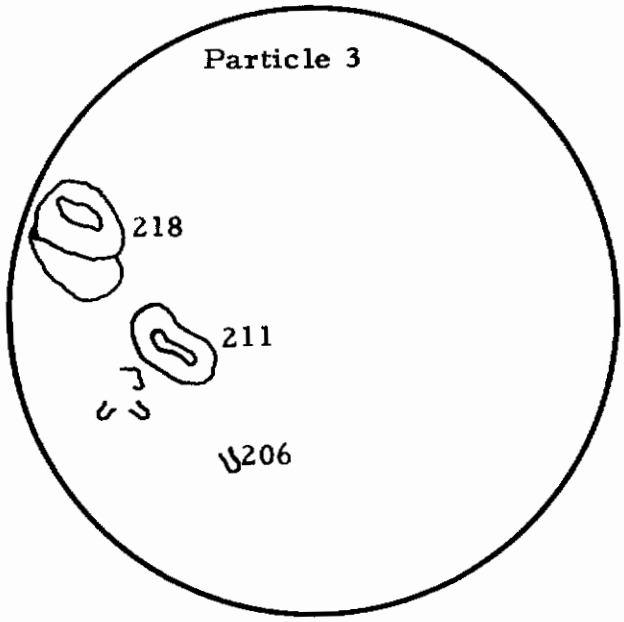

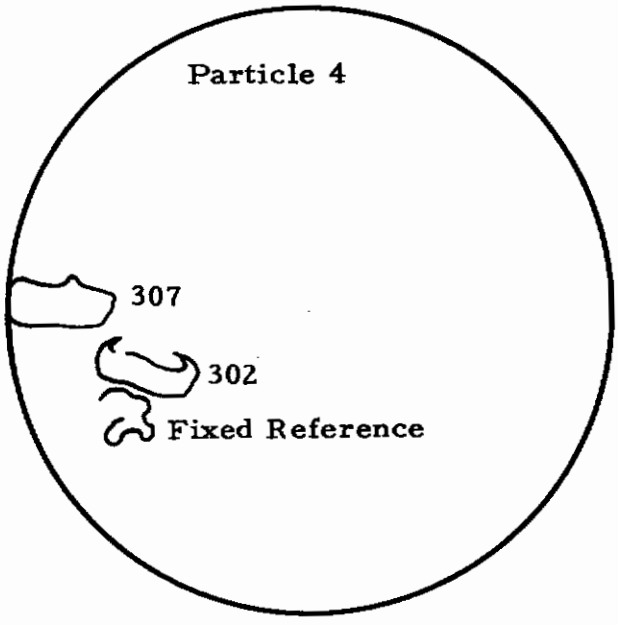

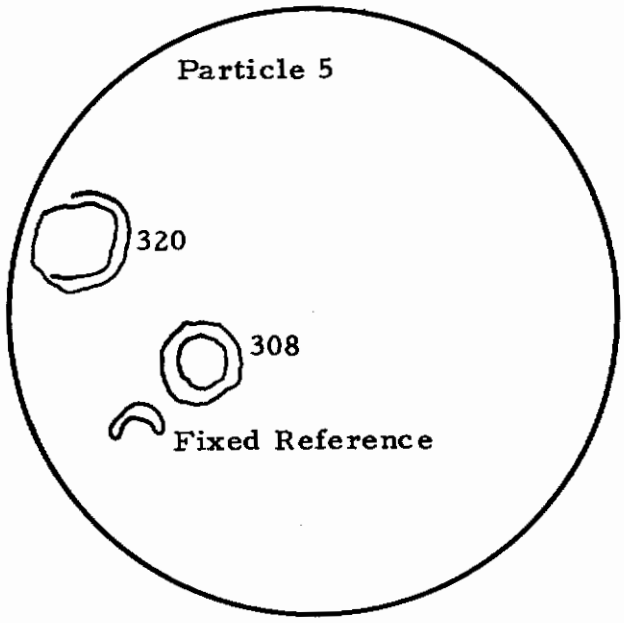

CINEMATOGRAPHIC DETERMINATION OF PARTICLE VELOCITY

SEQUENCE 3

Particle No.	Particle Size	Frame No.	Distance Traveled Between Positions	ΔFrames	Distance/ Frame	Velocity
	mm		mm		mm	mm/min
1	0.0070	26 35	0.0283	9	31.45×10^{-4}	12.072
2	0.0188	35	0.0240	6	40.00×10^{-4}	15.360
		41 47	0.0295	6	49.20×10^{-4}	18.870
3	0.0175 to 0.0088	206	0.0205	5	41.00×10^{-4}	15.750
		211 218	0.0283	7	40.40×10^{-4}	15.510
4	0.0188 to 0.0075	302 307	0.0193	5	38.60×10^{-4}	14.820
5	0.0138	308 320	0.0317	12	26.40×10^{-4}	10.140

Sequence 4

frame rate - 64 frames per sec

magnification - 600 x

Velocities of four particles

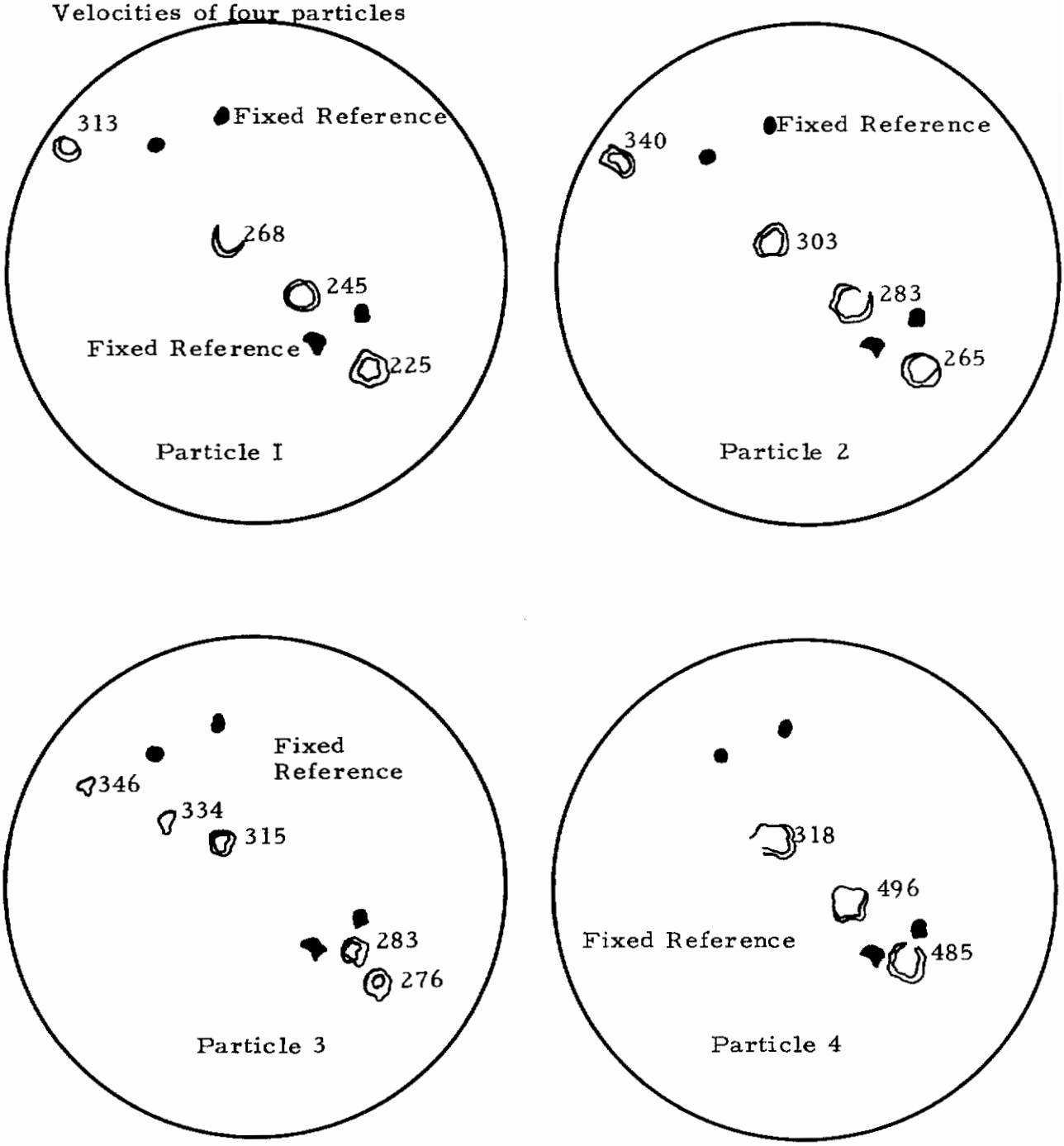

The particles can be seen to be moving through scattered debris.

CINEMATOGRAPHIC DETERMINATION OF PARTICLE VELOCITY

SEQUENCE 4

Particle No.	Particle Size	Frame No.	Distance Traveled Between Positions	Δ Frames	Distance/ Frame	Velocity
	mm		mm		mm	mm/min
1	0.0075	225	0.0215	20	10.75×10^{-4}	4.128
		245	0.0200	23	8.70×10^{-4}	3.336
		268	0.0398	45	8.85×10^{-4}	3.398
		313				
2	0.0075	265	0.0205	18	11.39×10^{-4}	4.374
		283	0.0214	20	10.70×10^{-4}	4.110
		303	0.0375	37	10.13×10^{-4}	3.888
		340				
3	0.0058	276	0.0093	9	10.33×10^{-4}	3.972
		285	0.0375	30	12.50×10^{-4}	4.800
		315	0.0125	19	6.58×10^{-4}	2.526
		334	0.0188	12	15.67×10^{-4}	6.012
		346				
4	0.0075	485	0.0175	11	15.90×10^{-4}	6.114
		496	0.0210	22	9.55×10^{-4}	3.666
		518				

The beating cilia can be seen. The circulatory motion of debris on top of the cilia suggests the turbulent nature of the fluid flow in the region of the cilia tips, which caused particles to be dislodged from larger agglomerations. These particles were carried by the general motions of the stream in the laminar layer of fluid motion beginning no more than 0.0050 mm from the top of the cilia.

These measurements have been made in a region free of debris about 0.0175 mm to the left and 0.0125 mm to the right of the 2 fixed reference particles in the fourth quadrant of the field. The line of particle travel passes between the reference marks and the above dimensions measured.

DISCUSSION

In summary, techniques have been developed to measure the ciliary beat rate by direct cinematographic observations. In addition, the beat rate can be measured by an inferential procedure, i.e., by observing particles of debris trapped adjacent to the cilia blanket. Ciliary beat rate has been measured by both techniques and the results were consistent.

Cinematographic evidence has shown that the mucus region adjacent to the cilia is characterized by turbulent flow. In addition, evidence suggests that the region in the mucus sheath peripheral to the cilia is characterized by laminar flow.

Techniques have been developed to determine particle velocities for debris moving in both the turbulent and laminar regions. The velocities of many such particles have been recorded and are tabulated in this report.

More definitive analyses have not been possible because of the lack of high speed cinematography. This would permit more accurate measurement of cilia beat rate in addition to recording the motion of the cilium in sufficient detail to allow determination of the energy associated with both working and recovery strokes. Energetics of this nature may be related to the energy required to move the mucus blanket. The ability to document an energy balance would provide fundamental insight into the properties of the mucociliary apparatus. In addition, high speed cinematography would yield information on the metachronal patterns associated with cilia movement.

ELECTROPHYSIOLOGY STUDIES

There is general agreement (ref 16) that the fluids secreted by the mucosa of the respiratory tract play an important role in shielding the epithelial surfaces from insult from inhaled gases, particulates, and mixed gas-particulates, many of which are irritant to this tissue. In addition to a non-specific mechanical protection, the mucoproteins present in the secretions probably contribute the properties of a buffer system to the host's resistance to these irritants.

Miller (ref 12) attempted to relate the motion of dyes and particles of carbon black mixed with lycopodium spores placed on the mucus surface to the depth of the mucus blanket. In an in vitro experiment, he found the height of mucus above the cilia to be a factor in relating the metachronal wave properties to the velocity of the particulate matter moving in the mucus sheath. His data indicated that with increasing height of mucus layer, the velocity of particulate transport increased. Further, he suggested a positive and direct relationship between the metachronal wave length and increasing mucus depth. In observations made on two cats with castor oil added to the mucus surface, he noted increased velocity of the natural debris embedded in the mucus compared to mucus transport values in a shallow medium. These results with castor oil are important since they indicate that mucus transport may be governed by a least two factors, namely, the height of the mucus blanket and its viscosity.

The human cervical mucus, in the pre- and post-ovulatory phases, has been reported to contain approximately 93 per cent water. The water content of aspirated human respiratory mucus determined in these Laboratories was approximately 90 per cent (ref 17) suggesting that mucus volume may be quantitatively determined in mammalian trachea via water content determinations.

It was the purpose of this phase of the study to examine electrophysiological method(s) whereby the mucus thickness could be measured in vitro and correlated with water volume. If a positive correlation could be established, the former procedure would be potentially useful to measure the mucus height in vivo. To explore further the rationale for this proposed method, studies were performed on tissues under altered physiological conditions.

(1) Electrophysiological in vitro procedure. A continuous non-destructive monitoring system for determining mucus blanket thickness was explored in an effort to follow effects of experimental exposure. The apparatus consisted of platinum wire (1/4 to 2 mm diameter) metallic electrodes in contact with the mucus layer through which 200 mV, 1000 Hertz sine wave pulses were passed from a Heathkit Model 1G 82 Sine-Square Wave Generator. The electrodes were fixed in series with a known variable resistor and capacitor (Wheatstone balanced bridge circuit, fig 2). The signals were displayed on a Tektronix 502 dual-beam oscilloscope. Resistance or capacitance readings, or both, were made between two electrodes, varying their distance interval from 5 to 20 mm, but maintaining balanced were signals by adjusting the variable resistor and capacitor accordingly (fig 3).

Figure 2

Alternating Current Circuit for Impedance Measurement on the Thickness of Trachea Mucus

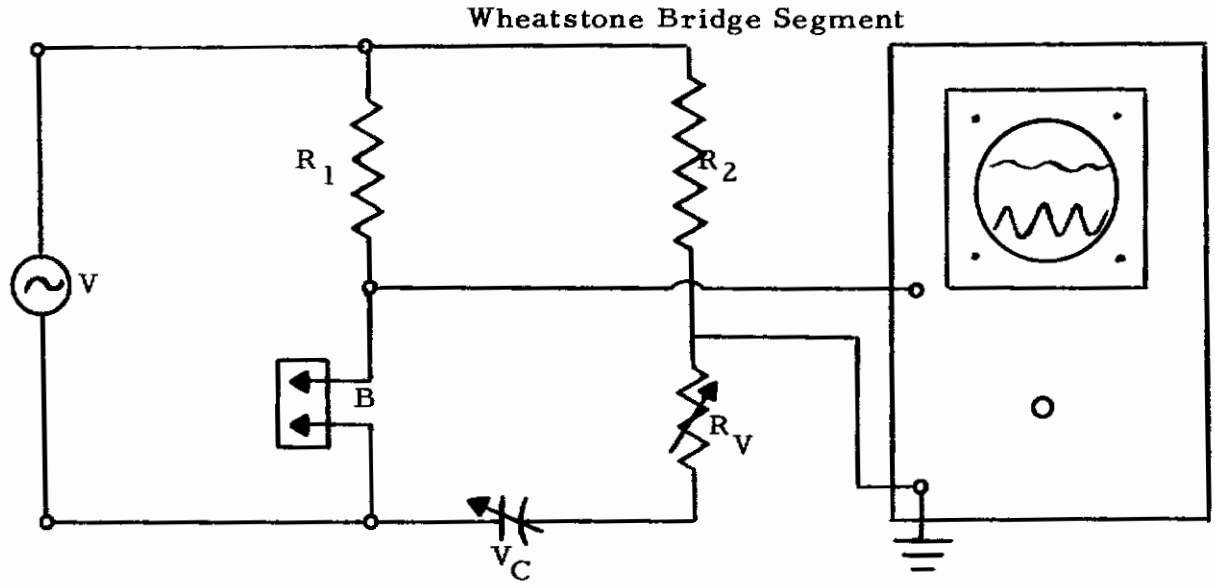

V = Output source from Heathkit Sine-Square Wave Generator

R_1-R_2 = 1 mega ohm

B = Platinum Electrodes for Electrophysiological Measurement on Trachea

R_V = Variable Resistor

V_C = Variable Capacitor

O = Oscilloscope

Figure 3

Oscilloscope Graph Showing Voltage Across Tracheal Mucus Layer

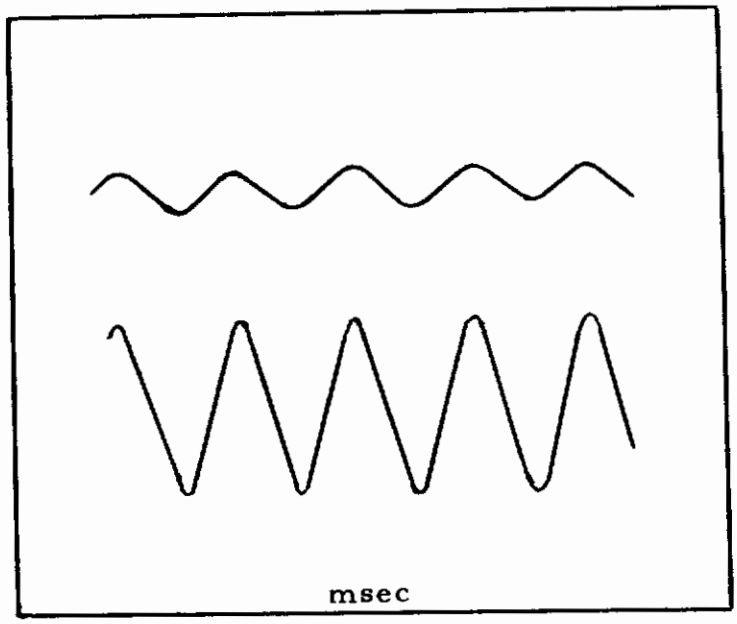

Upper beam= with setting of decade variable impedance networks, a smallest signal is obtained after balance.

Lower beam= a fixed voltage is passed across mucus, trachea and the circuit specified in Figure 2 (125 mV at 1000 Hertz)

A moisture chamber was employed to retard dehydration of mucus from the tracheal segments during these recordings. The tracheae were pinned down on a wax layer comprising 1/3 of the total depth of a 100 x 15 mm transparent plastic Petri dish. Wet cotton gauze was placed around the entire tracheal strip and the Petri dish containing the tissue was sealed with pressure-sensitive plastic tape. The electrodes, drawn to a shank length of greater than 5 cm, were passed through a 2 mm pre-drilled orifice in the center of the dish cover and, after contact was made with the mucus surface, self-sealing, thermoplastic parafilm was used to seal the gap between electrodes and the opening.

(2) Water content. Following excision of another group of tracheal strips (1 cm^2) the striated muscle and fat were dissected free and the tissue was placed in a tared aluminum moisture dish (30-gauge, 50 x 7 mm) and weighed. A longitudinal incision was made along the midventral surface of the trachea and a microscope cover glass placed on the ciliated surface to maintain a flat area for measurement with a calibrated rule. The tracheal segments were then dried to constant weight at 75°C for six hours in a forced air oven.

Mucus volumes of tracheal strips were estimated from the following equations:

(a) F (% moisture content) $= \frac{\text{Loss in weight following drying}}{\text{wet weight}} \times 100$

Since mucus is composed of approximately 10 per cent solid material, the estimated mucus volume is calculated as:

(b) G (estimated mucus volume μl) $= \frac{(0.1 \times F) + F}{100}$

Dividing the estimated mucus volume (G) by the surface area (H) of the excised tracheal strip provides a constant relationship:

(c) $\frac{G}{H} = \mu l/mm^2$

for comparing various different tracheal segments.

Although these formulae represent changes in tissue water content, constancy in any given tissue permits estimating mucus volume changes, since the latter represent the major variable in experimental conditions.

RESULTS

(1) Electrophysiological in vitro procedure. Resistance values between two electrodes on an excised tracheal strip increased rapidly when the trachea was exposed in a non-humidified atmosphere. This increase was retarded by application of a plastic film (pressure-sensitive tape) on the mucus surface which reduced the evaporation of water and prevented reduction of mucus thickness. The resistance values of the non-protected tracheal strip obtained from Guinea Pig 1 (fig 4) increased from about 20,000 to 45,000 ohms in 30 minutes. However a second strip, covered to retard evaporation and consequent alterations in mucus thickness, con-

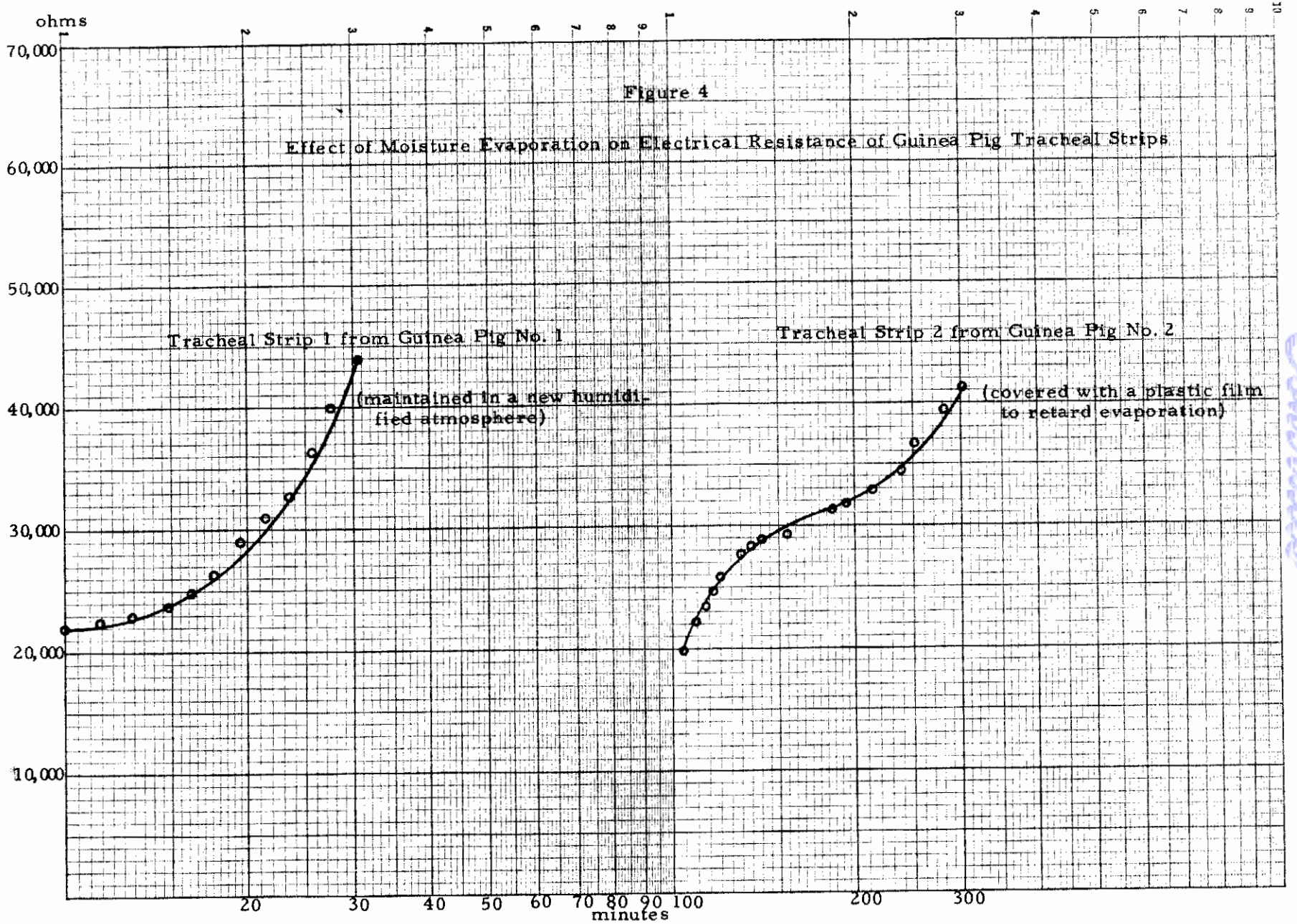

Figure 4

Effect of Moisture Evaporation on Electrical Resistance of Guinea Pig Tracheal Strips

tinued to exhibit a resistance of 20,000 ohms at 100 minutes after excision, and increased to about 40,000 ohms by 300 minutes. This difference in response suggests that when evaporation was retarded, the preparation was protected, as judged by the changes in resistance values. The time base over which the observations were made indicate a ten-fold increase in time prior to achieving equal resistance values.

The mucus surface of a third strip from the same trachea was covered with parafilm for 24 hours to retard moisture evaporation, after which resistance measurements were performed. In this strip the initial resistance was about 20,000 ohms and increased to approximately 45,000 ohms in 800 minutes. Although definitive information is not now available, it is possible that the reduction in time from 200 to 800 minutes for a resistance increase in strips 2 and 3, may have resulted from change(s) in the labile mucopolysaccharide structure of the mucus during the 24-hour holding period.

Resistance values were markedly constant when the tracheal strips were placed in a moisture chamber. Data for two tracheal strips from two different cats maintained in the moisture chamber are shown in fig 5 and resistance measurements recorded as described. No change in resistance from basal levels were seen for 300 and 750 minutes in segments 1 and 2, respectively. A resistance of 45,000 ohms was reached approximately 1500 and 2900 minutes after excision of the segment from the animals.

Resistance studies were also carried out with rabbit trachea, varying the treatment of the animal prior to excision of the tissue for recording. In one, the segments were taken from animals terminated immediately prior to dissection. In another study, the segments were taken from animals that died 24 hours earlier, in which the dead rabbits were wrapped in plastic bags to retard fluid loss, and the tracheal tissue was excised 24 hours later.

The procedures used, were as described in the previous section, but varied to the extent that recordings were made from both the serosal and mucosal epithelium, and the cartilage. This simultaneous procedure involved extensive exploratory work before it was feasible to carry out all recordings in the same animal.

Comparative resistance recordings made on the serosal, mucosal, and cartilaginous surfaces of rabbit tracheal tissue under a variety of conditions are detailed in table V. They are illustrated by the values obtained with animal No. 26, one of the first successful runs for simultaneous or sequential recordings. Resistance measurements made on the serosal surface were 12,900 ohms. Measurement of the resistance of cartilage of this tracheal segment one minute later, showed a 2.5-fold increase in resistance. Resistance measurements on mucosal surface 100 minutes after removal of the segment from the animal were 7,900 ohms when a mucus layer was still observed as present. With evaporation the mucus layer was observed visually (microscopically) regressing, and the resistance increased over the next 25 minutes to 106,900 ohms.

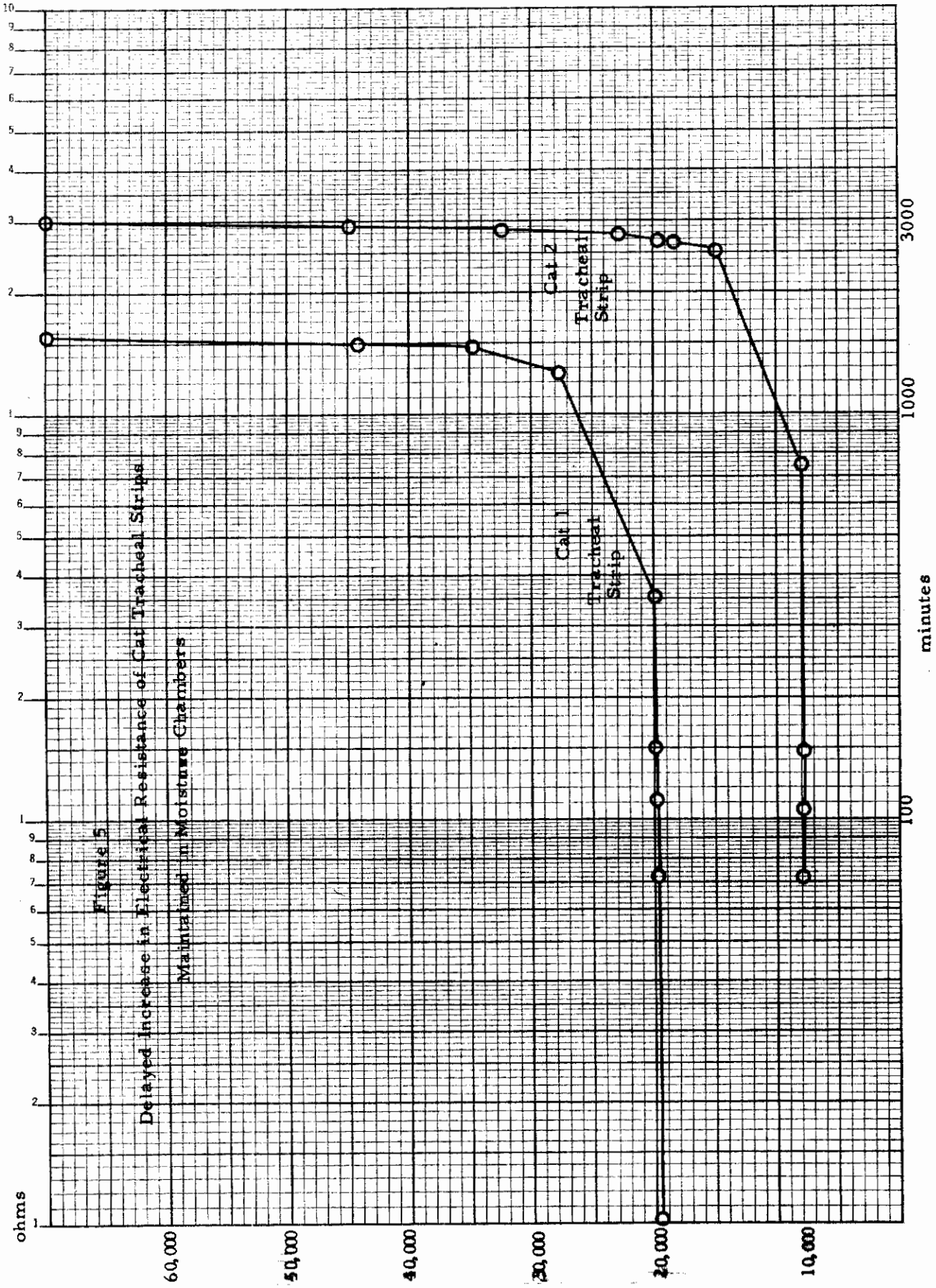

Figure 5

Delayed Increase in Electrical Resistance of Cat Tracheal Strips Maintained in Moisture Chambers

TABLE V

RESISTANCE MEASUREMENTS IN RABBIT TRACHEAL SEGMENTS

Rabbit No.	Electrode Placement	Elapsed Time	Resistance
		min	ohms
26	Serosal surface	0	12,900
26	Cartilage surface	1	34,000
26	Mucosal surface	100	7,900
		120	40,000
		125	106,900
24	Serosal surface	1440*	40,000
		1442	46,500
		1450	75,000
		1455	143,000
		1461	234,990
24	Mucosal surface	1466*	19,400
		1470	23,300
		1473	27,100
		1522	200,000
24	Serosal segment stored for 4 hours in a sealed Petri dish	1680*	70,200
24	Mucus layer from above strip	1685*	24,990
		1690	42,000
		1695	120,000
		1698	260,000

* All values for Rabbit No. 24 include the initial post-mortem period of 24 hours before the tissue sections were excised.

Rabbit No. 24 died 24 hours prior to initiation of measurements. The tracheal segments were not removed from the animal during that time period. Immediately following removal of the tracheal segment, measurements of resistance on the serosal surface (1440 minutes after death) yielded values of 40,000 ohms table V. Over the next 21 minutes, during which evaporation was uncontrolled, resistance increased to 234,990 ohms. Recording from the mucosal surface yielded values of 19,400 ohms. Continued resistance measurements for the next 66 minutes during which time the mucus level regressed (evaporation) resulted in an increase to 200,000 ohms.

The second segment of tracheal strip obtained from the animal, dead for 24 hours, was placed into a humidity chamber for four hours and exhibited serosal surface resistance values of 70,000 ohms (1680 minutes after the death of the animal). Five minutes later, values approximating 25,000 ohms were recorded from the mucosal surface of this strip. During the next 13 minutes, as the mucus thickness decreased, the resistance rose to 260,000 ohms.

These results indicate that the serosal surface of the trachea, lacking a mucus layer, has an intrinsically high electrical resistance. The resistance of the mucosal surface of the same strip with its mucus layer intact is markedly lower. As surface moisture is lost from the mucosal surface, resistance increased from the prior base line values. Thus, indirect evidence is available to indicate that the presence of a mucus layer correlates with a relative low electrical resistance on the mucosal surface.

Data showing electrical resistance measurements on tracheal strips subjected to various experimental conditions in three species of animals are presented in table VI. From the initial measurements, it can be seen that the resistance of the mucosal surface of tracheal strips obtained from monkeys is slightly less than that obtained from rabbits. Tracheal strips obtained from guinea pigs exhibit electrical resistance far in excess of the other two species. Microscopic observations of the mucosal layer suggests that the mucus thickness in guinea pigs is less than that found in either rabbits or monkeys.

Resistance measurements performed for 55 or 218 minutes with monkey tracheal strips in a partial or complete humidified atmosphere indicate little change in electrical resistance, though slight increases were seen.

Maintenance of the tracheal segment from the rabbits for 200 minutes in a moisture chamber prevented an increase in resistance. When a similar segment was tested under non-humidified conditions, resistance increased about five-fold. Similarly resistance increased two-fold in the guinea pig tracheal segment exposed to a non-humidified atmosphere. After 110 minutes in an humidified atmosphere, no increase in resistance was seen in a second guinea pig tracheal segment. In each of the species, therefore, maintenance of the integrity of the mucus sheath by humidification helped maintain the basal resistance values of the tissue system.

TABLE VI

SPECIES DIFFERENCES IN THE ELECTRIC RESISTANCE AND MUCOSAL SURFACE OF TRACHEAL SEGMENTS

Species	Animal No.	Initial Reading Resistance	Final Reading Resistance	T_0-T_f [1]	Remarks
		ohms	ohms		
Monkey	1028	5, 210	7, 041	218	Tested under humidified atmosphere
Monkey	1104	4, 740	5, 491	55	Partially open moisture chamber
Rabbit	1027	7, 600	5, 600	200	Frozen trachea tested inside moisture chamber
Rabbit	26	7, 900	40, 000	20	Tested under non-humidified atmosphere
Guinea Pig	1018	21, 030	43, 600	31	Tested under non-humidified atmosphere
Guinea Pig	1019	20, 000	20, 000	110	Tested inside moisture chamber

[1] T_0-T_f= Time interval between initial reading and final reading

Electrical data from a section of rabbit trachea frozen for eight days and then thawed are shown in table VII. When electrical resistance and capacitance measurements were made on the serosal surface, the resistance decreased slightly but capacitance increased for the first 95 minutes. For the next 105 minutes, there were no additional significant changes although a slight increase in resistance is suggested by the data (fig 6).

By shifting from alternating to direct current and by increasing the voltage 15-fold, the resistance reading increased only 13-fold. The difference may be due to a DC-boundary potential existing between the electrodes and the mucus table VII.

During the period of DC voltage application, reversal of the electrode polarity caused resistance to increase 113.2 per cent within one minute. This returned rapidly when the polarity was reversed to its original direction. A change in polarity and large increases in current appear to induce changes in the tissue (i.e., denaturation) as shown by the increased resistance in table VII. This finding justifies the use of alternating current of low to moderate intensity in all future work.

(2) Water content. Volumetric estimation of tracheal mucus thickness appears to provide a means of detecting differences among the several animals species examined. Within the same species, the pathological changes associated with excessive drying were reflected in the variation of tracheal mucus thickness shown in table VIII.

The total water content of the mucus layers, the tissue fluid in cartilage, connective tissue, smooth muscle, and elastic fibers are similar in rabbits and rats as judged by the recordings discussed, and slightly less than found in monkeys.

The estimated order of decreasing mucus thickness is, respectively, monkeys, rabbits, and rats. The data in table IV suggest that the estimated mucus thickness is independent of the total water content of the tissues. Corroborative data provide further demonstration, i.e., rats continuously exposed to ozone for 80 days exhibited a significant decrease in mucus thickness while the total water content of the tracheal segment remained unchanged.

TABLE VII

CHANGES IN ELECTRIC CHARACTER OF FROZEN AND THAWED RABBIT TRACHEA

Alternating Current (minutes after measurements started)	Placement	Resistance	Capacitance
		ohms	microfarads
0	Electrodes on	7,600	0.019
1	serosal surface	6,991	0.020
20	of frozen trachea	6,191	0.020
45	within a moisture	5,990	0.021
65	chamber	5,770	0.022
83		5,600	0.0223
95		5,490	0.0233
146		5,600	0.0238
200		5,600	0.0238
Direct Current 1.5V[1] (minutes after measurements started)			
0		78,000	
3		70,000	
10		76,000	
50		78,000	
95		71,000	
165		68,000	
		reversed polarity	
166		145,000	
		reversed polarity	
167		62,000	
168		40,000	
Alternating Current[2] (minutes after second measurement started)			
0	Electrodes con-	2,500	0.031
33	tacted mucus	2,800	0.031
41	laminated tracheal	2,900	0.031
94	inner surface	3,060	0.03147
95		3,066	0.03146
97		3,073	

[1] Shifted from 100 mV, 1,000 Hertz alternating current to 1.5V direct current.

[2] The trachea strip was frozen at -25° C for 16 hours, then thawed at room temperature; resistance was measured again by contact electrodes on the fresh mucus surface of the above mentioned tracheal strip.

Figure 6
Electric Resistance Fluctuation Character on the Outside Wall of Frozen Rabbit Trachea

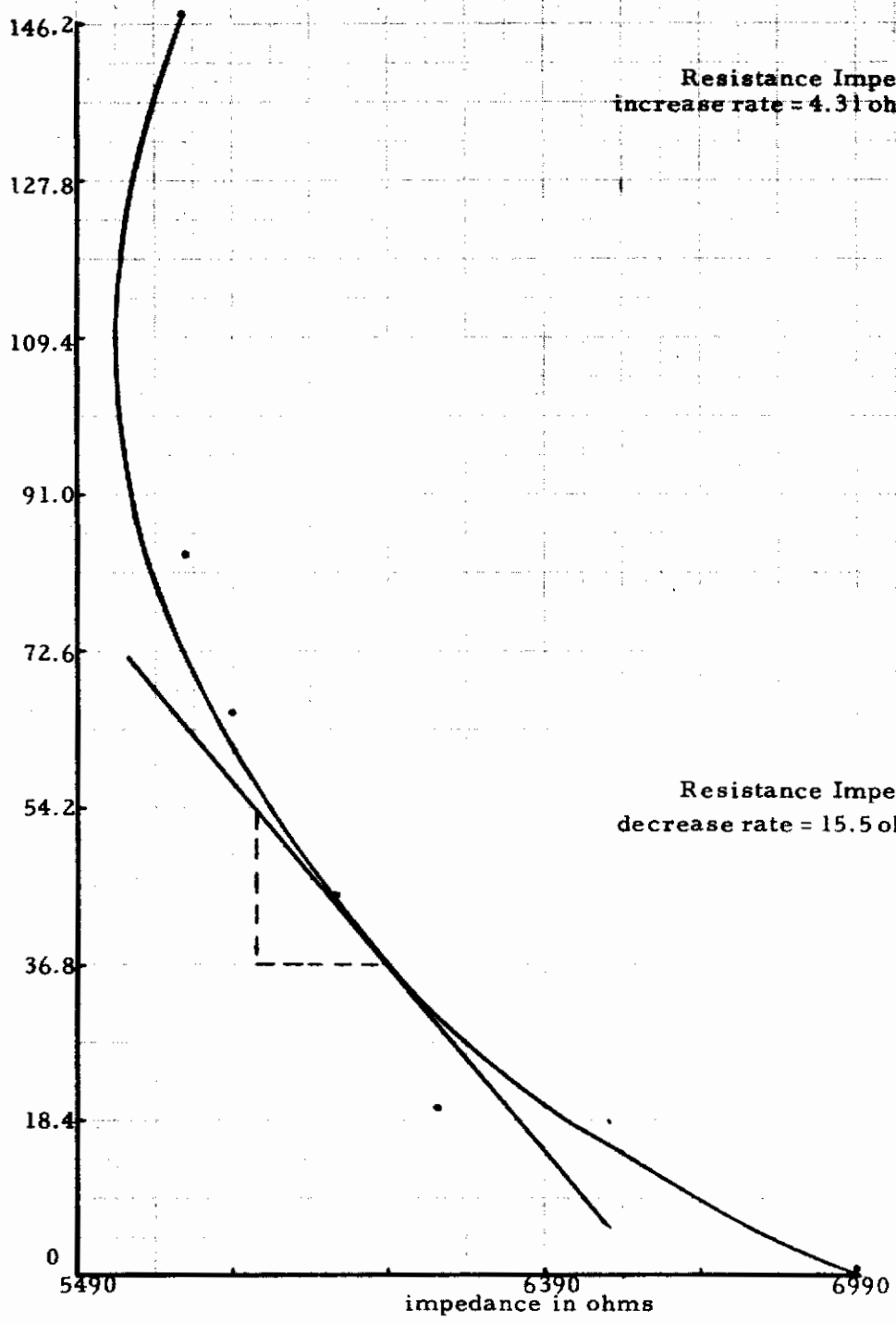

TABLE VIII

VOLUMETRIC ESTIMATION OF THE THICKNESS OF MUCUS LAYER OF MAMMALIAN TRACHEA

Species	Animal No.	Estimated Mucus Thickness $\mu l/mm^2$	Total Water Content In Wet Trachea (g/g of wet trachea)
Monkey	3141	0.735	0.7107
	3142	0.742	0.7196
	3805	1.182	0.7726
	5	0.773	0.7220
	4	0.912	0.7370
	3820	1.126	0.7398
	152	0.866	0.7450
	153	0.921	0.7335
	154	0.762	0.7476
	155	0.820	0.7456
	3817f	0.766	0.7339
	3821f	1.012	0.7336
	3819f	0.767	0.6961
	3822f	0.763	0.7320
	3824f	0.759	0.7140
Average		0.860 ± 0.047	0.7322 ± 0.0182
Rabbit	313	0.497	0.5857
	T6	0.621	0.5870
	211	0.797	0.7178
	213	0.719	0.7176
	214	0.708	0.6964
	215	0.647	0.6612
	216	0.822	0.7027
	217	0.696	0.6470
	218	0.635	0.6550
	219	0.744	0.6680
	220	0.692	0.7260
	221	0.814	0.6640
	222	0.720	0.5820
	223	0.603	0.6890
	224	0.515	0.6120
	304	0.805	0.5520
	305	0.954	0.6370
	306	0.851	0.5790
Average		0.717 ± 0.109	0.6490 ± 0.0533

TABLE VIII (continued)

VOLUMETRIC ESTIMATION OF THE THICKNESS OF MUCUS LAYER OF MAMMALIAN TRACHEA

Species	Animal No.	Estimated Mucus Thickness $\mu l/mm^2$	Total Water Content in Wet Trachea (g/g of wet trachea)
Rat	313f	0.392	0.6945
	307	0.345	0.6340
	308	0.457	0.5950
	3010	0.288	0.5800
	3011	0.240	0.6700
	3012	0.265	0.5450
	3013	0.275	0.6000
	311	0.348	0.6100
	312	0.360	0.6000
Average		0.327 ± 0.067	0.6160 ± 0.0434
Rat (exposed in ozone gas for 80 days)	A71	0.242	0.615
	A72	0.274	0.666
	A73	0.320	0.637
	A74	0.278	0.531
	A75	0.291	0.602
Average		0.281 ± 0.029	0.6100 ± 0.0505

DISCUSSION

The observations made in these studies involved the investigation of the relationship between electrophysiological properties of the mucosal surface of the tracheal segments in vitro with the thickness of the overlying mucus blanket. Utilizing surface resistance recordings, it has been demonstrated that a tissue possessing an intact mucus layer has less resistance than the area lacking this layer. The serosal surface of the tracheal segments yielded high resistance values compared to the mucosal surface values. The integrity of the mucus layer plays an important role as indicated by the changes in values as the mucus layer decreased with evaporation of moisture, as in a non-humidified atmosphere. Under these conditions, the resistance recorded from the mucosal surface increased markedly. Maintenance of the integrity of the mucus layer, as obtained by exposure of the tracheal strips in a humidified atmosphere, caused no elevation of resistance which was associated, in every instance, with drying and thinning of the mucus.

In vitro experiments performed to correlate electrical resistance with tracheal mucus thickness indicate that the electrical resistance obtained from the mucosal surface of tracheal segments of monkeys in less than that found in rabbits, while the reverse is true for mucus thickness.

Although absolute water content of the mucosal surface of guinea pig tracheal strips was not determined, the electrical resistance of these segments is high compared to values found with monkeys or rabbits. However, visual observations, using light microscopy, revealed that the mucus cover is much thinner in the guinea pigs examined than in the monkey or the rabbit.

From studies performed with rats, it appears that this species has a thinner mucus layer than found in rabbits or monkeys. Further, exposure of rats to ozone, a respiratory irritant, reduces the moisture content of the mucosal layer still further. These observations relating to thinness of mucosal coat in rats and guinea pigs should be considered in still another context. From the point of view of intrinsic secretory activity of the goblet cells, the population of these cells and their activity is among the lowest in the animal kingdom on a comparative basis.

It is therefore evident that in terms of defining the mucus layers that electrophysiologic measurement, i.e., resistance and to a less well characterized extent capacitance, can be utilized to estimate the thickness of the mucus layer of mammalian trachea. The results indicate that resistance is a function of the moisture content of the mucus. Further, while an irritant substance has the capability of reducing the thickness of the mucus layer, it does so without affecting the total water content of cellular components of the tracheal strip. With proper methodology it appears feasible to implant electrodes within the trachea of an animal and subsequently to record electrical resistance in vivo, while subjecting the animal to various experimental conditions, i.e., nitrous oxide, ozone, pure oxygen, and recording changes in the electrical resistance of the mucosal surface of the trachea during these exposures.

MUCOCILIARY RESPONSES TO IRRITANT EXPOSURES

The irritant exposure sequences referred to in the introduction were initiated early, since they provided biological material for integrated evaluation and characterization of normal and induced responses, as measured by mucus flow and ciliary beat. (These have been described (ref 6, 9) and independently verified by a number of other laboratories (ref 18)). Thus, a basis was provided in order to introduce methods for photographic visualization, possible electrophysiological studies, wave form analysis using cinematographic recordings, biochemical studies, and electron microscopy.

The correlation between chemical, physical, and biological events is essential if characterization of energy requirements of the non-innervated cilia in health and disease are to be made.

PROCEDURE

Initially, acute procedures were employed wherein correlative recordings from tracheal tissues of mucus flow, viscosity, and ciliary beat frequency could be made in situ. These tissues were then rapidly excised and mounted for studying laminar and turbulent flow patterns, as well as ciliary wave form in vitro.

Following this, subacute exposures were carried out in an attempt to correlate work being conducted in other centers with continuous pure oxygen exposures at 0.33 atmospheres and ozone exposures under ambient conditions.

Due to technical problems all the nitrogen dioxide exposures were acute.

ACUTE STUDIES

Pure oxygen exposures. Inhalation chambers and ancillary exposure apparatus were used to provide optimal conditions for exposure of cats to humidified pure oxygen. The oxygen was delivered at the rate of 5 liters per minute into a 3-cubic foot plexiglass exposure chamber in which a group of 3 to 5 healthy non-fasted young cats were housed. A small vessel containing sodium peroxide was placed into the chamber to absorb any CO_2 which was not cleared from the apparatus by continuous flow conditions. Exposure periods varied within the range of 15 to 30 minutes. Mucus flow rate measurements were recorded immediately after termination of exposure and continued for as long as 30 minutes post-exposure.

To ascertain whether O_2 flow via a small animal mask* would result in differential changes, and to record effects during such treatment, exposures were initiated with a flow rate of 500 ml oxygen per minute. This procedure permitted direct visualization of responses during exposure to irritants. Mucus transit time and "apparent average viscosity" (ref 5) was recorded. Stroboscopic illumination was used with selected animals to determine changes in ciliary beat frequency.

*Mine Safety Appliances Co., 201 N. Braddock Ave., Pittsburgh, Pa. 15208

Nitrogen dioxide. A group of cats was exposed to nitrogen dioxide gas at 35 and 75 µg per kg body weight generated by the action of nitric acid on metallic copper. Dosages were determined by the calculation of rate of oxide generation, tidal volume and the number of respiratory excursions allowed each animal.

Measurement of mucus velocity and viscosity. For these measurements the mask is left in place throughout the exposure or as called for by the protocol. The introduction of the pollutant or irritant into the face mask does not affect the method of velocity nor of viscosity recording.

Young cats (750 and 1500 g) of either sex are anesthetized with pentobarbital sodium (35 mg per kg), placed on a surgical tray in a supine position, and incised to a length of 3 cm through the skin, muscle, and fascia covering the trachea. Exposure of the trachea is performed by blunt dissection to avoid injury to nerves and blood vessels.

Following a period for acclimatization, the animal is placed in a prone position on a platform over a thermostatically controlled water bath to maintain body temperature (fig 7). A Wild binocular dissecting microscope with a calibrated ocular is inverted and focused on the trachea. Cotton pledgets moistened with saline are used to avoid tissue dehydration when readings are not being performed. A cold light is maintained in juxtaposition to the trachea to utilize its translucent properties. Equal weights of carbon black, triturated with lycopodium spores to insure uniform size, are introduced into the lumen through a syringe with a 22-gauge needle inserted between the bifurcation of the trachea and the point of observation. Movement of marker material floating on the mucus surface is clearly visible through the ocular. Reintroduction of the marker material may be made at each transit time recording.

Test materials are introduced via a small animal face mask of 200 cc capacity fitted with a rubber dam headport assembly which permits the insertion of the animal's head. Pure test materials are introduced via a Vaponefrin nebulizer as aerosols or as a gas from a source container with appropriate gauge and valve assembly.

The "viscosity" determinations are made with an electromagnetic coil set around the neck of the cat and oriented so that the lines of magnetic force are coaxial with the tracheal mucosa. A controlled current is passed through the coil until a steel ball 0.02 inches in diameter is made to move to the center of the field. This ball is inserted into the lumen through a small gauge needle and floats in the mucus. The current value is recorded when the ball passes to the center of the field. In animals with normal appearing mucus and normal mucus flow rates, movement of the ball (about 15 mm per minute) requires 1/3 to 1/7 less current than in animals with viscid mucus or little or no mucus flow. The flow velocity rates, using steel balls in normal animals do not differ significantly from those obtained with lycopodium spores.

Although true viscosity cannot be measured with this technique in a laminar non-Newtonian polymer, changes are indicative of altered viscidity. Studies performed in a large number of healthy and infected cats (upper respiratory infection) suggest that values in excess of 500 cs should be considered as outside of normal limits.

Figure 7. Schematic of the Apparatus for Observing In Vivo Mucus Flow

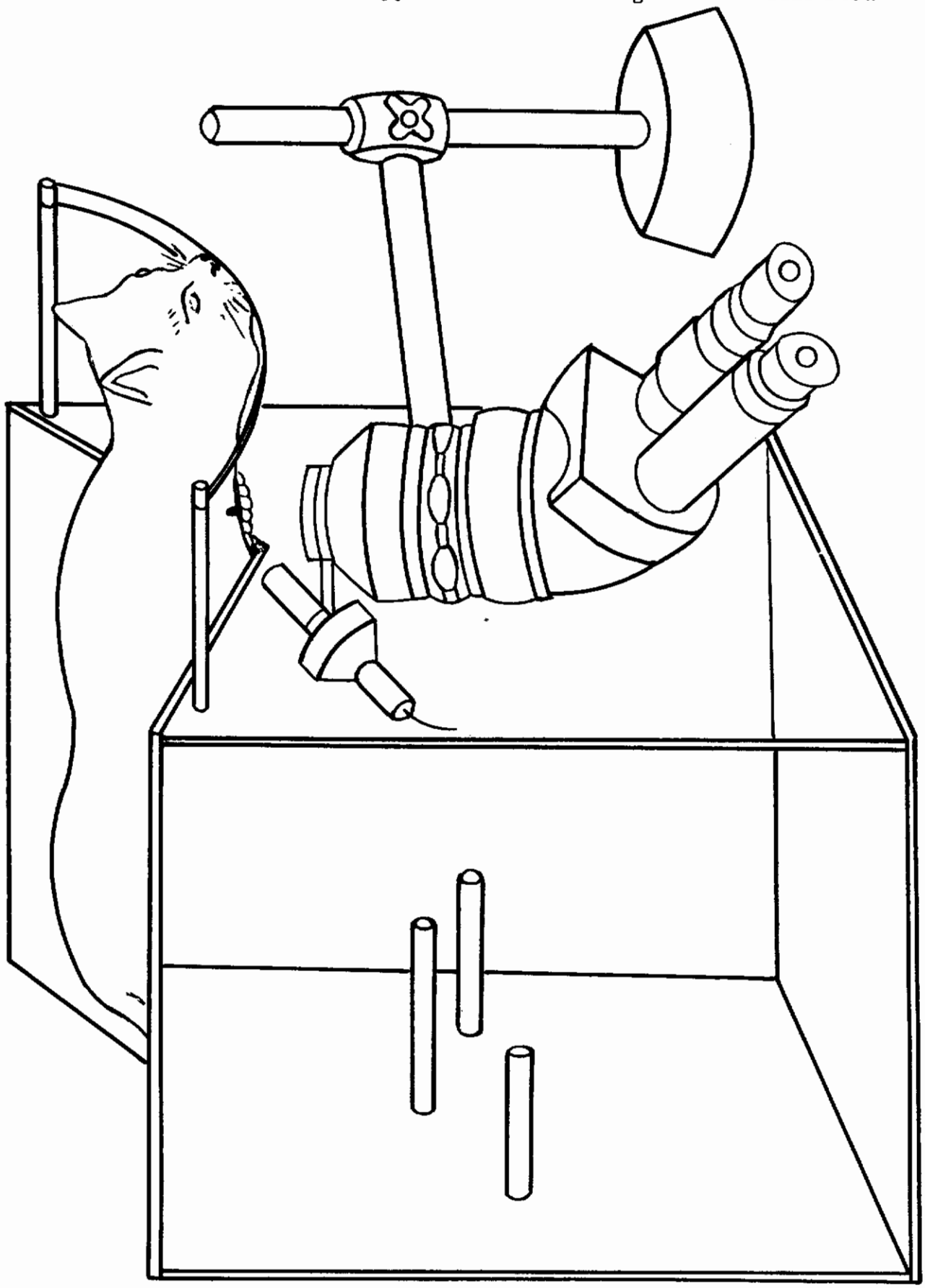

RESULTS

Pure oxygen exposures. The comparative velocities after exposure to humidified pure oxygen in a chamber system for 15 and 30 minute periods are shown in table IX and X, respectively. Inasmuch as no pre-exposure values can be obtained in these animals, all data shown refer to post-exposure readings, and other references must be made to a universal norm of 13.2 to 15 mm per minute. The data show no significant differences at one minute following cessation of exposure between the animals receiving oxygen for 15 or 30 minutes. Similar results were obtained at 2 minutes post-exposure. Although the data are insufficient, it appears that at 3 minutes there may have been a difference between the two groups.

No differences in mucus velocities were seen after exposure at 4, 5, 10, 15, and 30 minutes between the two groups, even though animals shown in table X received twice the exposure concentration as those in table IX. These data are significant since they indicate that a maximum level of response was achieved in the 15-minute exposure sequence, and prolonged exposure of 30 minute duration does not intensify the changes. Within 10 minutes post-exposure a large proportion of the animals returned to normal and at 15 minutes all animals in both groups returned to normal velocity readings.

Pure oxygen. Utilizing the same experimental material, pure oxygen, the results of the face mask exposures for 3, 10, and 30 minutes, respectively, are shown in tables XI, XII, and XIII, respectively.

In the 3-minute exposure series (table XI) there appears to be a slight diminution in flow which does not fall below 70 per cent of basal flow values. In all except two animals, a peak depression was observed at the third minute of exposure. The readings at one minute show a tendency toward diminution in some animals; others however remain at their basal levels. Of interest is the apparent correlation in viscosity readings which indicate an increase to approximately 174 per cent of basal levels. However these are considered to be within the normal maximum limits for healthy cats. As indicated previously, 500 cs is the maximum normal viscosity reading. One animal showed a reading of 505 cs which is not considered significant but falling within experimental variation.

The values in the cats exposed by face mask for a 10-minute period show graded diminution between 3 and 10 minutes of exposure (table XI). The maximum depression in basal flow being approximately 46 per cent of the pre-test value. In all animals peak diminution was observed at 10 minutes. At 15 minutes, all except two of the animals had returned to flow velocities of 13 mm per minute and by 30 minutes all values were in the normal range. Corroboration of changes in mucus flow velocity can be seen in the viscosity data which reveal an apparent peak increase in viscidity of the mucus occurring at 10 minutes after initiation of exposure. The post-exposure recovery was very rapid, all animals being within normal range at 15 minutes after cessation of oxygen flow.

TABLE IX

EFFECTS OF HUMIDIFIED PURE OXYGEN EXPOSURE ON MUCUS VELOCITY IN CATS

(15-Minute Chamber Exposure)

Cat No.	Body Weight	Velocity (Post-exposure, minutes) 1	2	3	4	5	10	15	30
	g	mm/min							
702	1215	9.5	10.2	10.2	9.9	12.3	13.1	15.8	15.0
703	890	9.4	11.5	11.5	11.1	11.8	11.3	13.7	14.6
715	975	8.7	---	---	---	---	14.7	15.0	15.0
716	1010	8.8	---	---	---	---	13.7	13.1	14.0
717	1120	10.0	---	---	---	---	12.3	14.6	14.3
718	840	8.5	---	---	---	---	14.3	15.0	14.0

TABLE X

EFFECTS OF HUMIDIFIED PURE OXYGEN EXPOSURE ON MUCUS VELOCITY IN CATS

(30-Minute Chamber Exposure)

Cat No.	Body Weight	Velocity (Post-exposure, minutes) 1	2	3	4	5	10	15	30
	g	mm/min							
693	560	10.7	10.3	8.4	9.4	11.6	11.1	13.1	12.6
700	1050	9.4	10.6	8.1	8.5	8.4	11.6	14.3	14.6
701	835	9.0	9.5	9.4	10.7	11.8	12.8	15.4	14.6
694	940	8.2	---	---	9.9	9.4	14.3	13.7	14.0
695	1105	9.9	9.7	11.1	11.6	12.0	11.8	14.3	15.4
696	780	10.2	11.1	11.6	12.0	12.8	15.4	15.4	15.0
697	920	9.0	---	---	---	---	15.0	14.3	13.4
698	955	8.7	---	---	---	---	11.6	15.0	16.2
699	1120	8.1	---	---	---	---	12.5	15.0	15.0

TABLE XI

EFFECTS OF HUMIDIFIED PURE OXYGEN EXPOSURE ON MUCUS VELOCITY AND VISCOSITY IN CATS (CONTINUOUS 3 MINUTES FACE MASK EXPOSURE)

Cat No.	Body Weight	Basal Flow	mucus flow velocity, mm/min - during exposure			post-exposure						Per cent Basal Flow
			1	2	3	1	2	3	4	5	10	
	g		minutes									
729	980	15.4	15.8	16.2	14.0	13.6	14.3	14.6	15.4	15.4	15.4	88
730	1100	16.7	15.4	15.0	14.3	14.3	15.0	15.4	15.0	15.0	15.8	86
731	790	11.8	12.5	12.2	12.2	12.8	13.6	13.3	13.0	12.8	12.8	103
732	1210	12.0	12.2	12.0	10.3	10.7	10.9	11.8	11.8	11.8	11.5	86
733	870	14.6	14.3	13.6	---	11.8	11.1	12.2	12.8	12.8	14.0	76
734	1340	13.6	14.6	14.3	12.0	---	12.0	13.6	14.0	14.3	14.0	88
735	920	13.3	13.6	13.0	12.2	12.0	11.8	13.0	13.3	14.0	13.6	89
736	1420	13.0	12.8	13.0	10.7	12.2	12.8	---	12.5	13.0	13.0	82
737	1110	15.8	15.4	15.0	11.5	11.8	12.0	13.0	14.0	15.0	15.0	73
738	910	15.0	13.6	14.3	10.5	---	11.1	11.8	12.2	13.3	13.0	70
			viscosity readings, cs*									
729	980	210	330	---	365	---	-	-	-	300	255	174
730	1100	285	310	---	-	---	-	-	-	275	265	109
731	790	365	360	---	330	---	-	-	-	350	365	-
732	1210	400	410	---	505	---	-	-	-	405	420	126
733	870	290	320	---	-	415	-	-	-	305	320	143
734	1340	325	305	---	365	---	-	-	-	300	320	112
735	920	340	390	---	415	---	-	-	-	345	355	122
736	1420	280	310	---	460	---	-	-	-	305	285	164
737	1110	305	300	---	480	---	-	-	-	325	315	157
738	910	315	320	---	405	---	-	-	-	340	345	127

*See table XII, footnote 2

TABLE XII

EFFECTS OF HUMIDIFIED PURE OXYGEN EXPOSURE ON MUCUS VELOCITY AND VISCOSITY IN CATS (CONTINUOUS 30 MINUTES FACE MASK EXPOSURE)

Cat No.	Body Weight	Basal Flow	mucus flow velocity, mm/min								Per cent Basal Flow
			1	2	3	4	5	10	15	30	
	g		minutes								
739	940	16.7	16.2	16.2	14.3	12.5	10.3	10.5	10.9	10.3	62
740	1170	15.4	15.4	15.4	14.6	14.3	12.2	9.2	9.1	9.4	59
741	1240	13.6	14.3	14.6	13.0	12.2	11.3	8.3	8.8	8.5	61
742	890	12.2	12.8	-	9.2	9.4	28.3	7.5	NF*	6.8	56
743	910	15.4	15.4	15.8	14.3	12.8	10.0	8.8	9.0	9.0	57
744	880	15.0	14.6	14.3	10.5	9.7	10.7	7.9	7.7	7.6	51
745	610	14.6	14.6	14.6	11.3	9.7	7.7	7.6	7.3	7.4	50
746	1120	15.8	16.2	15.4	13.3	12.2	10.7	10.3	10.3	10.5	65
747	960	14.3	14.3	14.3	9.8	-	7.9	8.1	7.9	8.0	55
748	920	13.6	13.6	14.0	10.0	9.8	8.8	7.7	7.7	7.6	56
			viscosity readings, cs**								
739	940	280	295	315	380	-	420	439	440	430	157
740	1170	315	285	300	325	340	495	530	535	520	170
741	1240	385	395	380	375	420	420	515	540	560	145
742	890	370	---	330	415	420	510	540	525	540	146
743	910	265	300	300	---	---	420	500	485	470	189
744	880	285	260	---	---	---	395	---	---	710	249
745	610	400	---	---	---	---	740	---	---	650	185
746	1120	395	---	---	---	---	620	---	---	500	157
747	960	310	---	---	---	---	680	---	---	645	219
748	920	340	---	---	---	---	590	710	---	800	235

*NF = no flow

** cs shown are based on gauss readings taken from a comparison with a standard Newtonian fluid using an electromagnetic probe apparatus, Carson, S., Goldhamer, R.E., and Weinberg, M.S. Characterization Intact Animal, Ann. N.Y. Acad. Sci. 130, 869 (1966).

TABLE XIII

EFFECTS OF HUMIDIFIED PURE OXYGEN EXPOSURE ON MUCUS VELOCITY AND VISCOSITY IN CATS (CONTINUOUS 10 MINUTES FACE MASK EXPOSURE)

Cat No.	Body Weight	Basal Flow	mucus flow velocity, mm/min during exposure						post-exposure		Per cent Basal Flow
			1	2	3	4	5	10	15	30	
	g		minutes								
719	840	15.4	14.6	14.6	13.6	11.1	9.7	8.8	14.0	15.0	57
720	980	17.1	15.8	16.2	15.0	---	10.0	8.1	15.4	14.6	47
721	1105	15.0	15.0	15.0	14.3	13.6	11.3	9.0	13.6	14.6	60
722	1220	16.2	16.2	14.6	14.3	10.7	10.2	7.4	14.3	15.0	46
723	780	13.0	13.6	13.6	11.8	10.0	9.0	7.8	13.0	14.3	60
724	970	13.3	13.6	14.3	10.5	10.5	11.1	7.6	13.6	13.3	57
725	890	12.5	12.8	13.0	11.5	10.0	7.8	6.8	12.2	13.0	54
726	1350	14.3	14.6	14.3	---	12.2	10.3	8.7	14.0	14.6	61
727	1290	15.8	14.0	---	14.0	12.8	12.0	7.9	15.4	13.6	50
728	1110	14.6	13.6	13.6	13.3	12.2	11.1	7.1	12.8	13.6	49
			viscosity readings, cs*								
719	840	295	285	270	305	300	510	595	300	320	202
720	980	360	355	330	430	-	590	845	340	360	235
721	1105	355	370	360	380	370	465	720	405	345	203
722	1220	240	280	270	300	480	600	1140	375	305	475
723	780	400	400	---	---	---	---	700	---	---	175
724	970	345	340	360	500	385	425	740	340	325	214
725	890	275	275	300	460	625	785	855	305	315	311
726	1350	305	300	335	---	675	705	760	340	325	249
727	1290	280	---	---	320	315	290	---	305	290	114
728	1110	300	---	345	335	390	425	870	380	365	290

*See table XII, footnote 2.

The pattern of responses in the cats exposed for 30 minutes (table XII) to pure oxygen did not appear to be quantitatively different from the data obtained in the 10-minute exposure except for approximately 5 cats that showed values below 10 mm per minute in the 4 and 5 minute periods. Despite this diminution, the peak effects likewise occurred late in the exposure period. With respect to the magnitudie of depression, the effect is no more marked at 30 minutes than at 15 minutes except in one animal (No. 742). The viscosity readings in this group of cats showed maximal increases in the 5 to 30 minute period without the consistency apparent in the 10 minute exposure group. The magnitude in the increase of viscosity is generally that seen in the continuous 10 minute group (table XIII) again indicating that the 3-fold increase in exposure time did not enhance the change in mucus flow obtained under these experimental conditions.

Nitrogen dioxide. The results of the acute exposure to nitrogen dioxide (table XIV) at the two graded dosages of 35 and 75 μg per kg per cat, calculated on the basis of known tidal volume and chamber concentration, indicated that the increased concentration of the irritant produced a slightly greater effect than the lower dose. The magnitude of the difference appears graded to the concentration of the irritant.

Other studies in these Laboratories indicate that nitrogen dioxide inhalation at similar concentrations for 72 to 96 hours results in marked pulmonary edema and pathologic changes in the respiratory tract.

The post-exposure changes in viscosity show a trend toward significant difference in the two groups inasmuch as more than 50 per cent of the animals showed values in excess of 500 cs.

TABLE XIV

ACUTE NITROGEN DIOXIDE EXPOSURE ON MUCUS VELOCITY AND VISCOSITY IN CATS

Cat No.	Body Weight, g	Mucus Flow Velocity, mm/min		% Basal Flow	Viscosity, cs	
		pre-exposure	post-exposure		pre-exposure	post-exposure
			75 µg per kg			
943	685	13.0	7.3	56.2	310	510
944	745	15.8	9.4	59.5	240	735
945	1015	12.2	8.6	70.5	345	700
946	1205	12.2	9.4	77.0	295	480
947	975	12.8	7.9	61.7	380	715
948	1085	13.0	7.7	59.2	425	605
949	745	15.4	9.5	61.7	300	640
950	980	15.0	9.1	60.7	365	585
951	870	15.8	11.3	71.5	310	495
952	940	14.3	8.3	58.0	320	600
			35 µg per kg			
952	900	13.6	10.5	77.2	275	510
953	1125	12.8	11.3	88.3	405	435
954	965	12.5	8.9	71.2	310	400
955	805	12.2	11.8	96.7	275	360
956	595	15.0	9.1	60.7	285	415
957	810	14.3	10.9	76.2	275	400
958	1115	11.8	10.3	87.3	350	495
959	1040	13.0	9.8	75.4	315	475
960	765	14.3	11.8	82.5	290	450
961	930	14.3	10.2	71.3	255	480

SUBACUTE EXPOSURE STUDIES

Two major subacute inhalation series were conducted for this program using a continuous exposure system.

Pure oxygen studies. Exposure was maintained at 0.33 atmospheres for a 21-day period in a 3 cubic foot exposure chamber. Due to the unavailability of bypass equipment, the chambers were open one hour during the day for feeding and sanitation purposes, then resealed and exposures reinitiated. Thus, the effective time of contact in the oxygen exposure series involved 23 hours per day for a 21-day period.

Upon cessation of exposure the animals were removed from the chambers and the mucus velocity determined immediately and again one hour later. Where no mucus flow could be measured, NF was recorded. Concurrent viscosity determinations were also performed to provide correlation under similar conditions.

Ozone studies. In this series, cats were continuously exposed for 24 hours per day, in a room 6 x 8 x 8 feet. Ozone was generated with shielded G4511 ozone producing lamp, the circuitory of which is diagrammed below.

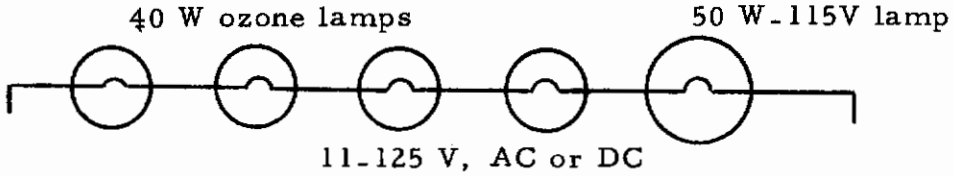

For the purpose of maximizing the exposure to ozone, all animals were caged within 2 feet of the device. A constantly circulating fresh air source was passed across the experimental animals. Sanitation and feeding were carried out in a minimum time period during the exposure. Upon completion of the 14-day exposure period, the cats were removed from the chamber, anesthetized and mucus velocity and viscosity determined as described previously.

Although in the 21-day oxygen exposure series, a 1-hour post-exposure reading was made, it was not done in the ozone series, the extensive mucostasis being sufficiently severe to obviate its necessity. Tissues from these animals were taken in accordance with procedures that are to be described later for biochemical evaluation and for electron microscopic visualization of the subcellular morphology. Animals maintained in these Laboratories without exposure were selected for control biochemical determinations and electron microscopy.

RESULTS

Pure oxygen studies. The results of the 21-day studies with pure oxygen do not reveal adverse physical changes as judged by the body weight of the cats. This is indicative of the good health of the animals since mucostasis and ciliastasis are usually associated with loss in body weight.

Mucus velocity values for these animals are shown in table XV and represent recordings made immediately after the final exposure to oxygen and one hour later. Velocity was markedly altered in all cats, several animals being as low as 50 per cent basal flow, which generally ranges between 13.2 and 15 mm per minute. Mucostasis was found in three cats.

Within one hour after removal of the cats from the chamber, all of the animals had demonstrable flow, except Cat No. 1203, which exhibited some increase in mucus velocity. The three cats with frank mucostasis showed no change. This finding is not considered irreversible since animals with extensive damage have been shown to exhibit normal mucus flow and ciliary frequency following removal from the irritant atmosphere.

In general the viscosity data confirm the changes in mucus flow. The values at one hour are lower than those recorded immediately after cessation except in Cat No. 1215.

The mucus viscosity of the cats with NF readings increased, which confirms unpublished findings with other environmental irritants. However, the changes were of less magnitude than found with material classified as air pollutants. Nevertheless, the change in velocity due to 0.33 atmospheres of pure oxygen over a 21-day period is of intrinsic interest and suggests the need for possible re-evaluation of the use of oxygen as the sole respiratory environmental component in an enclosed system.

Ozone studies. The cats exposed to ozone for 14 days (table XVI) showed frank evidence of respiratory difficulty; and several a slight loss in body weight. At necrospy, patchy edematous areas in the respiratory tract were noted. The tracheal mucosa were thickened and bronchioles appeared congested. These effects were characterized by markedly decreased mucus flow (except in Cat No. 994) and increased viscosities.

TABLE XV

PURE OXYGEN EXPOSURE AT 0.33 ATMOSPHERE[1]
ON MUCUS VELOCITY AND VISCOSITY IN CATS
(21-day exposure)

Cat No.	Body Weight, g		Mucus flow velocity, post-exposure, mm/min		Viscosity, post-exposure, cs	
	Initial	21-day	Immediate	1 hr.	Immediate	1 hr.
1201	860	990	8.7	10.5	425	410
1202	1106	1164	7.1	9.5	730	520
1203	725	940	10.3	10.3	400	440
1204	800	865	8.2	10.0	485	335
1205	740	795	10.2	10.9	390	380
1206	1215	1260	6.8	8.6	650	425
1207	1010	1045	9.4	11.5	415	390
1208	720	820	NF*	NF	690	1100
1209	955	1015	NF	NF	>850	1000
1210	865					
1211	605					
1212	1125	1270	7.3	9.4	620	485
1213	940	980	8.0	9.8	645	600
1214	950	1105	7.8	11.1	700	420
1215	1045	1120	8.8	10.0	580	610
1216	1265	1290	NF	NF	860	950
1217	950	1060	9.5	10.7	505	425
1218	820	915	7.7	9.7	580	435
1219	740	780	7.1	8.4	640	520
1220	1165	1175	7.8	11.1	665	360

*NF = no flow

[1]All readings taken at atmosphere

TABLE XVI

14-DAY OZONE EXPOSURE ON MUCUS VELOCITY AND VISCOSITY IN CATS

Cat No.	Body Weight, g		Velocity, post, exposure, mm/min	Viscosity, cs
	Initial	14-day		
986	565	575	NF*	>850
987	840	860	NF	>850
988	970	950	NF	>850
989	1320	1285	6.8	>850
990	1105	1200	8.8	685
991	1045	1040	NF	>850
992	845	820	NF	>850
993	895	935	NF	>850
994	730	750	15.8	>850
995	920	905	6.1	>850

*NF = no flow

PATHOLOGIC EXAMINATION

Following cessation of exposure to the pulmonary irritant gases, the animals were anesthetized with sodium pentobarbital, exsanguinated and submitted to detailed necropsy. Distribution of tissues was made at this time to provide material for (a) histomorphologic evaluation, (b) biochemical determinations, (c) electron microscopy for subcellular characterization, and (d) for chemical analyses including a variety of parameters. Ten tissues and organs of dogs and cats were examined as follows: liver, thyroid, parathyroid, lymph nodes, spleen, heart, trachea, eye, bone marrow, and kidneys. Subsequently, representative sections of thyroid, lungs and trachea from at least 10 cats per treatment were fixed in buffered formalin, stained with hematoxylin and eosin and examined microscopically.

The findings in three dogs and two cats in the preliminary ozone treatment revealed no significant histopathology. The eyelids of all dogs exposed show varying degrees of acute focal inflammation of the surface skin. The brains in these animals showed moderate generalized congestion. The changes in the lungs included congestion, areas of alternating atelectasis and compensatory emphysema, mild edema as well as evidence of organizing bronchopneumonia, acute bronchitis manifested by inflammatory exudate and moderate peribronchial inflammatory cell infiltration. Similar findings were seen in the cats.

Histomorphologic examinations of the cats exposed to 800 ppm nitrogen dioxide revealed marked changes in the lungs of these animals. Characteristic changes were bronchopneumonia, focal proliferation of bronchiolar and alveolar epithelium with metaplasia, emphysema, alveolar hemorrhage and macrophagic infiltration.

The histomorphologic changes in cats exposed to 5 ppm ozone for 40 or 72 hours were minimal. Of the eight cats that inhaled 5 ppm ozone for 40 hours one had focal atelectasis and a second animal exhibited a focal acute inflammatory reaction in the trachea. Intra-animal variations were found at each exposure period. No pattern of pathologic change was evident in these animals unlike the findings in animals treated with nitrogen dioxide.

One of the two groups of six cats treated with ozone for 72 hours exhibited little or no histologic changes in the respiratory tract while four of six cats in the second group demonstrated mild to marked pathologic changes. One cat in the latter group (No. 0314) had extensive pathology of both the trachea and lungs. The morphologic changes in the remaining cats were much less severe.

Focal chronic inflammatory changes were found in the thyroid glands of both the control cats and those exposed to nitrogen dioxide or ozone. These changes were non-specific.

In several of the dogs exposed to ozone and nitrogen dioxide, photographs were taken of the mucosal surface immediately following extirpation of the trachea. The vascular supply of the normal dog trachea exhibited a symmetrical evenly distributed capillary network. Following 25 minutes exposure to 800 ppm nitrogen dioxide, marked congestion and engorgement of the capillary vessels of the trachea are evident. In contrast, following 24 hour exposure to ozone, the capillaries of the trachea were constricted with evidence of tissue anoxia (fig 8).

Figure 8
Effect of Exposure to Irritant Gases on the Vasculature of Dog Tracheal Tissues

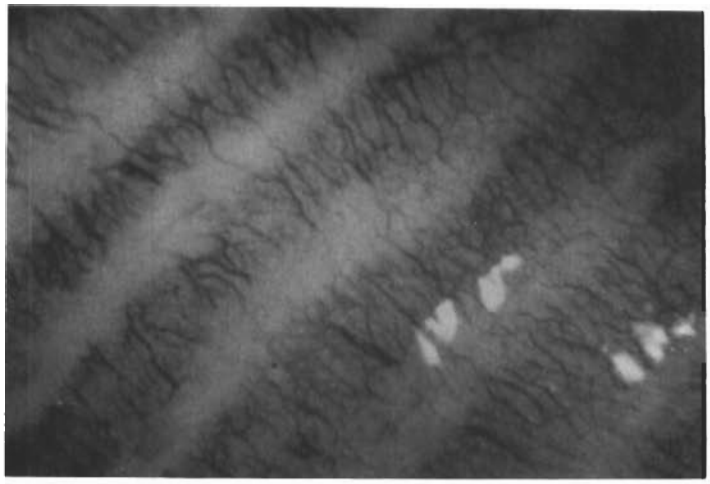

A. Normal

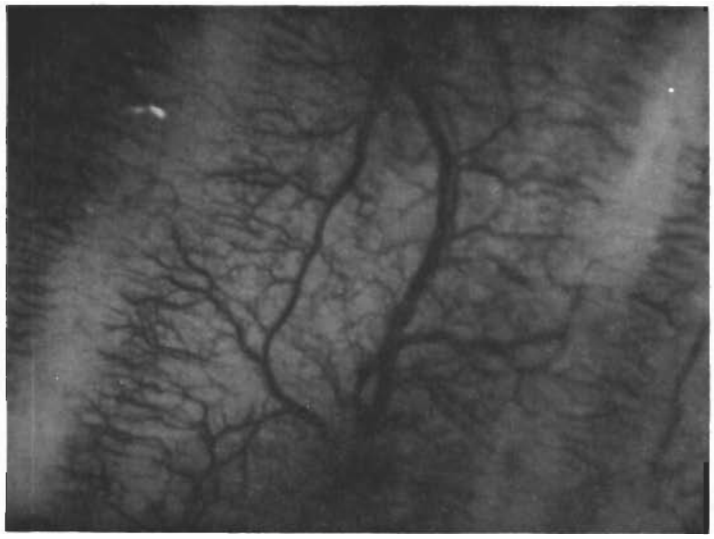

B. 800 ppm nitrogen dioxide

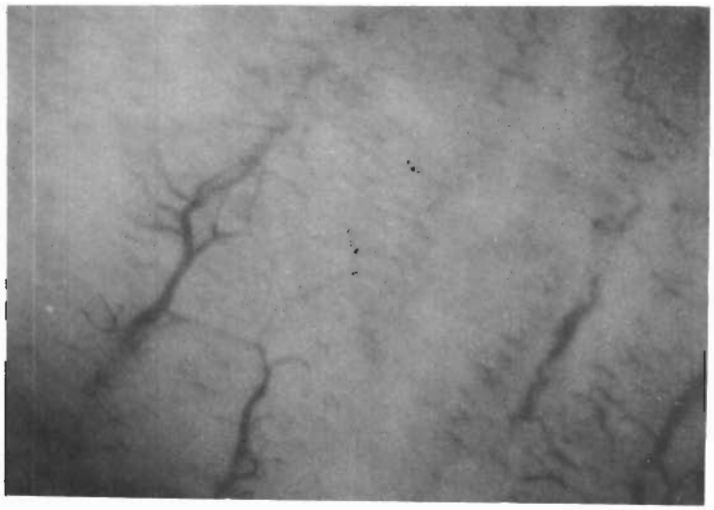

C. 0.5 ppm ozone

ANALYTICAL DETERMINATIONS ON RESPIRATORY TISSUE

It has repeatedly been pointed out that the phenomena associated with exposure to industrial environments; air pollution, and tobacco smoke, viz. changes in mucus flow, ciliary beat, "viscosity", represent the result of interaction of experimental treatment, ambient enviornment and previous clinical history of the host animal. Results provide information as to the effect of treatment deep within the respiratory pathways, rather than on the area of immediate impingement by the irritant.

A number of characteristics of mammalian respiratory tissue were selected for appraisal. Analyses was conducted for total lipid, fatty acids, amino acid and total N, sodium chloride and chloride ion.

LIPID ANALYSIS

On the reasonable assumption of qualitative parallelism with other active metabolic tissues, triglycerides are formed and stored in the trachea, and an alteration in the tissue may be caused by an imbalance of lipid content. Fatty acids and glycerol provide important energy pools as neutral fats or triglycerides, and combined with carbohydrates and phosphate are involved in the tricarboxylic acid cycle and in aerobic glycolysis.

Normal oxidation of fatty acids is relatively complete with degradation taking place by progressive release of two carbon segments in the form of acetyl coenzyme A. A major portion of the degradation occurs in the liver with the formation of acetoacetic acid which is subsequently distributed to peripheral tissues. Under pathologic conditions, accumulation of acetoacetic acid results in ketosis. Though well understood in hepatic metabolism, evaluation of the lipid content and character of tracheal or parenchymal lung tissue or both was undertaken in the effort to correlate possible changes with alterations associated with the energetics of mucociliary activity. Table XVII summarizes the method utilized for extraction and determination of tissue fatty acid content by gas chromatography.

Details of the effects of ozone exposures on tracheal and lung lipid content are described in table XVIII. Normal tracheal tissues taken from pooled or individual unexposed animals ranged from 55.4 mg per g of tissue in the monkey to 286 mg per g in the rabbit. Rat and dog values were 86.5 and 96.75 mg per g, respectively, while cat tracheal tissue appeared to be intermediate, 153.47 mg per g. Lipid content of monkey lung tissue ranged from 83.90 to 96.10 mg per g. Dog lung tissue had a lipid content of 97.10 mg per g.

After exposure to 30 ppm ozone for 96 hours, the pooled trachea from 37 cats reveal a marked decrease in tissue lipid. Similarly a single dog under the same test conditions showed that total lipid fell to 22.00 mg per g.

TABLE XVII
FLOW DIAGRAM FOR LIPID ANALYSIS[1]

tissue

↓

extract with acetone

↓

reduce to dryness (lipids and other acetone-soluble compounds)

↓

extract in hexane-ether-water (discard water phase)

↓

hexane-ether (lipids)

↓

dry over sodium sulfate (contains all major lipid classes)

↓

saponify with ethanol-KOH

↓

acidify with HCl

↓

extract with hexane

↓

esterify with 5% H_2SO_s-methanol*

↓

extract and wash with H_2O

↓

dry over sodium sulfate

↓

reduce in volume to dryness with N_2

↓

add chloroform

↓

gas chromatograph analysis for total fatty acids as methyl esters**

[1]American Oil Chemical Society Methods: * = Ce 2-66; ** = Ce 1-62

TABLE XVIII

EFFECT OF OZONE EXPOSURE ON TOTAL LIPID CONTENT IN TRACHEA AND WHOLE LUNG

Species	Tissue	No. of Pooled Tissues	Treatment	Lipid
				mg/g tissue dry weight
Rat	Trachea	18	Control	86.50
Rabbit		13		286.00
Cat		40		153.47
Dog		4		96.75
Monkey		13		55.40
Dog	Lung	1		97.10
Monkey		1		83.90
		11		96.10
		1		90.20
		1		95.00
Cat	Trachea	37	Ozone, 30 ppm-96 hrs	50.74
Dog	Trachea	1		22.00

The data suggest that under conditions of ozone exposure there is mobilization of lipids. These data require further studies for species differences and for possible effects graded to ozone concentration or duration of exposure. Also no conclusions as to significance of this depression in terms of mucus or tissue quality or quantity can be drawn on the basis of total lipids since the ratio of fatty acid fractions is still unknown. It is possible that the ratios of the fatty acids to each other remains constant and the total is diminished, or, that the ratio is disturbed and the missing fractions affect the total as a result of irritant effects on the tissues.

The fatty acids of mucosal epithelium, underlying subcutaneous tissue, cartilaginous C rings and smooth muscle of untreated monkey, rabbit, and dog trachea were analyzed by gas-liquid chromatography. The tissues were extracted, esterified and analyzed with 20 per cent DEGS on a Chrom "P" column.

The results, shown in table XIX, reveal quantitative variations among the species although the qualitative patterns are similar except for the linoleic acid fraction. These data are of interest with respect to the content and the distribution of carbon chain fractions. The results do not clearly define mucus composition as differentiated from epithelial tissue. Methods for "cleansing" the epithelial layer of mucus and quantitative separation from the underlying cartilage are not yet available. They in-

TABLE XIX

FATTY ACID COMPOSITION IN MAMMALIAN TRACHEA LIPIDS[1]

Fatty Acid-Methyl Ester	Monkey Trachea	Rabbit Trachea (pooled)	Dog Trachea
C10 capric	---	---	---
C12 lauric	---	0.3	---
C12 lauroleic	---	0.1	---
C14 myristic	1.7	4.7	3.1
C14 pentadecanoic[2]	---	1.0	---
C14[2]	---	0.4	---
C16 palmitic	25.8	45.0	33.5
C16 palmitoleic	3.4	5.9	8.2
C16[2]	---	1.6	---
C18 stearic	13.2	9.8	11.2
C18 oleic	39.8	30.2	34.2
C18 linoleic	16.1	0.1	9.8
	100%	100%	100%

[1]Extracted, esterified, and analyses performed by gas chromatography. Area normalization procedure used for calculations.

[2]Not clearly identified.

dicate the presence of cartilaginous protein as well as of epithelial tissue and blood. However further analyses of tracheal tissue should be conducted to permit more definitive interpretation.

The amino acid composition of an untreated dog trachea was determined after HCl hydrolysis by means of the Technicon amino acid analyzer.

The results are shown in table XX. Recovery was not complete with 84.88 per cent being accounted for. The ratio of aspartic acid and glutamic acid to the other components may be indicative of a relative content of free or bound substrate for enzymologic reactions. The lysine content is difficult to explain, but is often associated with tissue repair in relation to protein quality.

Concurrent determinations of Kjeldahl Nitrogen content from seven dogs is provided in table XXI and indicates good agreement between animals either as nitrogen or as the calculated protein (N x 6.25).

NaCl concentrations were determined in tracheal tissues. Comparison of electrolyte concentrations were made between normal cats and cats treated with 5 ppm of ozone for 72 and 96 hours, or treated with 1700 ppm of NO_2 for 15 minutes. For these determinations the tracheae of groups were pooled.

The results of these electrolyte analyses are shown in table XXII. The level of biological significance to apply to these data are as yet indeterminant, however a pattern of diminution in concentration is suggested. The question of its relationship to an inflammatory edematous response is speculative, yet some suggestion of correlation with edema is warranted.

TABLE XX

AMINO ACID* COMPOSITION OF DOG TRACHEA

Amino Acid	Calculated Protein**
	per cent
Aspartic Acid	14.27
Threonine + Serine	2.77
Glutamic Acid	12.82
Proline	22.22
Glycine + Alanine	1.35
Valine + 1/2 Cystine	0.67
Methionine	7.32
Isoleucine	0.19
Leucine	0.25
Tyrosine	0.28
Phenylalanine	0.57
Ammonia	0.90
Lysine	11.60
Histidine	2.09
Arginine	7.58

*after HCl hydrolysis

**Protein calculation = N x 6.25

TABLE XXI

KJELDAHL N DETERMINATIONS IN DOG TRACHEA

Dog No.	Per Cent N	Calculated Protein*
		per cent
10	8.03	50.18
7	8.04	50.15
14	8.11	50.68
8	8.57	53.56
13	8.79	54.93
22	8.95	55.70
17	8.74	54.62

*Protein calculation = N x 6.25

TABLE XXII

ELECTROLYTE CONTENT OF POOLED TRACHEAL TISSUE OF CATS

Treatment	No. of Animals	Findings	
		% NaCl	Cl^-, ppm
None	11	0.414	2.488
Ozone, 5 ppm-96 hrs	7	0.308	1.848
None	10	0.456	2.734
	11	0.455	---
Ozone, 5 ppm-72 hrs	11	0.409	2.457
	7	0.341	---
None	6	0.335	2.013
NO_2, 1700 ppm-15 min	8	0.308	1.848

SECTION III

BIOCHEMICAL STUDIES

The investigation has revealed that although the mucociliary apparatus is an integrated physiological function, experimentally induced mucostasis can be established without apparent change in ciliary activity.

The capacity of the ciliated epithelium to continue to function under normal conditions against the gradient of rheologic changes in the overlying mucus demands a system of high energy requirements involving the oxidative metabolism of the ciliated cells.

These investigations have at every turn been concerned with mammalian tissue and the biochemical studies of an invertebrate system were not included. Instead the irritant exposures were programmed to provide tissues for simultaneous biochemical, chemical, and electron microscopic examination.

In selecting the systems for appraisal, consideration focused on pathways and procedures described by many workers as bearing on the effect of the irritants on subcellular entities and tissue function. Because of the limitations imposed by the availability of amounts of tissue and the oxidative pathways and enzymes localized in the mitochondria.

PROCEDURE

In the initial study, classical manometic procedures for determining possible uncoupling of oxidative phosphorylation were examined.

Healthy young cats (500-1500 g body weight) were observed for in vivo mucus flow. Those which had flow rates between 17.2 and 12.0 cm per minute were sacrificed by overdosage of pentobarbital sodium, pieces of ciliated epithelium (cm^2) carefully excised and placed in shallow covered dishes containing physiologic saline or diluted DNP*. Examination of ciliary viability was made using a Strobotac-Strobolume Illuminator. An arbitrary scoring scale for viability was chosen due to the difficulty of characterizing precise beat frequency viz., normal beat, slow beat, and cessation of beat. The tissue strips were then incubated to DNP or saline for 10 minutes, followed by transfer to Warburg flasks containing 2.5 ml of saline, and oxygen uptake determined at 20 °C.

*2, 4 dinitrophenol sodium

RESULTS

The results are shown in table XXIII. Saline immersion did not affect ciliary viability nor oxygen consumption. Concentrations of DNP between 2.3×10^{-7}m - 1.5×10^{-4}m caused little or no change in ciliary motility nor in oxide uptake. At 2.3×10^{-4}m, ciliary beat was irregular and sluggish with increased oxygen uptake (171 per cent of normal). Increasing the concentration to 1.3×10^{-3} and 2.3×10^{-3} caused ciliastasis with oxygen consumption values of 169 and 152 per cent, respectively,

In this series of experiments, DNP induced changes in oxygen uptake and the effect on ciliary beat inhibition appear to be directly related. The results which indicated a trend toward alteration in pure oxygen uptake were however not highly significant and the methodology was cumbersome. Polarographic procedures were substituted to obviate some of the limitations on tissue sample and time required for the procedure.

POLAROGRAPH STUDIES

Mitochondria are the site of conversion of respiratory energy into phosphate bond to mechanico-chemical and finally to osmotic energy. The nature of this respiratory chain is a sequential multi-enzyme system for the acceptance of electrons from oxidized and reduced forms of nicotinamide adenine dinucleotide, dehydrogenase, and the fatty acid oxidation cycle. The 3 major components are the pyridine-linked dehydrogenase, the flavoproteins, and the cytochromes.

The basic concept involves the electron carriers arranged in a linkage of increasing oxidation-reduction potentials with the flow of electrons moving from electronegative substrates via pyridine nucleotides and flavoproteins to the electropositive cytochromes and then to oxygen. Inhibition of mitochondrial enzymes would be expected to interfere with the respiratory chain and decrease cellular efficiency. Succinic dehydrogenase, cytochrome reductase, and cytochrome oxidase were chosen for their importance in cellular function.

PROCEDURE

Groups of 15 healthy young cats (500 to 1500 g body weight) were exposed to high levels of ozone (>10ppm) or to nitrogen dioxide (80 ppm). The animals were killed by overdosage of pentobarbital sodium, the tracheae excised and the ciliated epithelium stripped from the cartilage and muscle of the trachea. The strips were pooled on cold saline-moistened filter paper.

TABLE XXIII

OXYGEN UPTAKE AND CILIARY MOTILITY IN THE EXCISED CAT TRACHEA AFTER INCUBATION WITH DNP*

No. of Runs	Ciliary Motility	Oxygen Uptake	DNP
		per cent	moles
16	Normal	100	---
4	Normal	97	2.3×10^{-7}
4	Normal	96	2.3×10^{-6}
4	Normal	107	2.3×10^{-5}
8	Normal	114	1.5×10^{-4}
8	Slow	171	2.3×10^{-4}
8	Cessation	169	1.3×10^{-3}
8	Cessation	152	2.3×10^{-3}

*2, 4, dinitrophenol sodium

Strips of cat tracheal epithelium were washed from the filter paper with 4.0 ml of 0.1 M Tris-HCl, 0.1 mM EDTA, 0.25M sucrose buffer, pH 7.5-7.6. The tissue was homogenized with a Potter-Elvehjem homogenizer. The plunger was passed four times through the tissue. The homogenate was centrifuged twice at a speed of 2000 g in a refrigerated centrifuge for five minutes, sedimenting cell debris and nuclei.

The precipitate was discarded and 0.2 to 0.5 ml of the supernatant used for the succinic dehydrogenase assay. In the cytochrome oxidase and reductase assays 0.2 ml was used.

All steps were done in a cold room with cold buffer and glassware.

SUCCINIC DEHYDROGENASE ASSAY

The measurement of succinic dehydrogenase activity was based on the rapid oxidation of reduced flavin adenine nucleotide by phenazine ethosulfate* and subsequent reoxidation of the reduced salt by oxygen. In these studies, 5.0 mM KCN was present in order to inhibit any cytochrome oxidase present and permit transfer of electrons from $FADH_2$ to oxygen via the phenazinum salt. The reaction was followed by measuring the rate of disappearance of pure oxygen dissolved in the reaction mixture (fig 9). The reaction mixture used for this assay is outlined in table XXIV.

MEASUREMENT OF OXYGEN UPTAKE

Oxygen uptake was measured at 25°C with a Clark O_2-electrode** polarized at -0.8 volt. The electrode was adapted to fit a plexiglass reaction chamber, 2 ml capacity, equipped with a magnetic stirrer and connected to a Varian Model G-14 graphic recorder. The final reaction mixture volume was 2.0 ml, 3 to 4 minutes were required for temperature equilibration. The succinic dehydrogenase assay was initiated by the addition of 0.001 M phenazine ethosulfate (0.2 ml) through an aperture in the glass cover of the chamber.

SUCCINATE-CYTOCHROME C REDUCTASE SYSTEM

The succinate-cytochrome c reductase system was measured. This reaction was followed by the appearance of 550 mμ absorbancy of reduced cytochrome c over a period of 4 to 5 minutes at 25°C (19). See table XXV for the reaction mixture used.

---

* Nutritional Biochemical Corporation, Cleveland, Ohio

** Yellow Springs Instrument Co., Yellow Springs, Ohio

Figure 9. Measurement of succinic dehydrogenase activity. Three to four minutes were allowed for temperature equilibration. The recorder speed was reduced and 0.001 M phenazine ethyl sulfate added to the well (0.2 ml) through an aperture in the glass cover of the chamber.

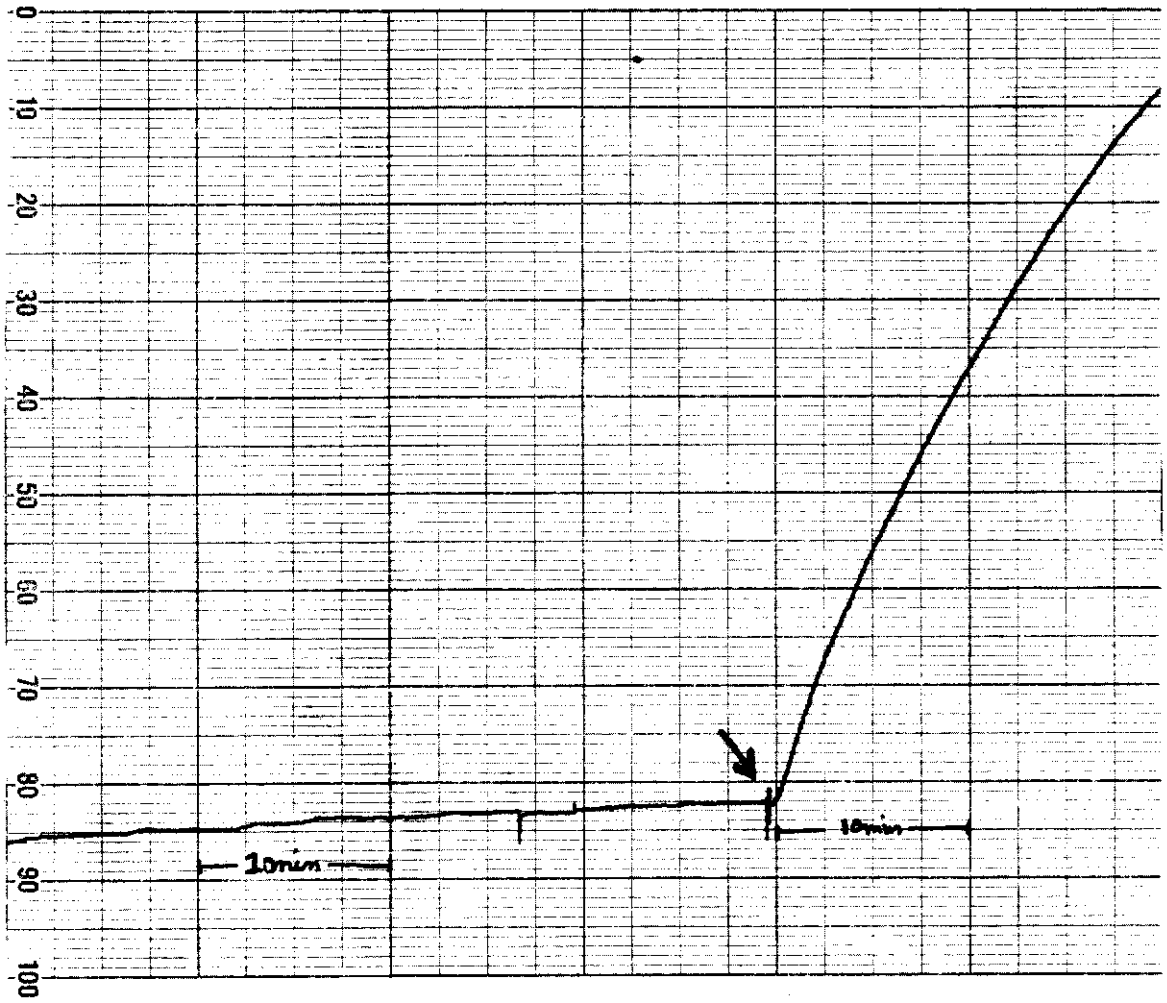

TABLE XXIV

SUCCINIC DEHYDROGENASE ASSAY

Final Concn.	Ml Used	Substance Added
0.006 M	0.06	$CaCl_2 \cdot 2\ H_2O$ (0.1 M)
0.005 M	0.1	KCN (0.05 M) 0.1 M Tris-HCl buffer, pH 8.0
	2.0	with 0.25 M Sucrose added
0.04 M	0.2	Na_2 Succinate
	0.5	Supernatant
0.001 M	0.2	Phenazine Ethosulfate (added to the well after the above reaction mixture has incubated for 3-4 minutes)

This assay was done at 37°C. See reference 1 for preparation of 0.1 M Tris-HCl buffer.

TABLE XXV

SUCCINATE-CYTOCHROME C REDUCTASE ASSAY

Final Concn.	Ml Used	Substance Added
	2.4	Na Phosphate Buffer (0.1 mM) pH 7.5[1]
2-3 x 10^{-5} M	0.1	Oxidized cytochrome c (1 %)[2]
0.005 M	0.1	KCN (0.05 M)
0.006 M	0.06	$CaCl_2 \cdot 2\ H_2O$ (0.1 M)
	0.2	Supernatant
0.04 M	0.2	Na_2 Succinate

The blank lacks cytochrome c. The reaction is started by the addition of succinate and the experimental tubes compared to a tube lacking sodium succinate. The experimental tubes are allowed to stand for five minutes before the succinate is added and the zero reading taken. Reaction is followed by the appearance of the 550 mμ absorbancy of reduced cytochrome c over a period of 0-5 minutes at 25°C.

[1]See reference 1 for the preparation of this buffer.

[2]See reference 7 for the preparation of oxidized cytochrome c. Type III horse heart cytochrome c was obtained from Sigma Chemical Co., St. Louis, Mo. Molecular weight assumed to be 14,000. Solution and stock crystals were stored in the freezer.

CYTOCHROME C OXIDASE

The cytochrome c oxidase activity was observed. This reaction was followed by observing the disappearance of the absorbancy of reduced cytochrome c at 550 mμ due to its oxidation over a period of 0 to 5 minutes (19). See table XXVI for the reaction mixture used.

PROTEIN DETERMINATION

The protein present in the homogenates was measured by ultraviolet spectrophotometry (20). This method was chosen for its sensitivity rather than the biuret or Folin-Wu methods. Each determination was processed against a balanced pooled sample of tissue from sham exposed normal cats. Final spectrophotometric determinations were performed on a Process and Instruments Split Beam Spectrophotometer.

RESULTS

The data shown in table XXVII are based on the presence of 1 mg of protein in the supernatant and are each composites of three runs of 15 animals each performed on separate days.

Exposure to ozone resulted in significant inhibition of the respiratory enzymes under investigation. Succinic dehydrogenase, cytochrome reductase and cytochrome oxidase were inhibited to the extent of 50, 31, and 10 per cent respectively.

Exposure to nitrogen dioxide caused 30 per cent inhibition of succinic dehydrogenase, 20 per cent inhibition of cytochrome reductase, and 0 per cent inhibition of cytochrome oxidase.

DISCUSSION

The complexes of electron carriers in the electron transport system of tissue respiration are shown below:

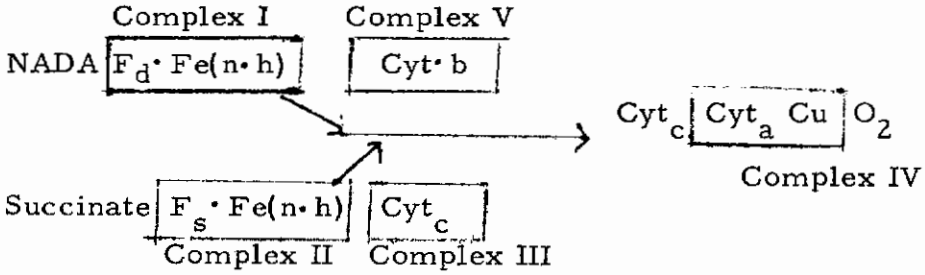

F_d = NADH dehydrogenase
F_s = succinic dehydrogenase
$Fe(n \cdot h)$ = non-heme iron

Interference either in formation or disassociation of these complexes can be expected to alter electron transport and oxidative phosphorylation thereby reducing cellular activity.

TABLE XXVI

CYTOCHROME C OXIDASE ASSAY

Final Concn.	Ml Added	Substance Added
	2.6	Na_2 Phosphate Buffer (0.1 M) pH 7.5
$2\text{-}3 \times 10^{-5}$ M	0.1	Reduced cytochrome c (1 %)[1]
0.006 M	0.06	$CaCl_2 \cdot 2H_2O$ (0.1 M)
	0.2	Supernatant

The blank lacks reduced cytochrome c. The reaction is initiated by the addition of the cytochrome c to the sample tube. The disappearance of the absorbance at 550 mμ due to oxidation of reduced cytochrome c is followed over a period of 0-5 minutes, and a final reading is taken after the addition of a drop of ferricyanide to totally oxidize the cytochrome c.

[1] See reference 8 for the preparation of reduced cytochrome c. These experiments were done at 25°C. See footnote 2 of Table 2.

TABLE XXVII

EFFECTS OF OZONE AND NO_2 ON MITOCHONDRIAL ENZYMES

Irritant	Succinic Dehydrogenase Inhibition	Cytochrome Reductase Inhibition	Cytochrome Oxidase Inhibition
	per cent		
Ozone	50 (40-60)	31 (30-35)	10 (5-15)
Nitrogen Dioxide	30 (20-40)	20 (18-23)	0 (0)

Succinic dehydrogenase activity should be related to cytochrome reductase because cytochrome reductase is the series of enzymes which run from succinic dehydrogenase through cytochrome c. Cytochrome oxidase is the terminal portion of the transfer chain and may not be related to the other two.

ELECTRON MICROSCOPY

As pointed out previously, the subcellular events that either regulate or are concerned with alterations in physical properties of mucus and which govern energy requirements related to ciliary function are critical factors in studying the mucociliary apparatus. Analyses of tissue samples were made to provide direction for correlating cellular ultrastructure with energy-requiring biochemical processes.

Data correlating the effects of drugs and enzyme function on mitochondria, lysosomes, and smooth and rough endoplasmic reticulum, have largely been limited to active metabolic organs such as the liver and kidney. Little emphasis has been placed on lung parenchyma and the specialized epithelial tissue lining of the trachea and bronchi.

Preliminary electron micrography of the trachea of cats exposed to ozone, 0.5 ppm levels of exposure, had revealed engorged capillaries, lipid vacuoles in the endothelial lining cells with swelling and large vacuoles in the overlying cells.

In the light of the effects on the enzymes, the absence of mitochondrial changes suggested that these were within limits which do not involve disruption or swelling of mitochondria. More intensive follow-up of a dosage range to determine these limits was done.

The results of intensive examinations of multiple specimens of representative animals exposed to ozone and NO_2 are shown on pages 82-127.

Ozone

The interpretation of whole lung sections reveal changes in the cytoplasm of the cell which were characterized by loss of electron density and numerous vacuoles as well as clustering of lysosomes. Although these are significant degenerative changes they do not appear to primarily involve the mitochondria. These alterations may indicate the advisability of reviewing enzymes related to protein formation and microsomal activity as a result of ozone exposure.

Review of the epithelial sections of several animals that had been exposed to ozone for 72 hours reveal a number of changes characterized in large part by superficial degeneration of the epithelium and a moderate degree of monocyte infiltration. These degenerative changes are somewhat variable from cell to cell but appear to include the presence of numerous vacuoles, numbers of lysosomes and an unusual increase in endoplasmic reticulum. The mononuclear cell infiltration has been described previously with other materials.

Ozone apparently precipitated the development of considerable cell damage which, though patchy, is characterized by marked edema, vesicle formation, loss of electron density and lysosome clusters. These lysosomes appear generally to be in relationship to the nucleus and are also associated with autophagic vacuoles. When the results obtained in these sections are compared with the results from blocks of whole tissue of cats exposed to NO_2, the superficial epithelial cells in the latter show a number of changes which are characterized by diffuse vacuolization, the development of numerous myelin figures and relatively large numbers of lysosomal bodies. The deeper cells show considerably less changes than those seen in the superficial areas. The intercellular organelles are normal and the cilia are normal.

Examination of the alveoli reveals that in large sections the lining is normal, basement membrane is of uniform thickness and the electron density of underlying septal cells though showing numerous small vacuoles may be pynocytotic in size. They are separated by the usual basement membrane. In some an increase in the amount of collagen is noted, although other than this, the sections appear to be normal. In other sections a somewhat engorged capillary filled with red cells has been seen with the pynocytotic vesicles. Supporting structures do not show any remarkable changes.

Nitrogen Dioxide (NO_2)

The NO_2 exposed animals on the other hand show less marked change and of a diffuse type. These changes are characterized by the development of numerous cytoplasmic vacuoles and numbers of myelin figures.

The epithelial strips of the NO_2 exposed animals show an occasional alteration in electron density or clusters of mononuclear cells. They are in large part characterized by prominent interdigitation which may be widely separated by an increase in intercellular space. Cilia appear to be normal although vacuoles are present. Occasional edema and myelin figures that were previously described above are seen. Mitochondria and nuclei do not appear to show any alterations in structure.

In summary the electron microscopic evaluation of whole blocks of lung tissue, epithelial strips or in some cases alveoli, fail to reveal any serious morphological alterations, although the indications of modifications in electron density, the increased lysosomal structure or clusters thereof, edema, and the occasional interdigitation reveal evidence of some effects. However the structures are characterized by the maintenance of the integrity of the mitochondrial elements. In view of the apparent slight modification in oxygen dependent enzyme function, the degree and intensity of the insult with ozone and NO_2 appear to be of lesser quantitative nature than would cause alteration in mitochondrial morphology. This is apparently indicative of reversible change and suggests that either longer exposure or higher levels of exposure may be required to produce sub-microscopic pathology at the biochemical and tissue level.

The swelling of the endoplasmic reticulum that is noted in many sections in both the ozone and NO_2 treated tissue and the lysosomal effects suggest that enzyme induction of drug metabolizing capacity has occurred at several levels of organization and may include protein formation and microsomal activity. Because the ozone and NO_2 are considered to be non-specific with respect to enzyme induction attention should be given to a spectrum of enzymes including highly specific as well as general classes that would be responsible for a variety of metabolic effects.

EPITHELIAL STRIPS FROM A CAT EXPOSED TO 0.5 ppm OZONE FOR 72 HOURS

Sample No. 1

1. Superficial cells show a number of interesting changes. There appears to be marked intercellular separation and interdigitations become exceedingly apparent. Within the upper portion of the cell there is an increase of lysosomes and an occasional vacuole. There is also an increased proliferation of the endoplasmic reticulum. Basal portions of the cells also show separation from basement membrane or collagen.

2. Other sections from basal portions clearly demonstrate an increase in cell interdigitations at the base, some vacuolization and swelling of a number of mesenchymal cells within supporting tissues.

3. Epithelial cells are again clearly demonstrative of the separation between the cells and increased prominence of interdigitation. Within the cells there are small vacuoles and increased number of lysosomes. Increased intercellular separation and interdigitation is present even at the base of the cell.

Sample No. 2

1. Portions of the lining on a number of sites appear normal. The basement membrane is uniform in thickness and electron density. Underlying septal cells show numerous small vacuoles which are almost pynocytotic in size. Cells are separated by the usual basement membrane.

2. These sections of alveoli show a normal pattern. The capillaries are filled by portions of red cells. The pynocytotic vesicles within the cytoplasm of the capillaries are readily apparent. Septal cells are not remarkable.

3. Alveolar walls are noted and significant changes described above are present.

Sample No. 3

1. Sections of alveoli are from areas where there is an increase in the amount of collagen. Other than this the sections appear to be within normal limits.

2. Other sections are those of supporting mesenchymal tissue with fibroblasts and abundant collagen readily apparent.

3. Within the alveolar wall there appears to be an engorged capillary filled with red cells. The walls show a number of pynocytotic vesicles. Supporting structures are not remarkable.

Sample No. 7

1. Sections of tracheal cells show evidence of loss of electron density. In general there is an accumulation of lysosomes and some myelin figures. Mitochondria are scattered but appear to be of normal outline. Within the cells there are prominent Golgi apparatus. The microvilli are not remarkable.

2. Areas of extreme degeneration with marked loss of electron density are seen. An increase in the number of lysosomes is present. These changes are believed to be real since adjacent epithelial cells show a relatively small amount of vacuolization with normal intact nuclei.

3. Electron micrograph demonstrates degenerated cells to the right and an essentially normal cell to the left. Findings are similar to those described previously.

4. Very pale degenerated cells are seen in the center of a cluster of normal cells. Normal appearing cells show occasional vacuoles, a few lysosomes and possibly an increase in endoplasmic reticulum.

5. In the deeper cells there is an increase in the interstitial space as described in Sample No. 1.

6. Areas of degenerated cells adjacent to essentially normal appearing cells are again observed. It is noteworthy that degenerated changes appear to primarily involve cytoplasm of the cell with nucleus apparently relatively intact.

7. Changes are again similar to those described previously for Sample No. 1.

8. Number of different cilia are seen some of which resemble a tree-rack. Mitochondria appear normal but there are a number of vacuoles and increased lysosomes.

9. Electron micrograph demonstrates changes previously observed.

Sample No. 27

1. Marked intercellular separation with tremendous apparent increase in interdigitation is seen. Individual cells have large nuclei. Relatively few organelles are seen within residual cytoplasm.

2. In the deepest portions of the supporting structure, there are a number of capillaries, collagen fibers, segments of nerve, all of which show an essentially normal pattern.

3. Large cells showing marked separation with large crenated nuclei centrally located. Within the cytoplasm of these cells, a moderate amount of Golgi apparatus is noted. Adjacent to this, there are other degenerated epithelial cells which are more difficultly characterized.

4. Superficial epithelial cells show the presence of cytoplasmic vacuoles. The mitochrondria appear normal. There may be some increase in endoplasmic reticulum.

5. Cluster of monocytes are seen many of which have cytoplasmic vacuoles, numerous lysosomes and small numbers of mitochondria.

Sample No. 55

1. Sections show columnar cells to be normally disposed. Beneath the nucleus are numerous lysosomes. At the right side of the photograph is a degenerated cell characterized by the development of vesicles, loss of clarity, increased number of lysosomes and other smudgy appearance.

2. In this section is a cell with marked swelling and associated electron lucidity. Adjacent to this is a sharp increase of lysosomes.

3. The bronchoepithelium is clearly identified and cilia noted. Beneath the intact cilia, epithelial cells show considerable degeneration. Adjacent to the cell another large pale epithelium was noted with clusters of electron dense lysosomes and an autophagic vesicle.

4. Electron micrograph show normal cilia. The mitochondria occur in clusters in the upper one-third of the cell. Adjacent to the nucleus are clusters of lysosomes and numbers of autophagic vesicles. Degenerated cells are also noted in which there are several alterations.

5. A high power section of superficial portions show marked loss of electron density, swelling, vacuolization, pallor and other degenerated changes within the epithelial cell. These changes occur in spite of essentially normal appearing cilia.

Photographs of the aforementioned samples follow.

Code for Photographs

N = nucleus
IS = intercellular space
BM = basement membrane
RET = reticulum
C = cilia
M = mitochondria
V = vacuoles
LY = lysosomes
GC = goblet cell
MY = myelin
ER = endoplasmic reticulum
GO = golgi
COL = collagen
CAP = capillary
RBC = red blood cell
AL = alveolus
DB = dense bodies

Sample No. 1

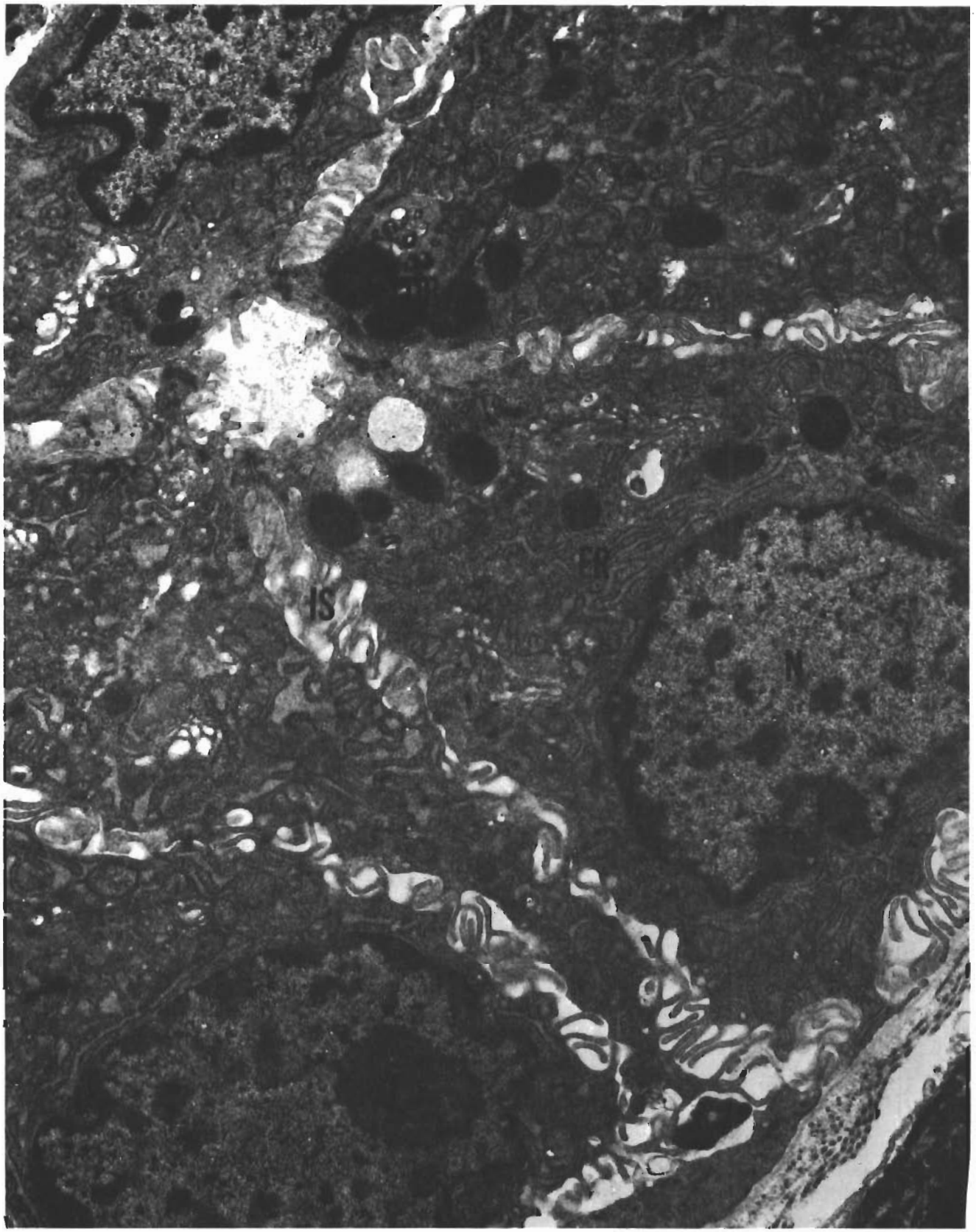

Sample No. 1

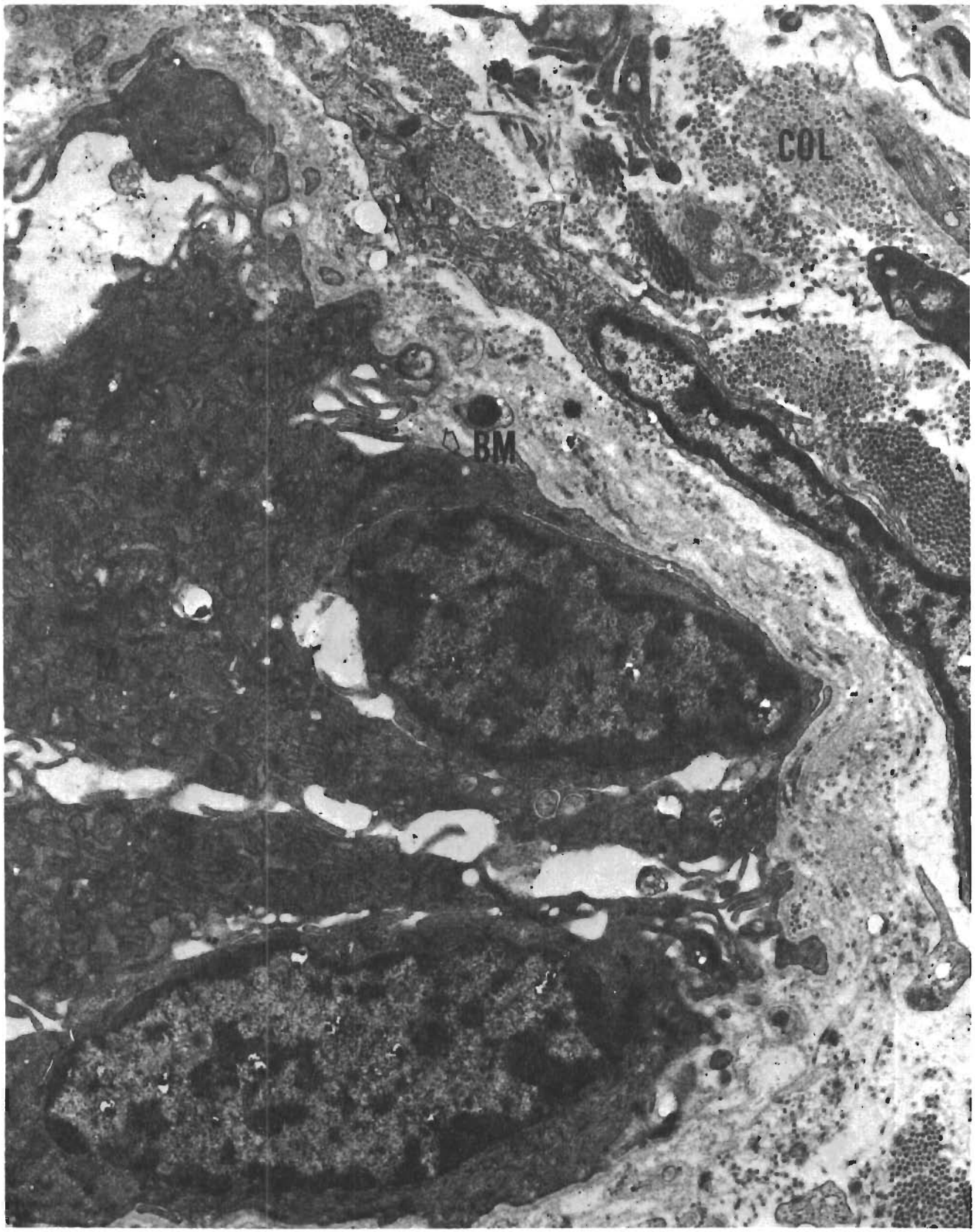

Sample No. 1

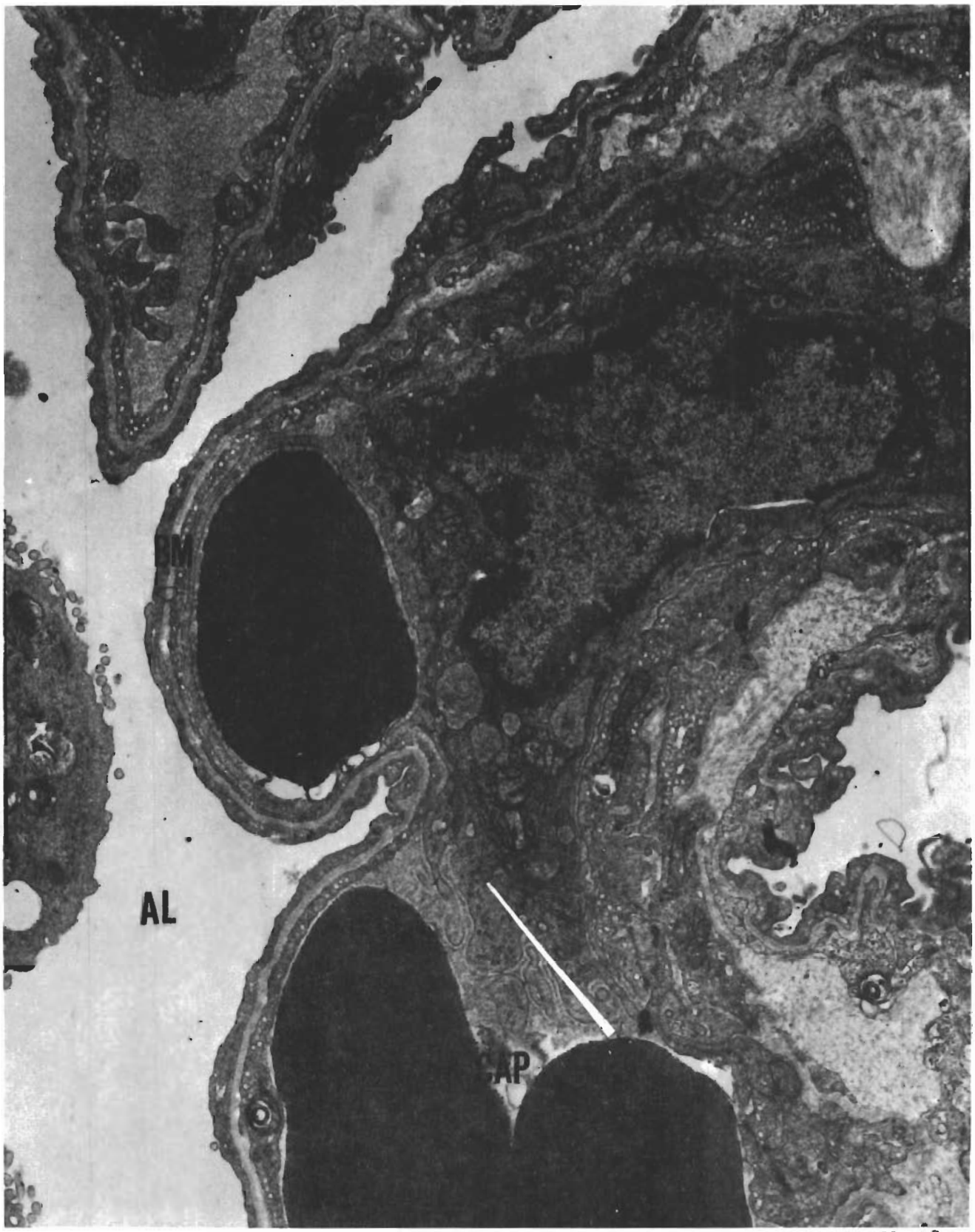

Sample No. 2

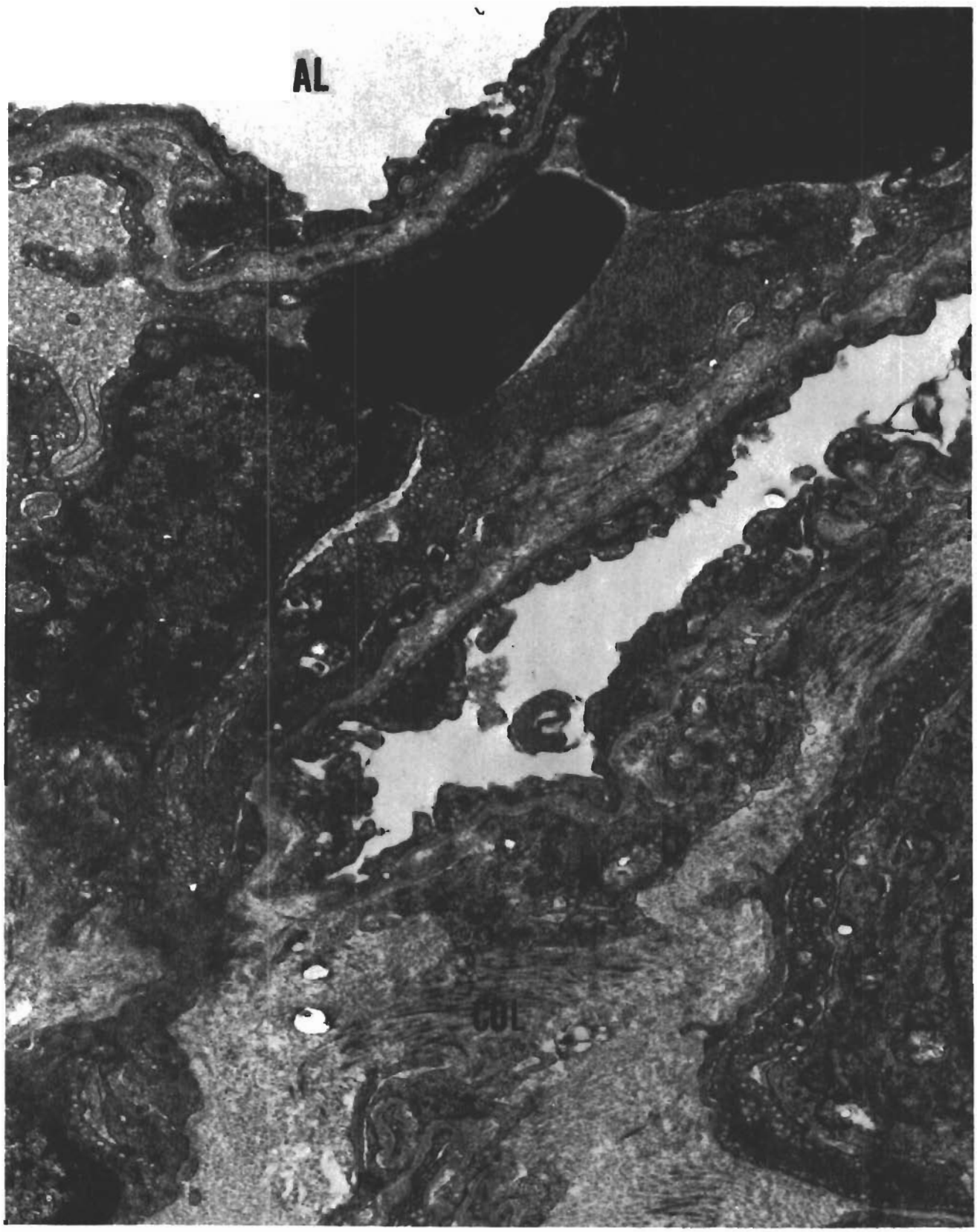

Sample No. 2

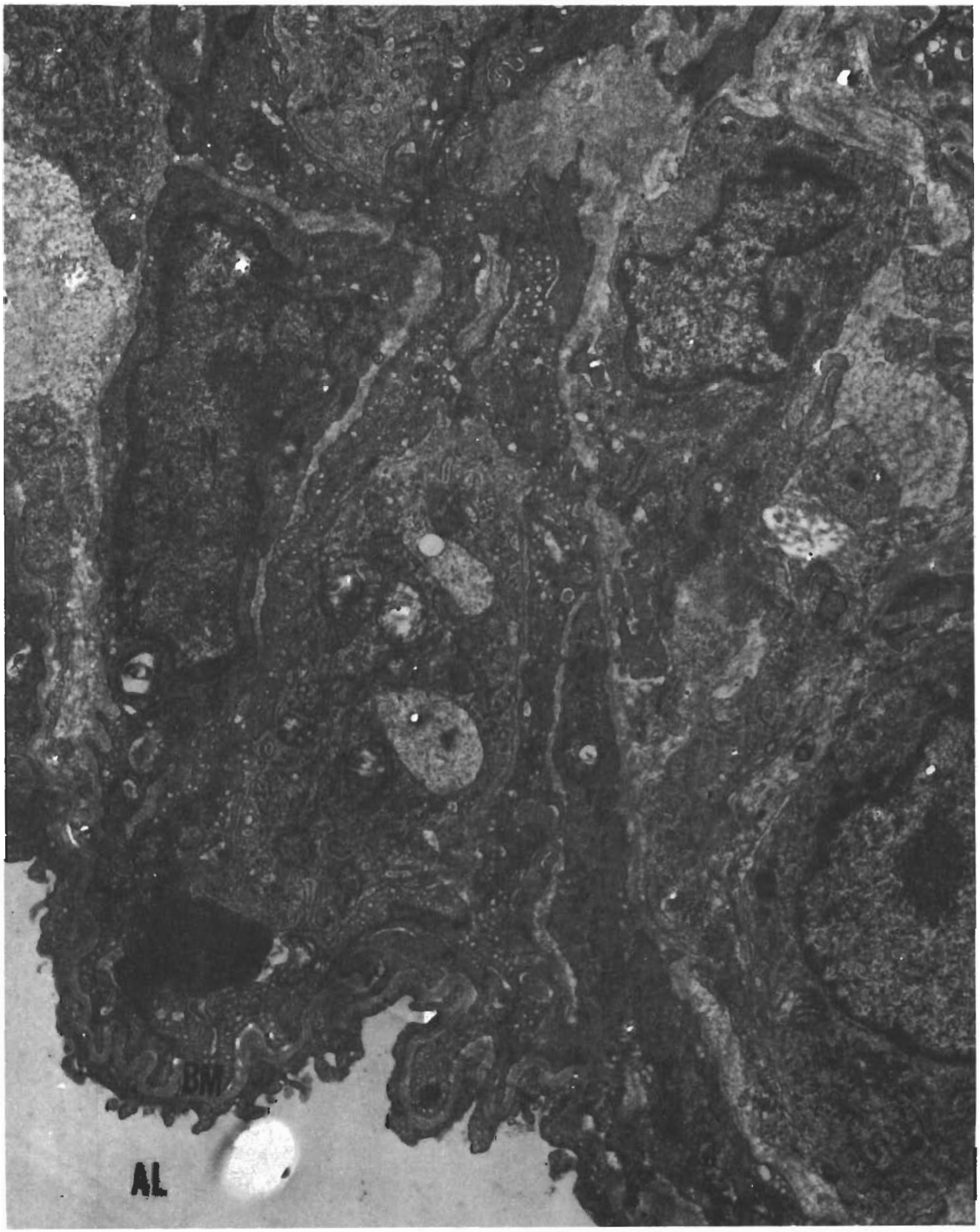

Sample No. 2

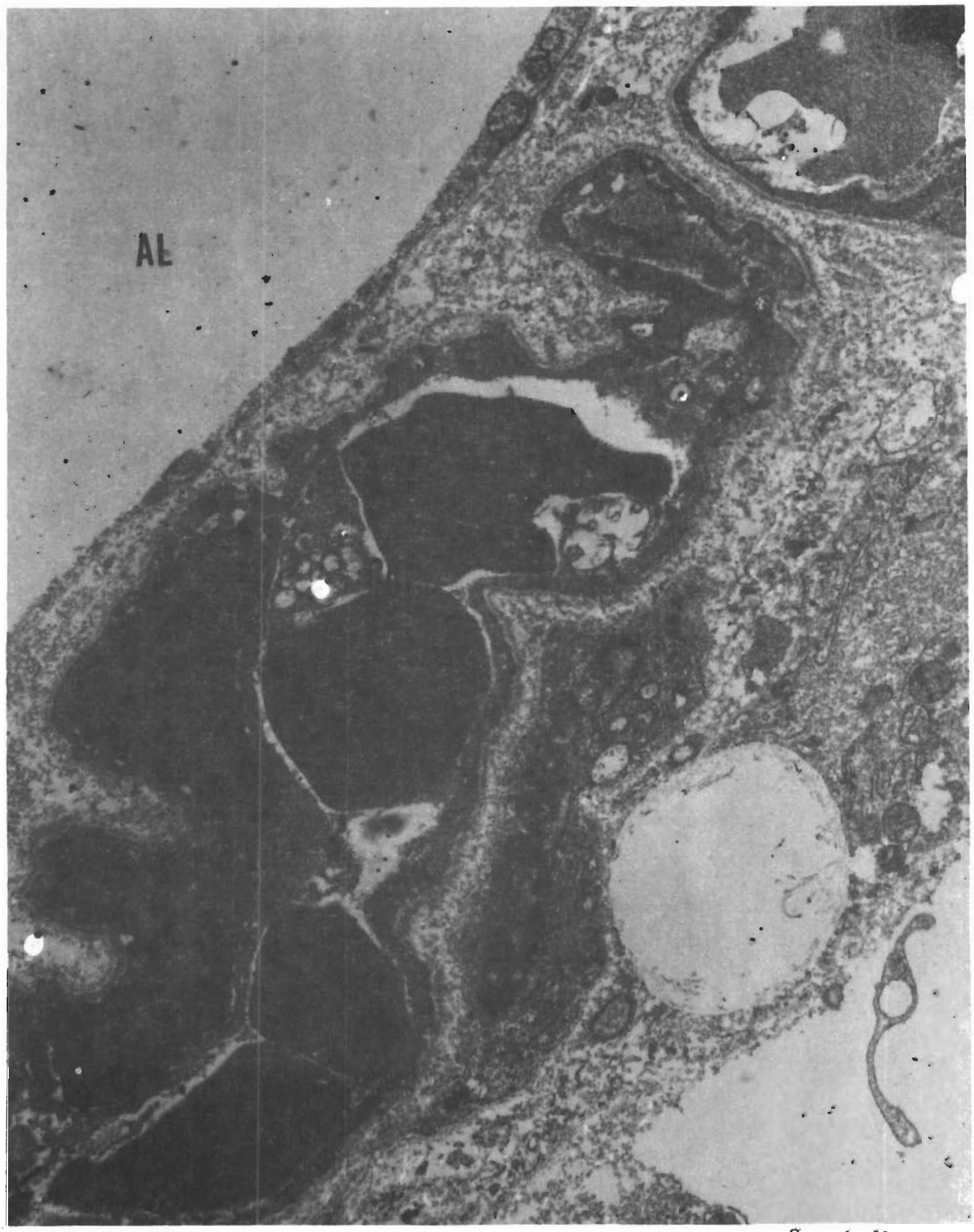

Sample No. 3

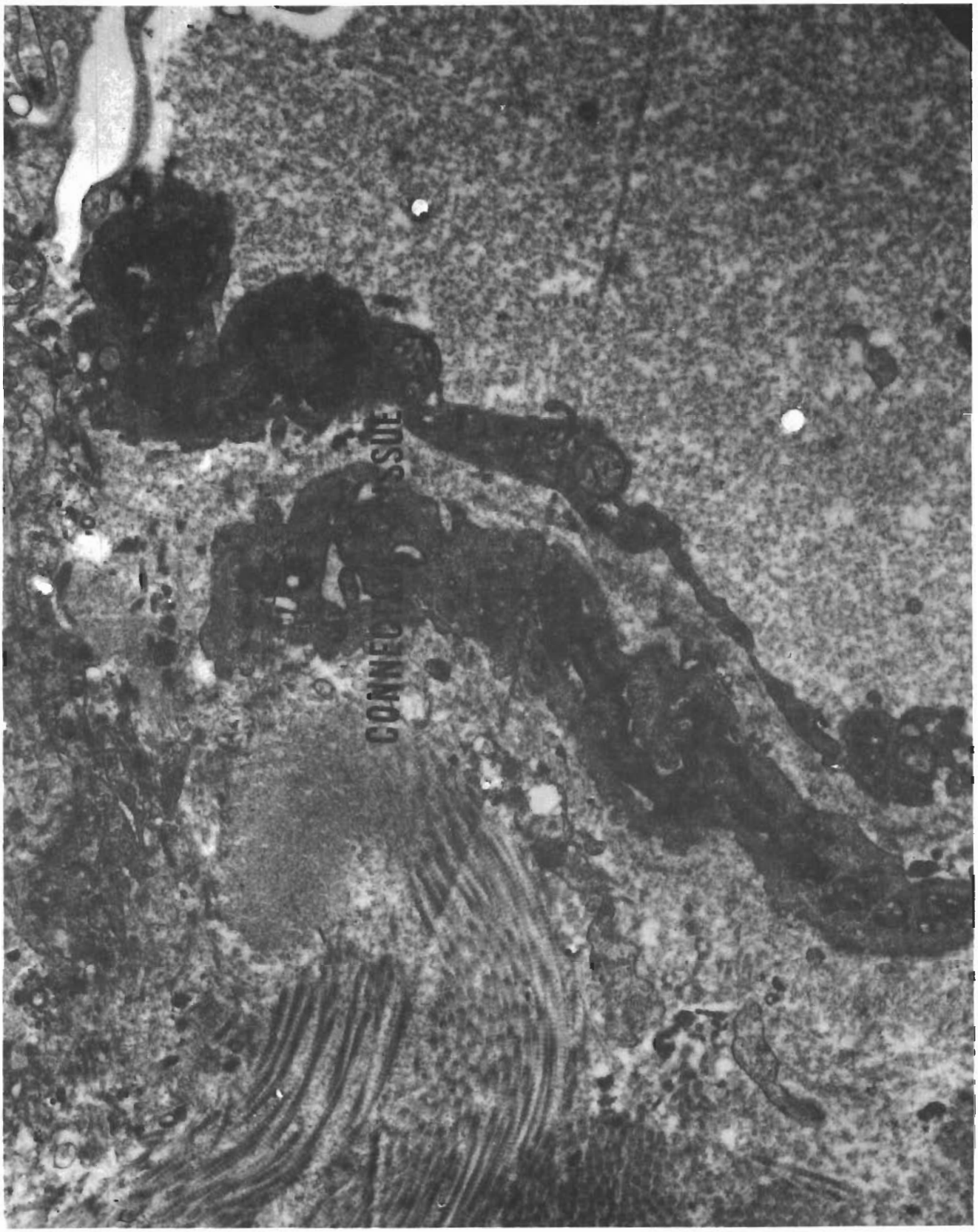

Sample No. 3

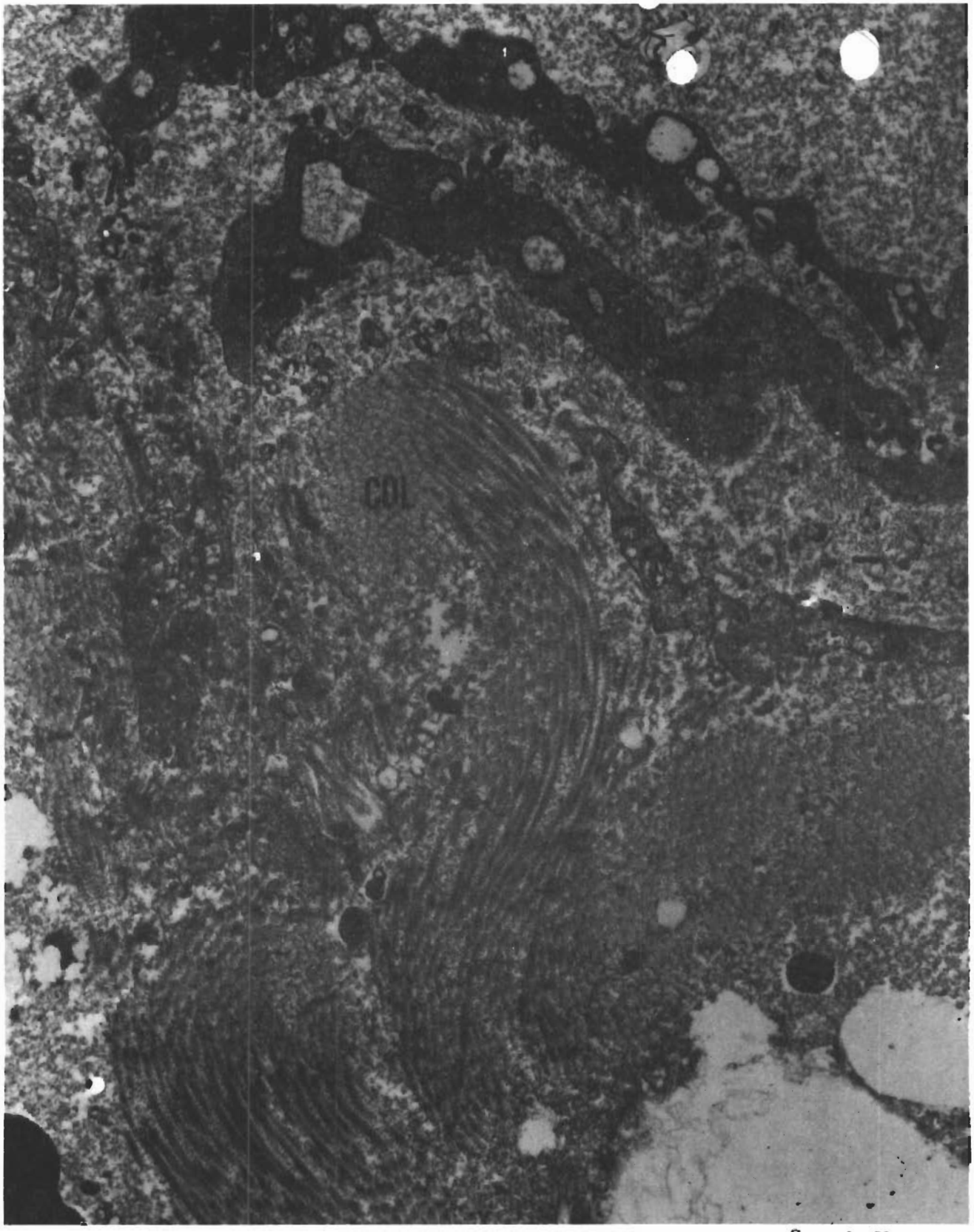

Sample No. 3

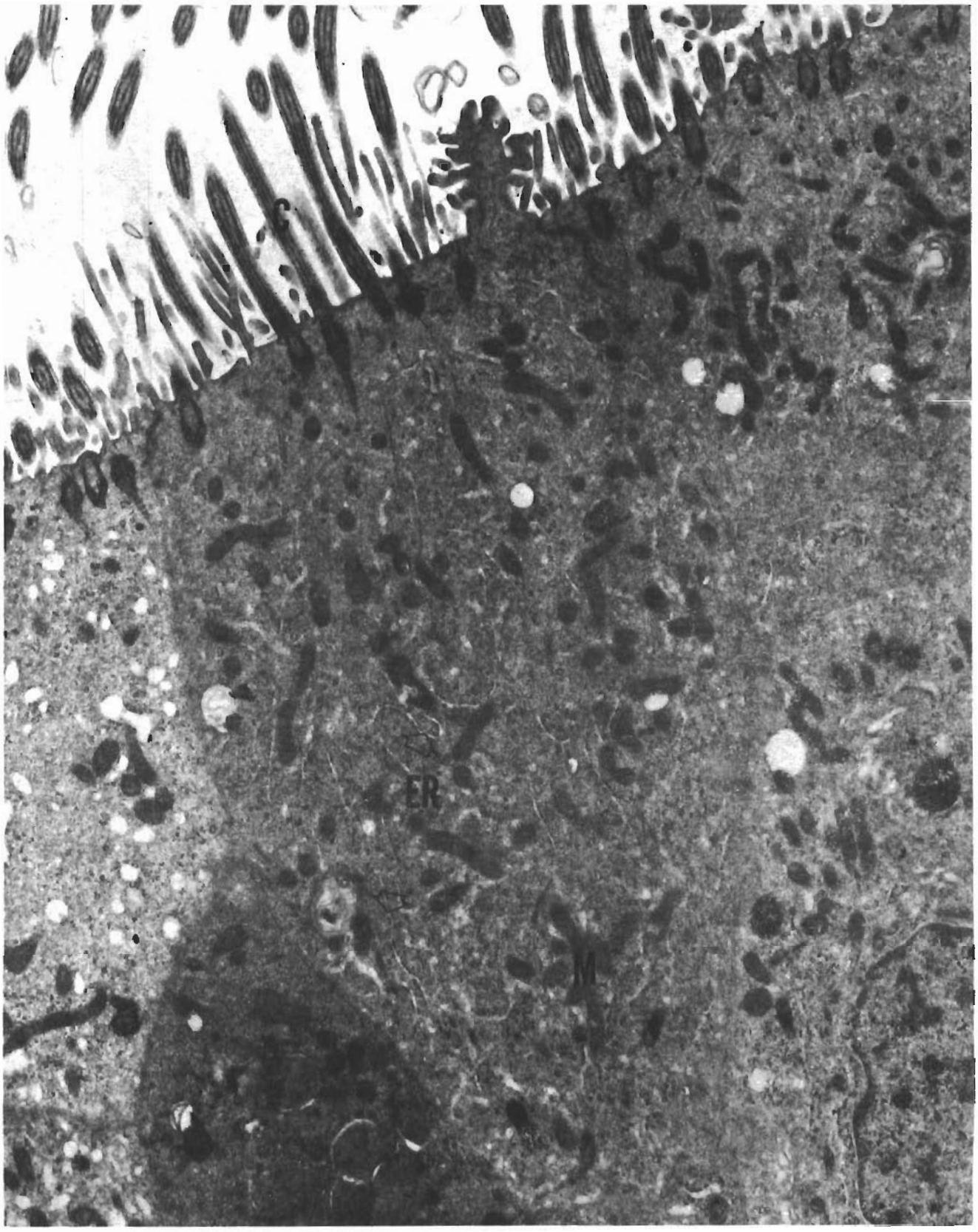

Sample No. 7

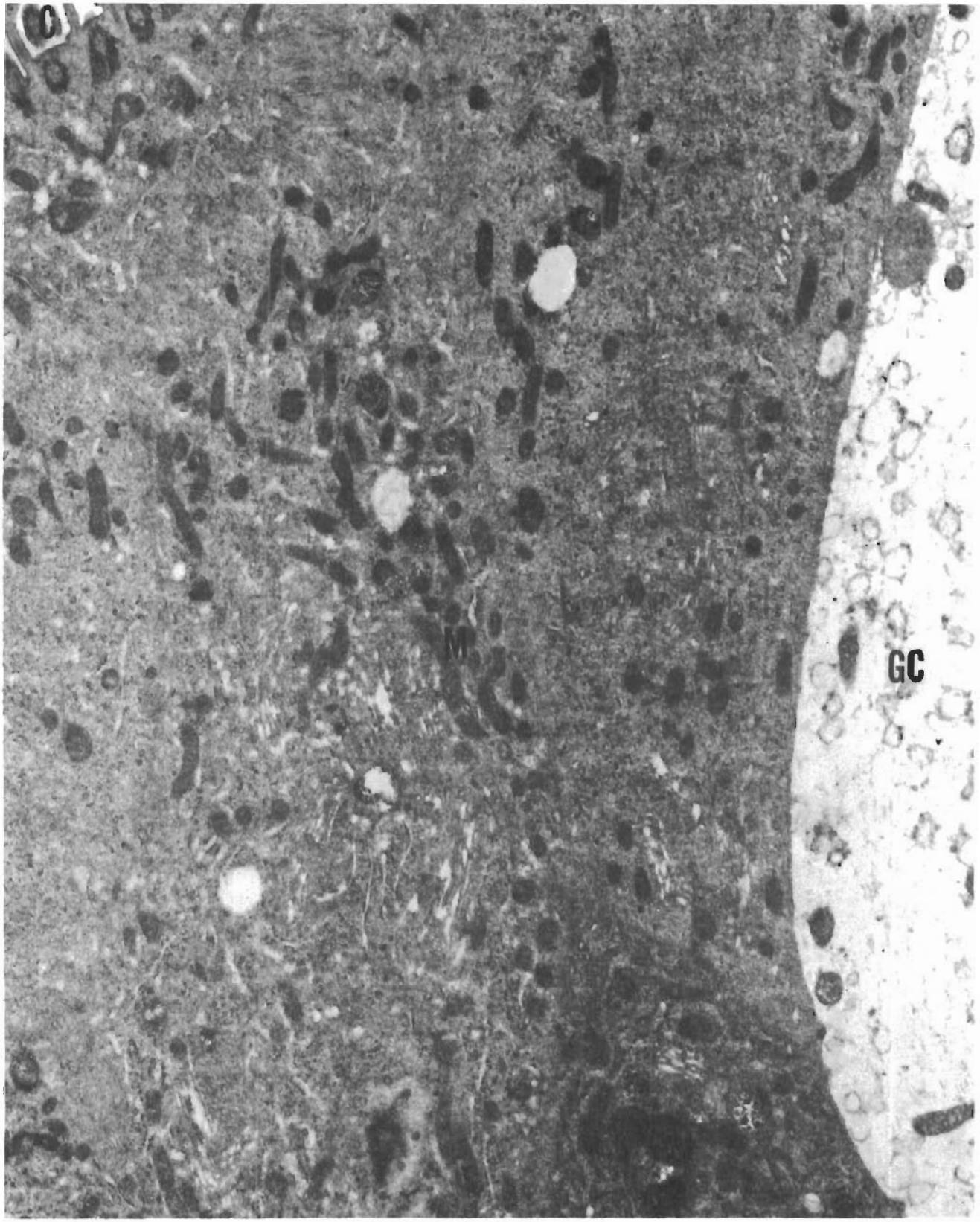

Sample No. 7

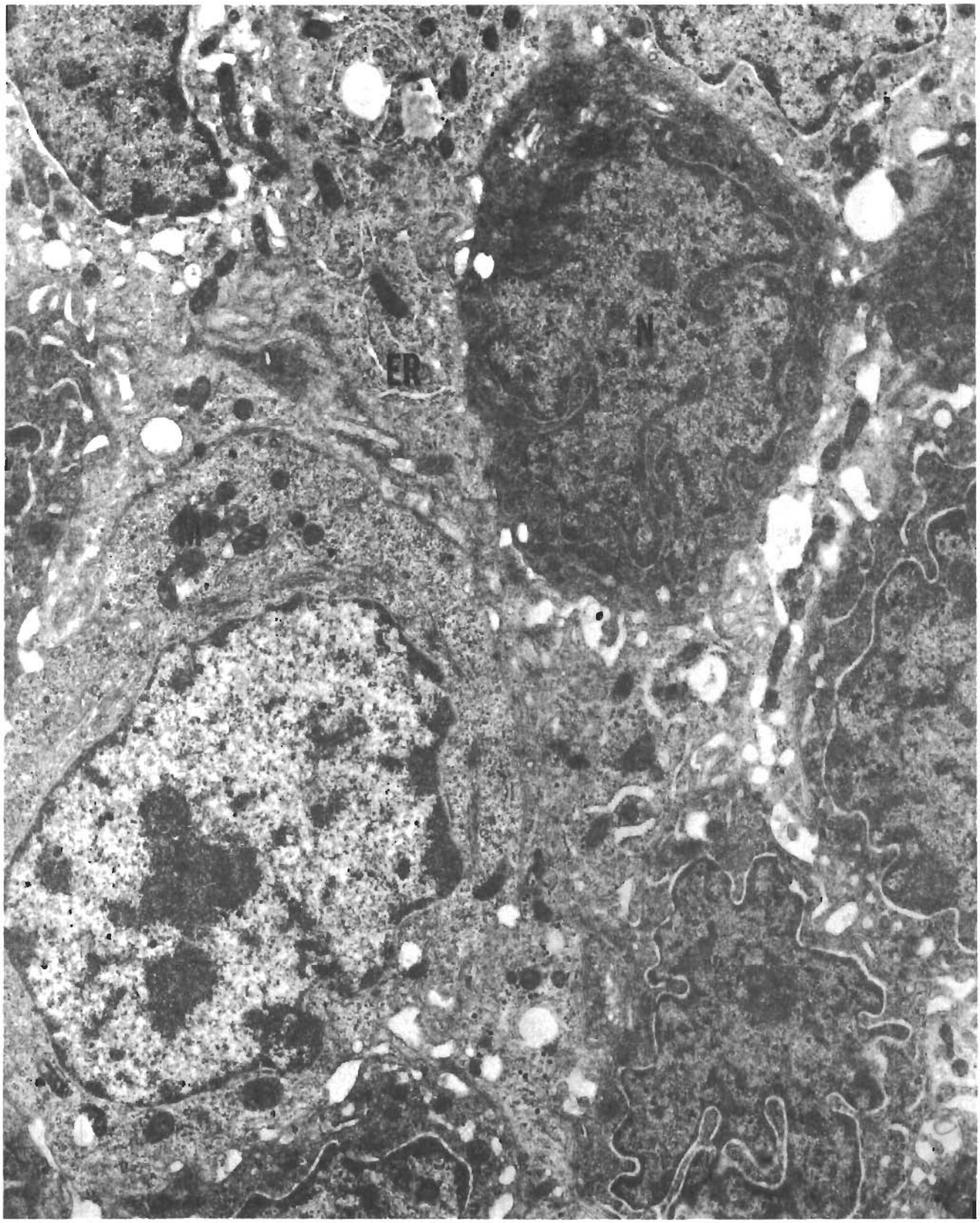

Sample No. 7

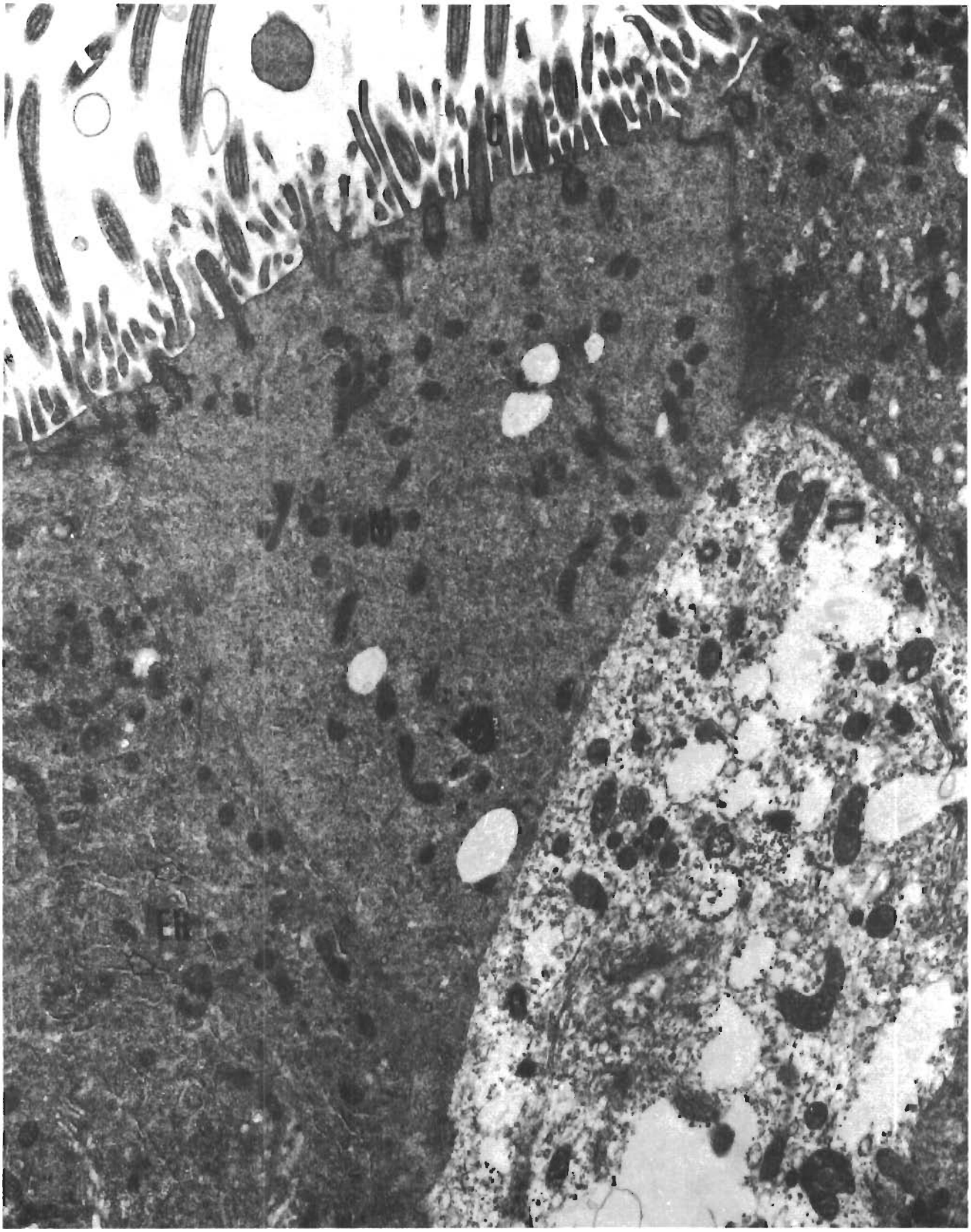

Sample No. 7

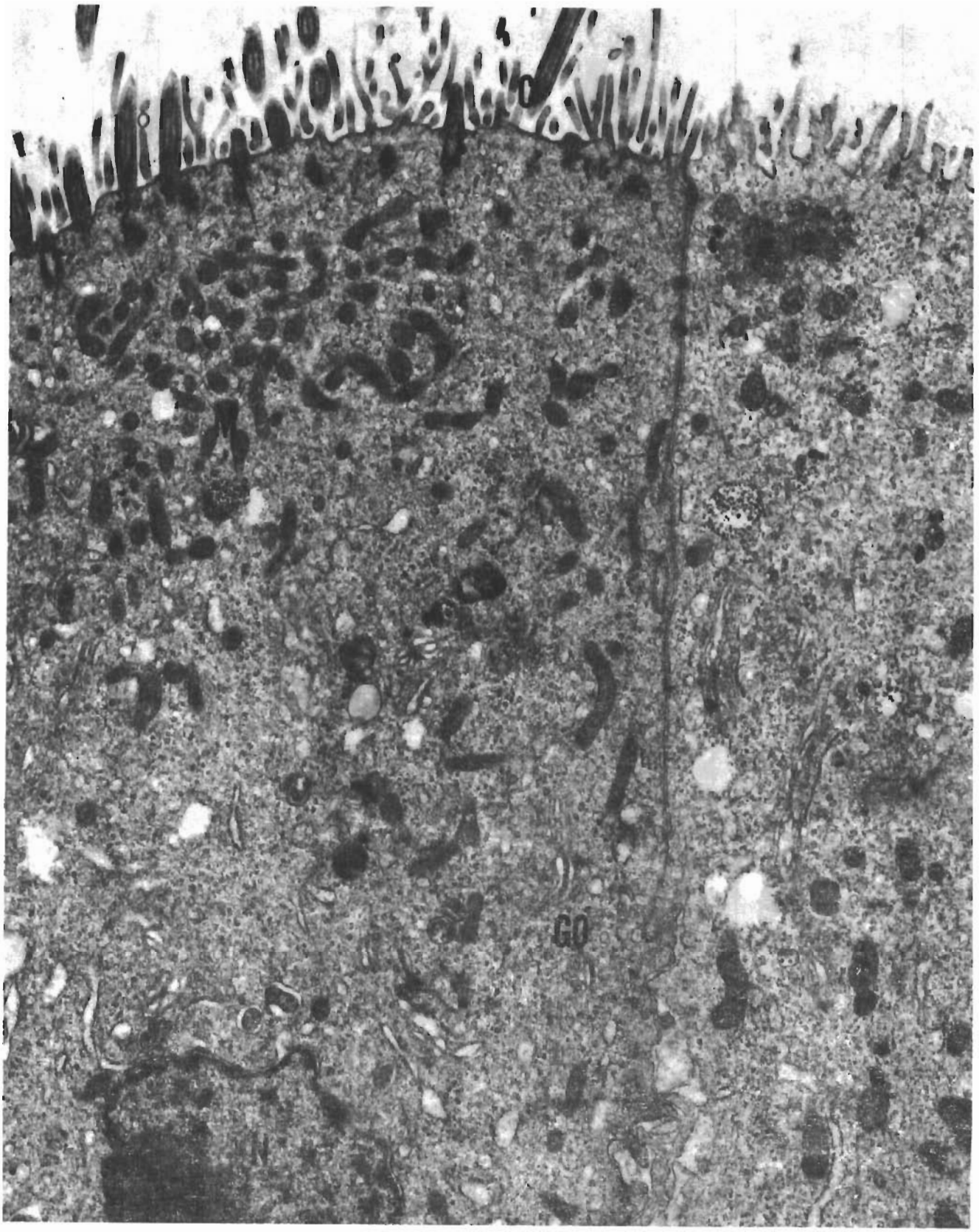

Sample No. 7

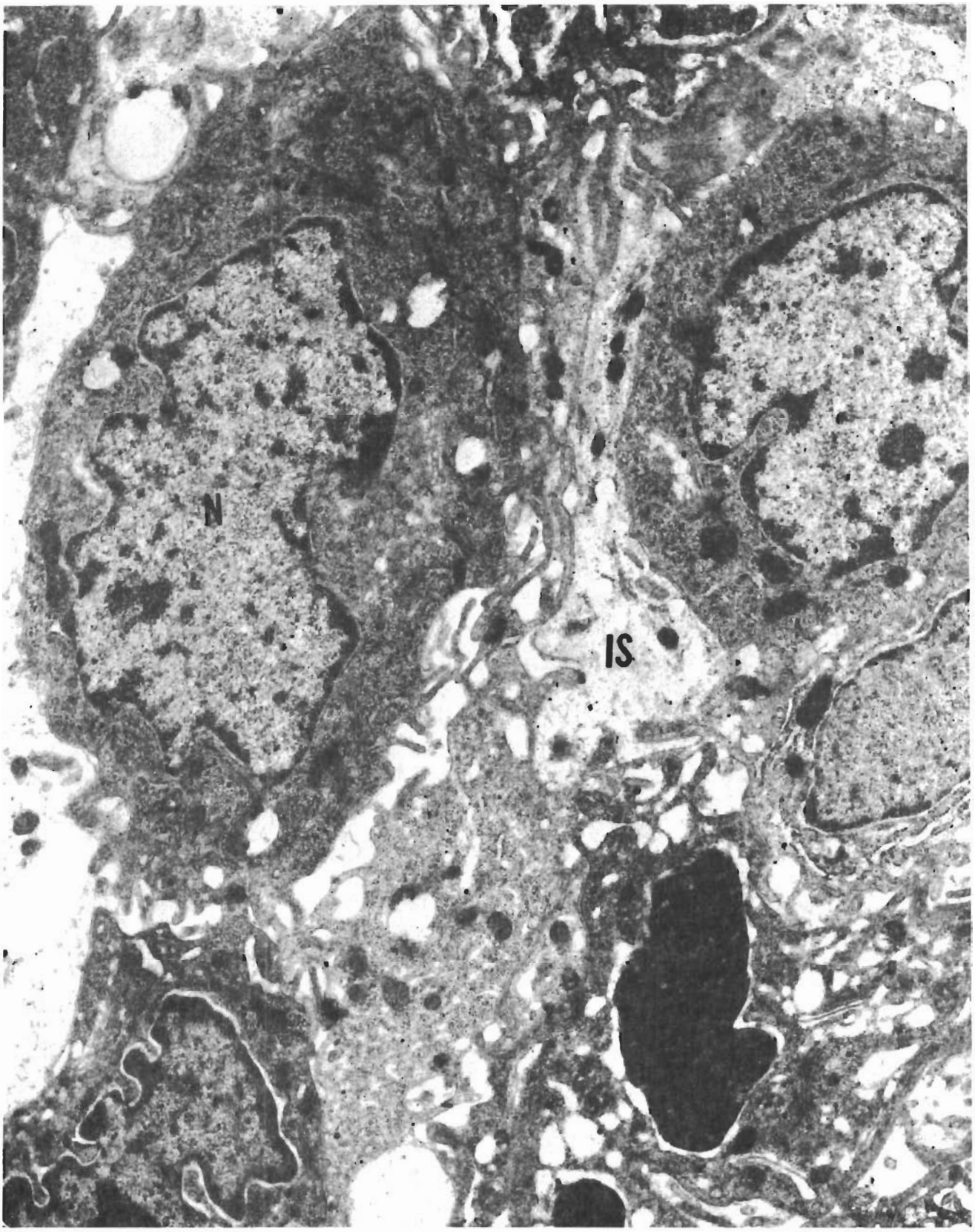

Sample No. 7

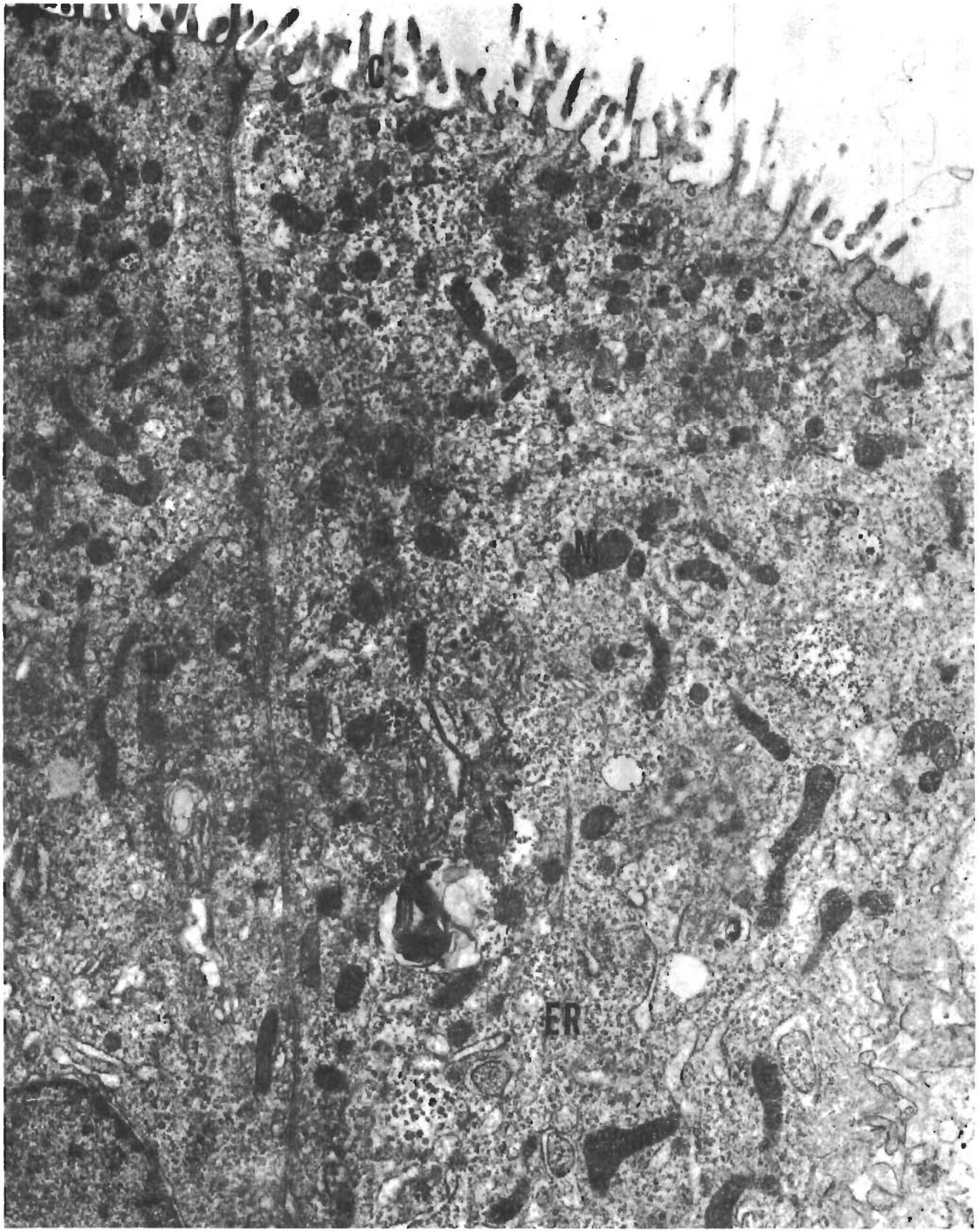

Sample No. 7

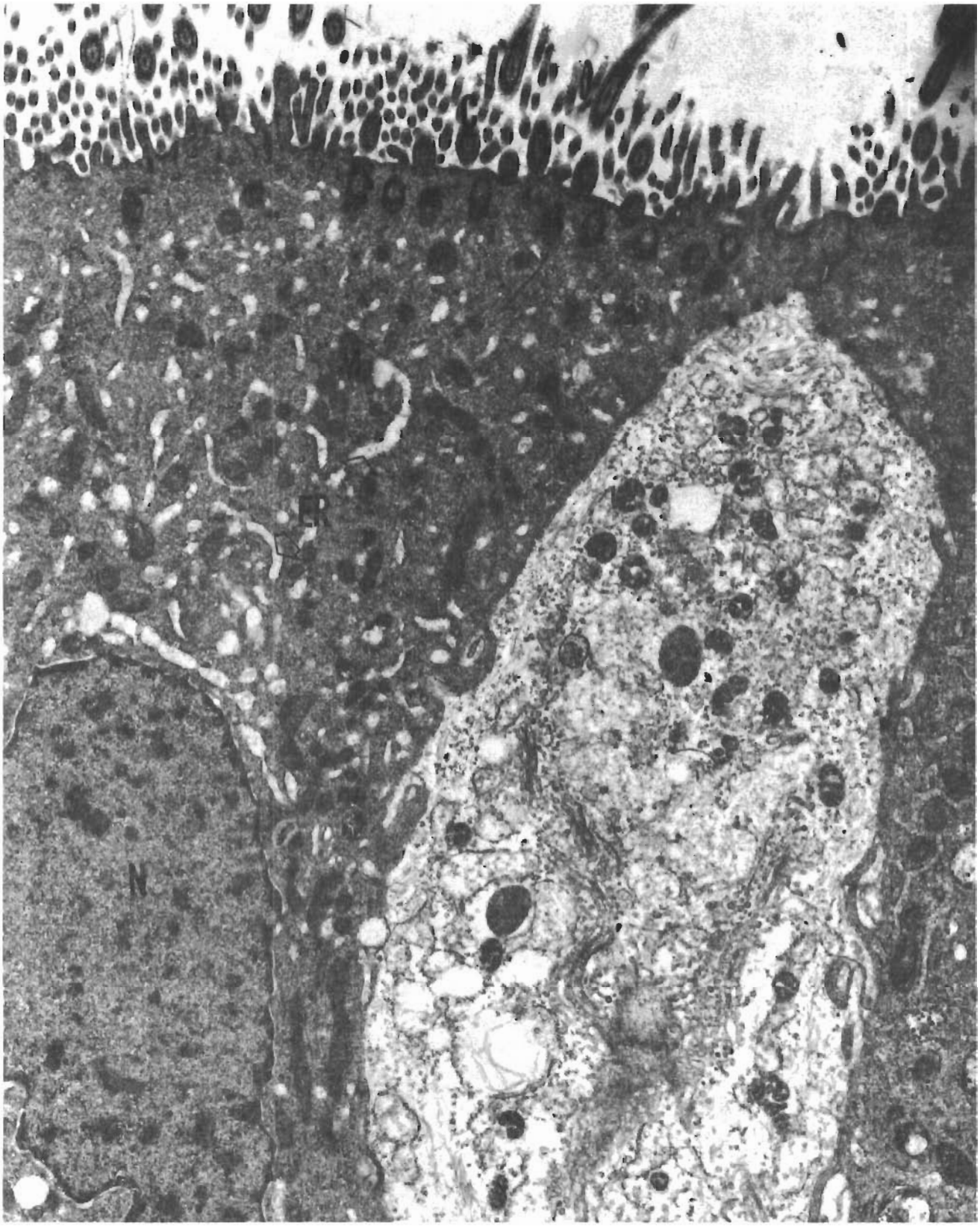

Sample No. 7

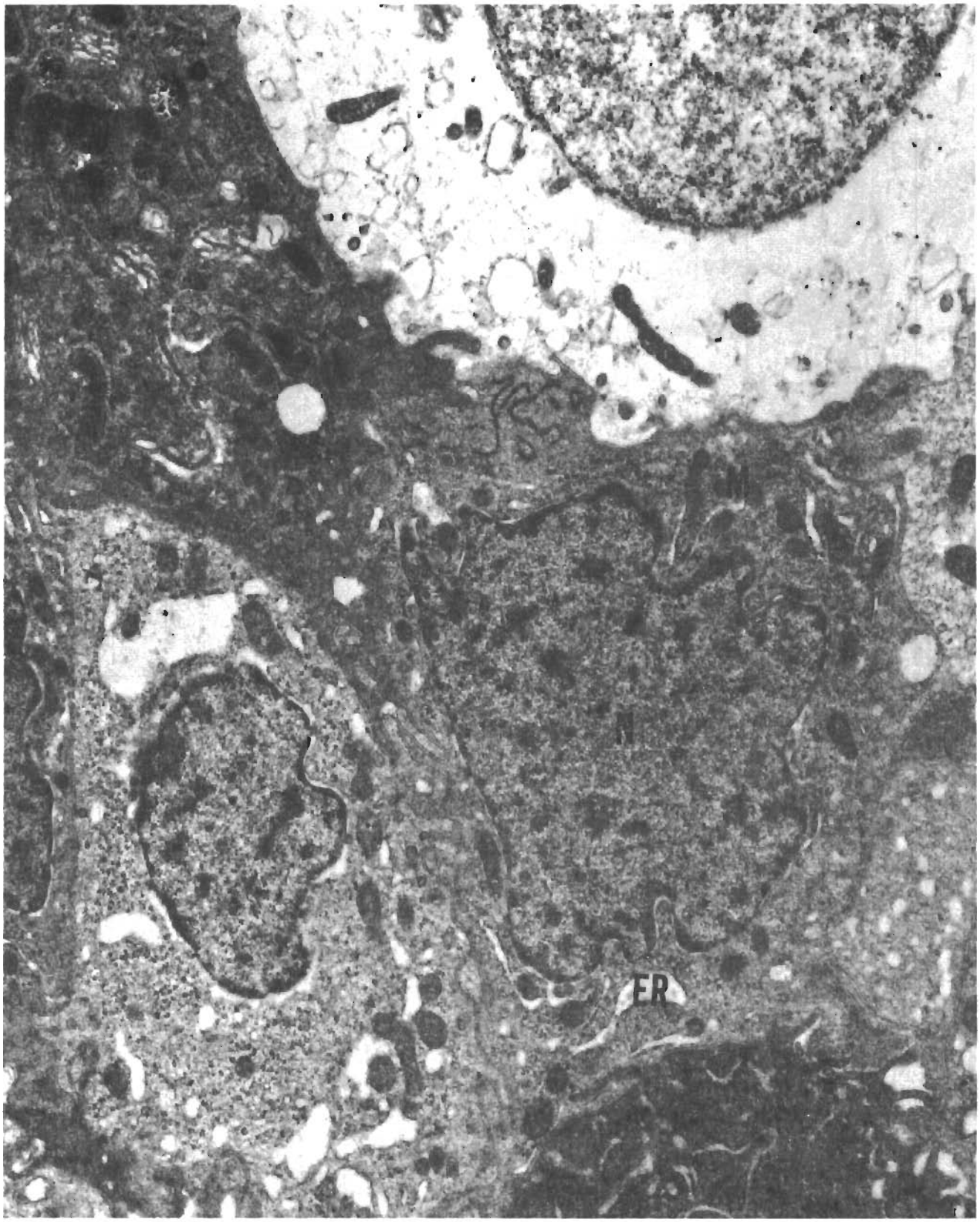

Sample No. 7

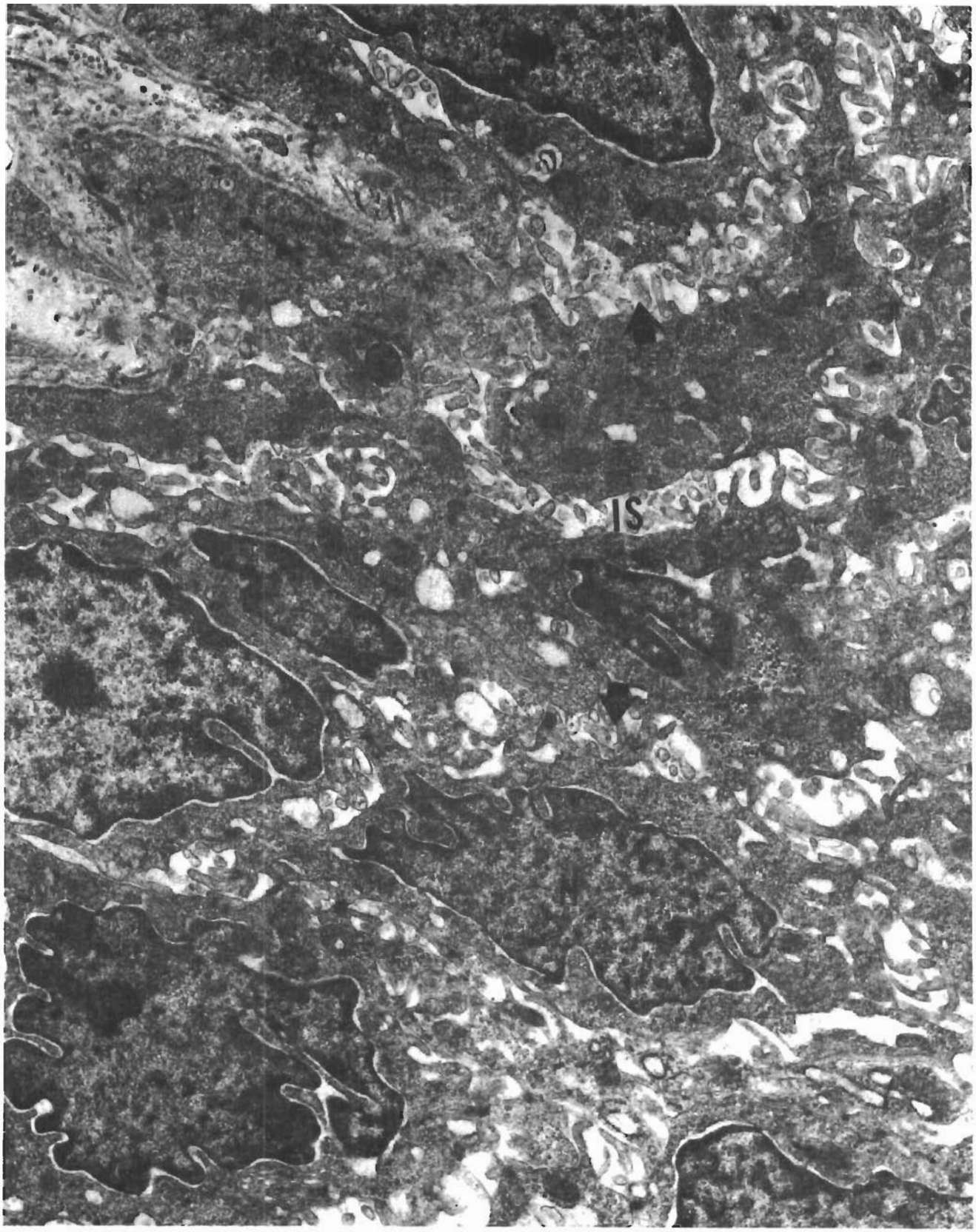

Sample No. 27

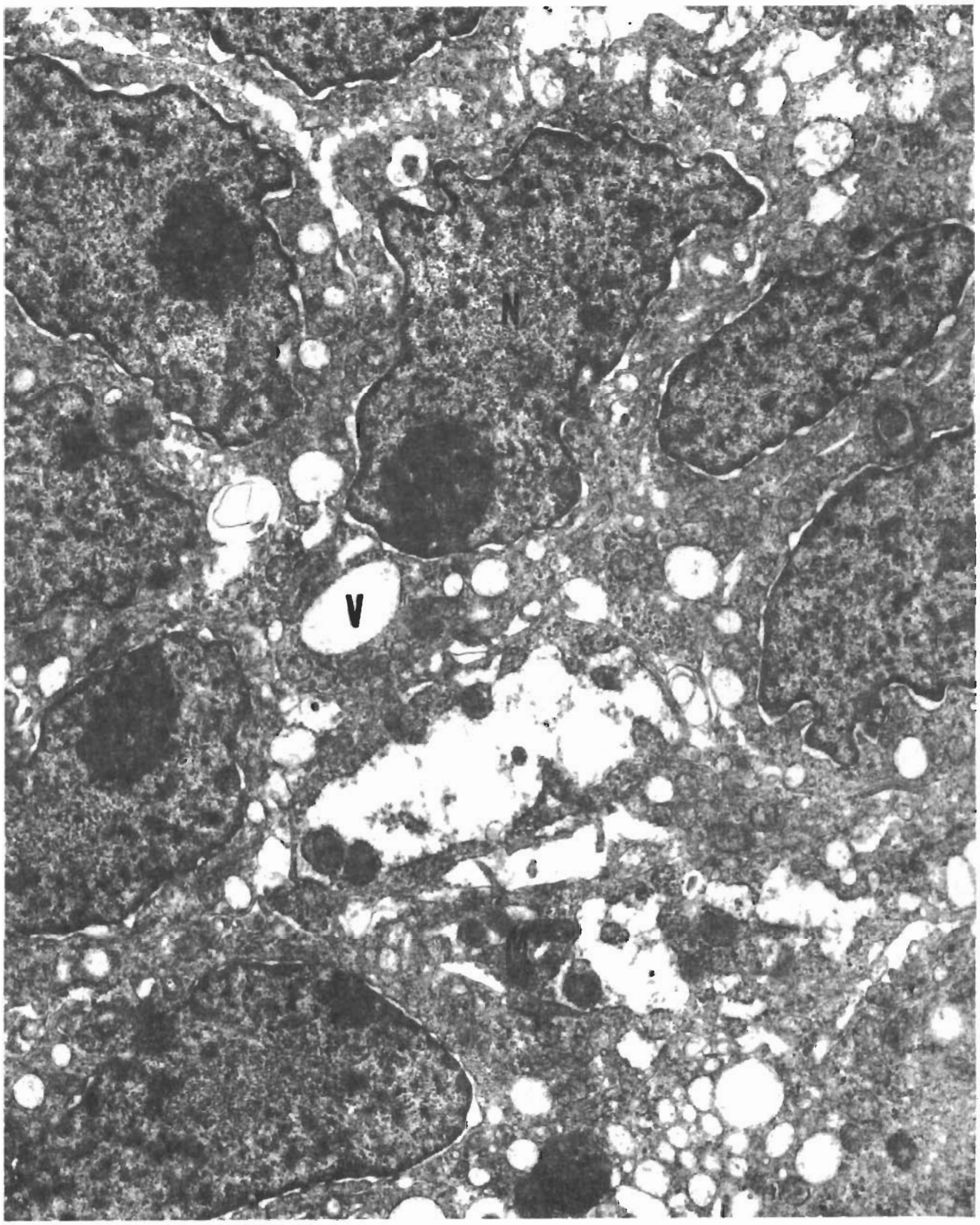

Sample No. 27

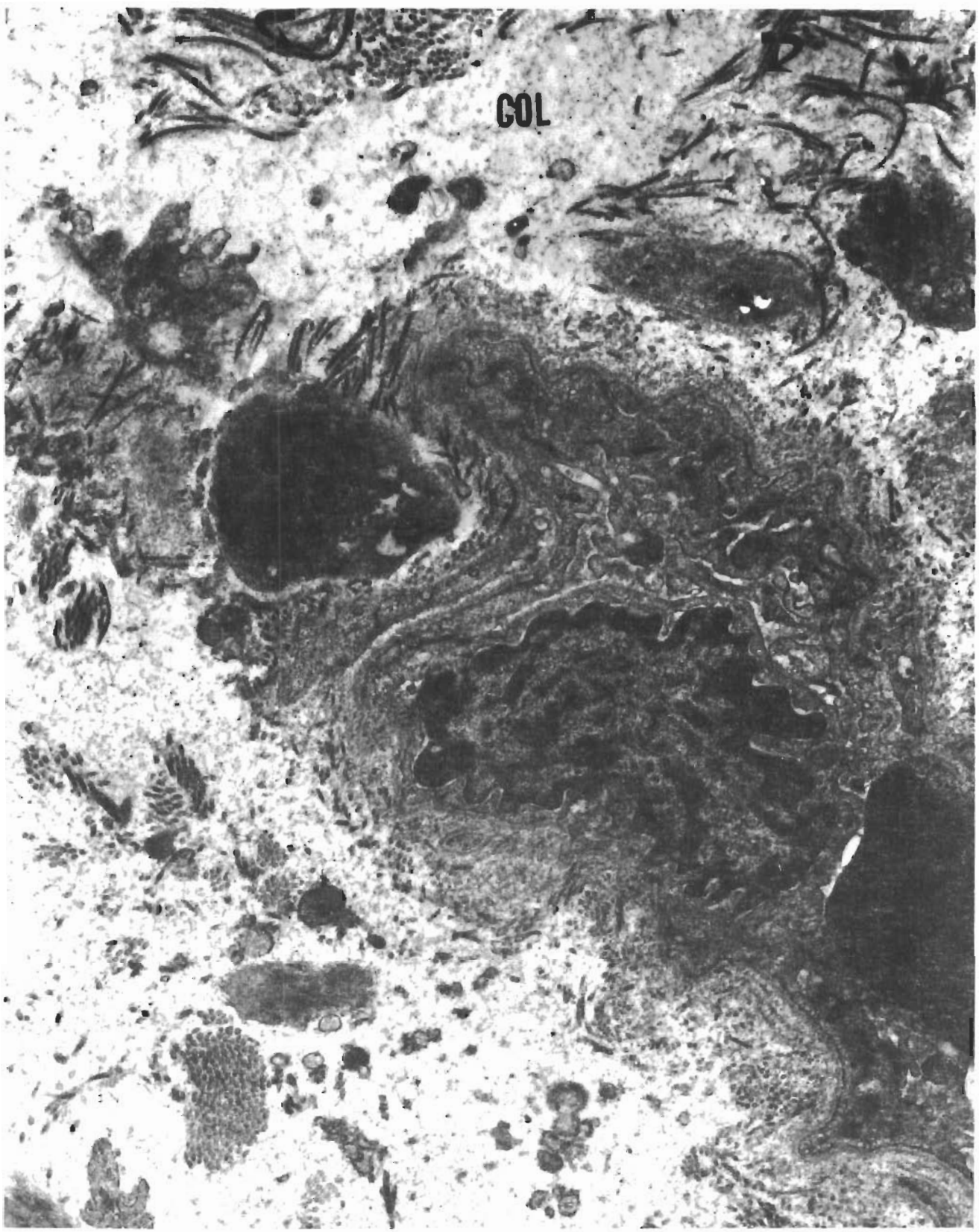

Sample No. 27

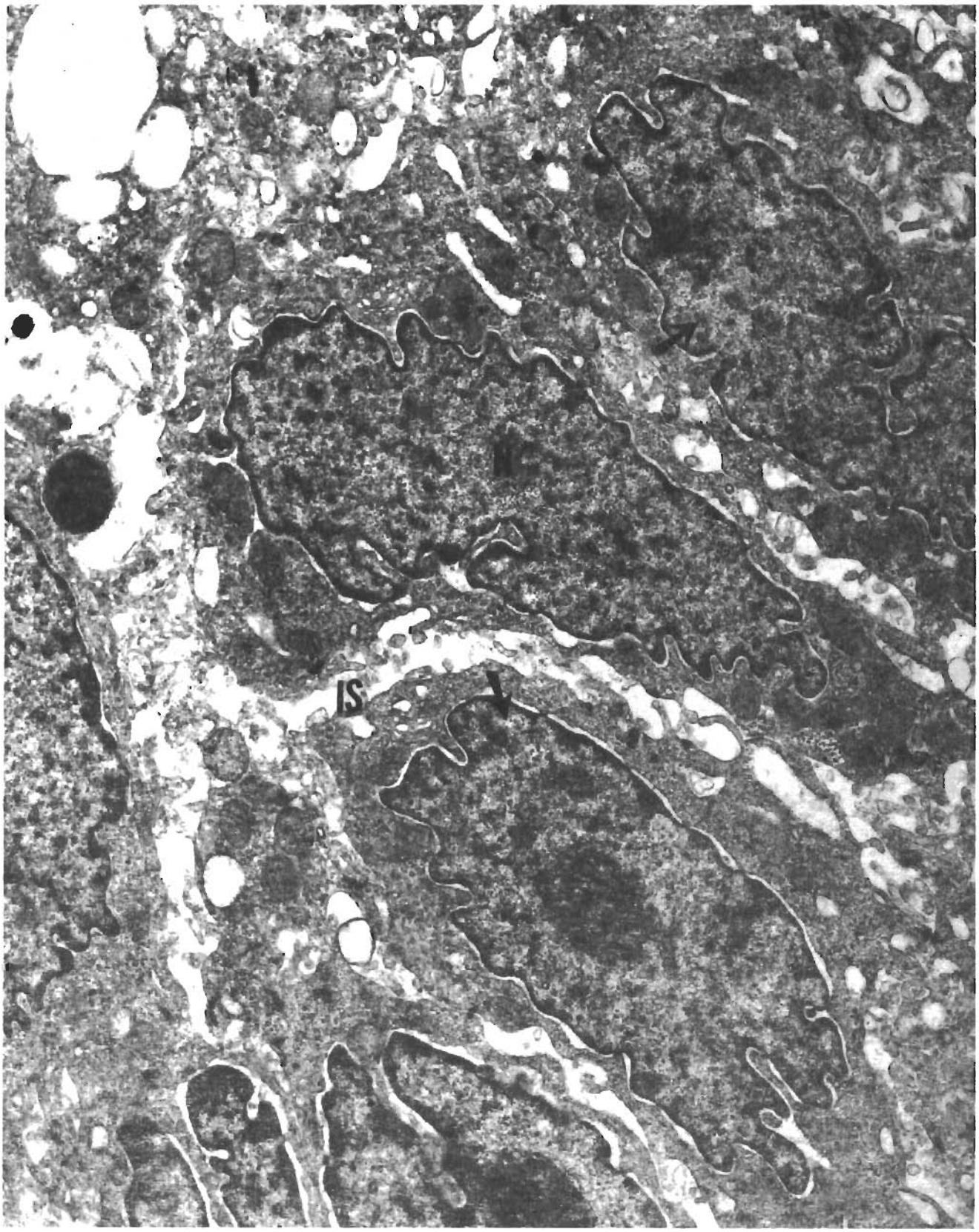

Sample No. 27

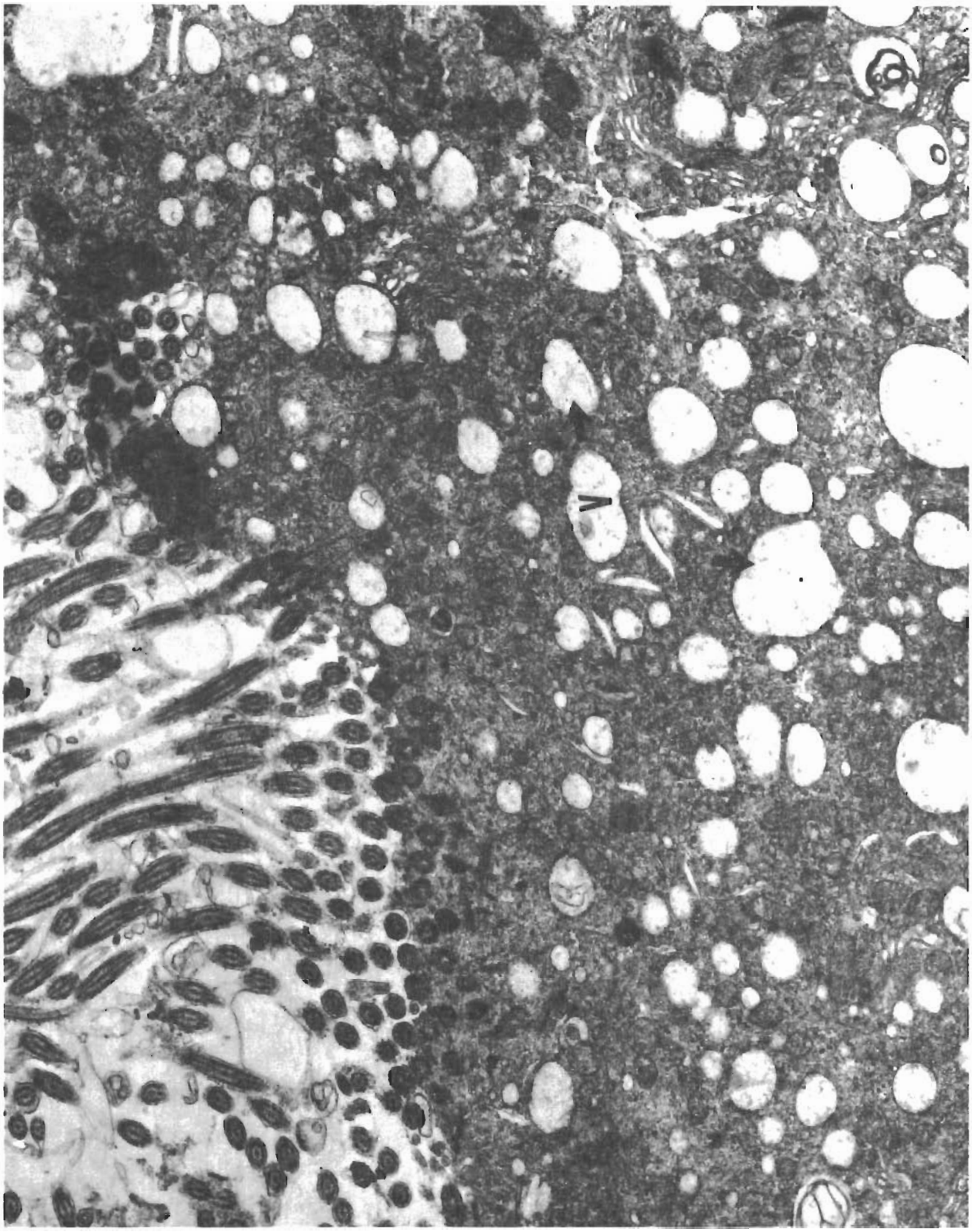

Sample No. 27

Sample No. 55

Sample No. 55

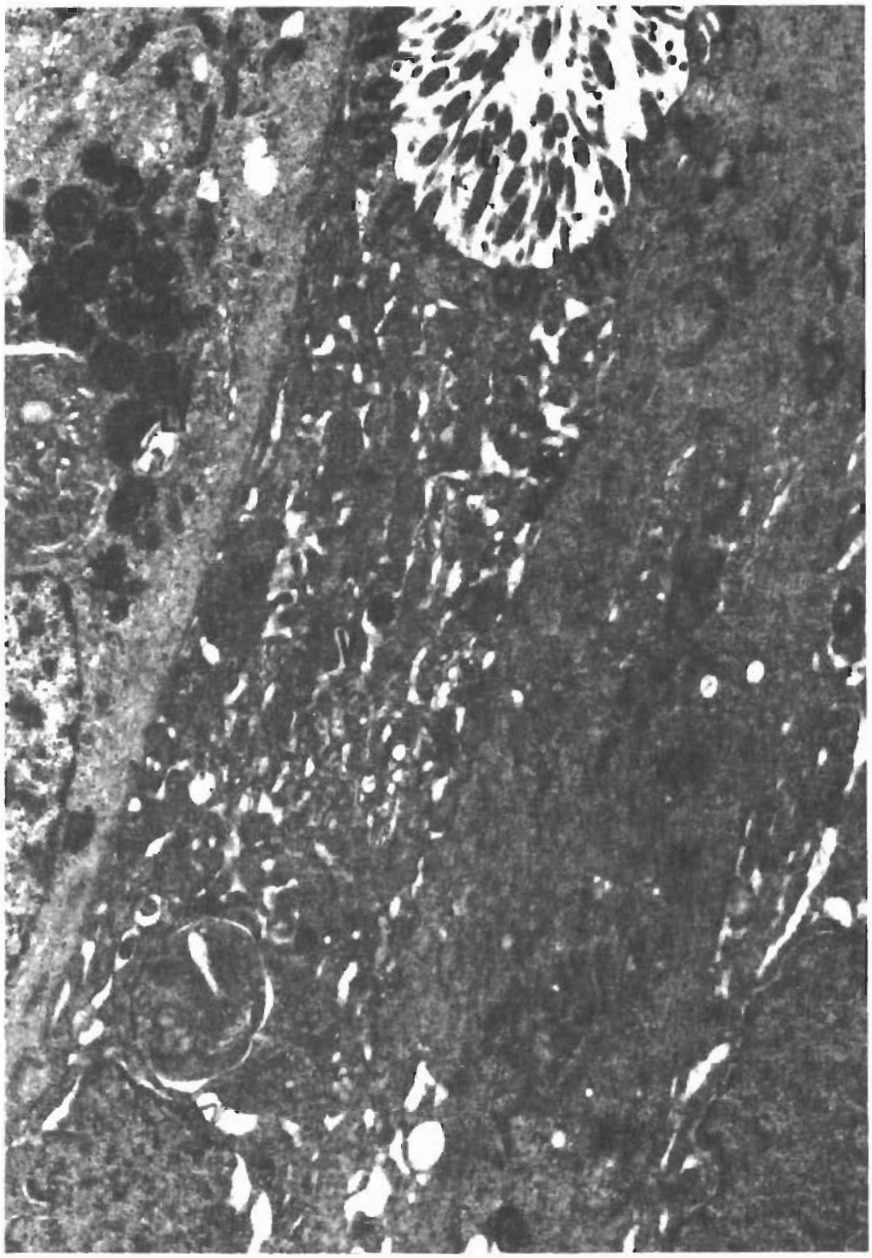

Sample No. 55

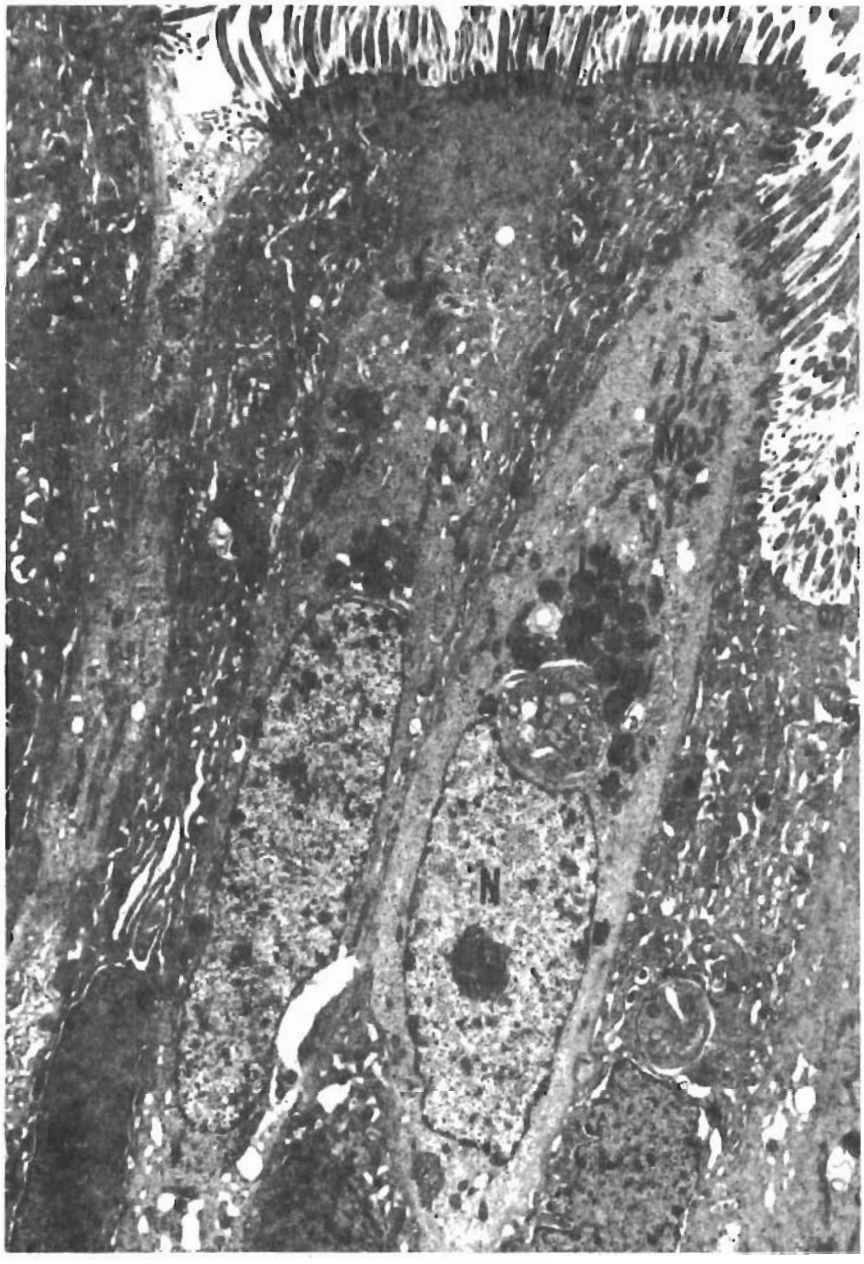

Sample No. 55

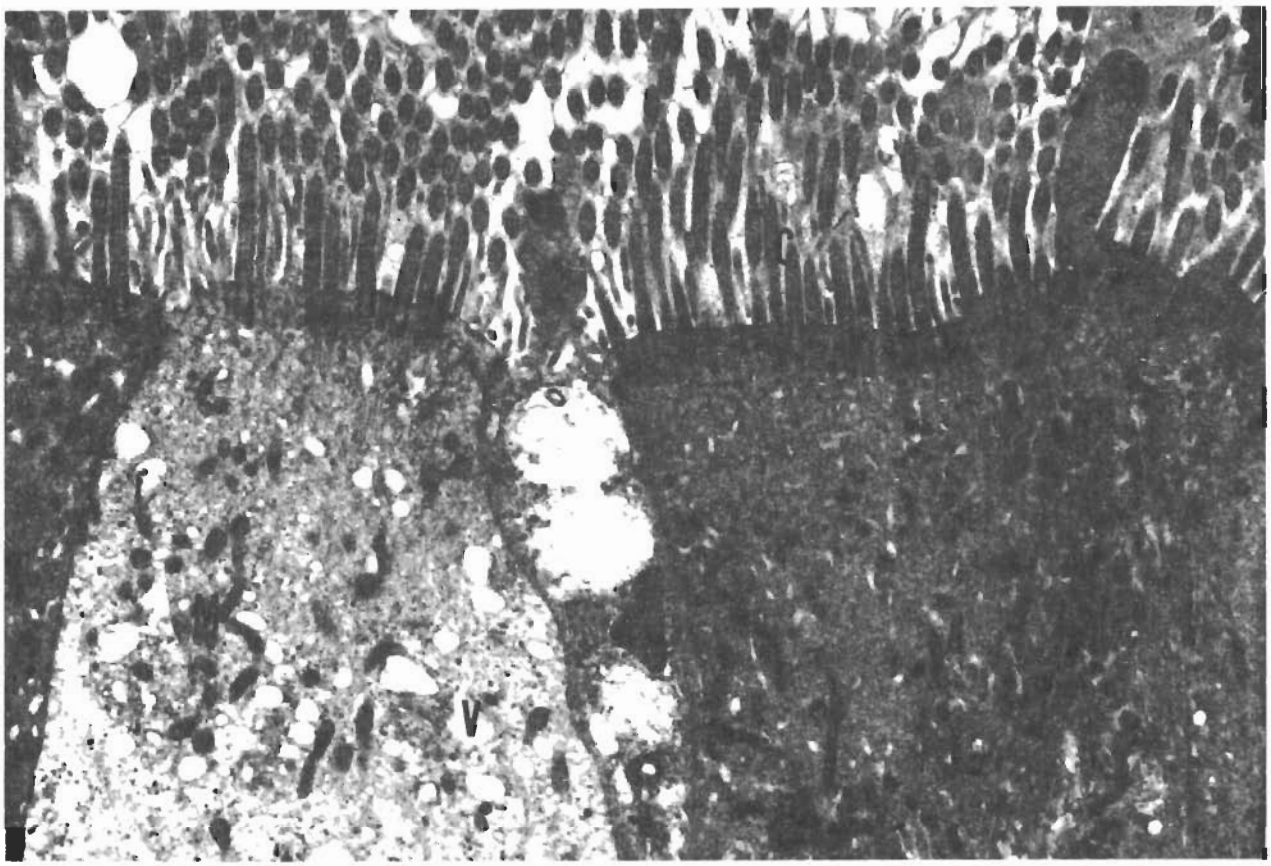

Sample No. 55

EPITHELIAL STRIPS FROM A CAT EXPOSED TO 80 ppm NO_2 FOR TWO HOURS

Sample No. 74

1. The sections again show a cluster of mononuclear cells characterized by prominent interdigitation widely separated by an increase in intercellular space.

2. Tracheal epithelial cells are characterized by variably sized electron dense uniform smooth looking droplets. Except for an occasional cytoplasmic vacuole, these cells appear normal.

3. Sections from the basal portion show mononuclear cells.

4. Superficial epithelial cells show cilia to be normal. Within the upper portion of the cytoplasm there are numerous vacuoles. The mitochondria appear normal.

5. Superficial epithelial cells show the same vacuolization, edema, and occasional myelin figures which have been previously described.

6. Epithelial cells illustrate marked diffuse vacuolization of a small fine nature previously described. Nuclei are normal and mitochondria appear normal in distribution.

Sample No. 101

1. Sections show cilia to be intact despite apparent variations in size. There obviously are several types of cilia some of which are arising at the peripheral margins of the cell. Within the surface of the cell are numbers of swellings of the endoplasmic reticulum which result in vacuoles. Occasional myelin figures are noted. The mitochondria appear intact. The intercellular space and desmosomes are intact.

2. Sections reveal areas of cell injury manifested by numerous cytoplasmic vacuoles, marked accumulation of lysosomes and increased electron lucidity in the cells. Mitochondria still appear normal.

3. These sections are illustrative of cytoplasmic vacuolization and numerous myelin bodies. Intercellular spaces are normal.

4. Injured epithelial cells show same basic pattern as previously described.

5. Virtually all of the cells observed show changes previously described including cytoplasmic vacuolization, small numbers of lysosomes, increased numbers of myelin figures, and no basic change in intercellular arrangements.

6. Same basic changes described previously.

Photographs for the aforementioned samples follow.

Code for Photographs

N = nucleus
IS = intercellular space
BM = basement membrane
RET = reticulum
C = cilia
M = mitochondria
V = vacuoles
LY = lysosomes
GC = goblet cell
MY = myelin
ER = endoplasmic reticulum
GO = golgi
COL = collagen
CAP = capillary
RBC = red blood cell
AL = alveolus
DB = dense bodies

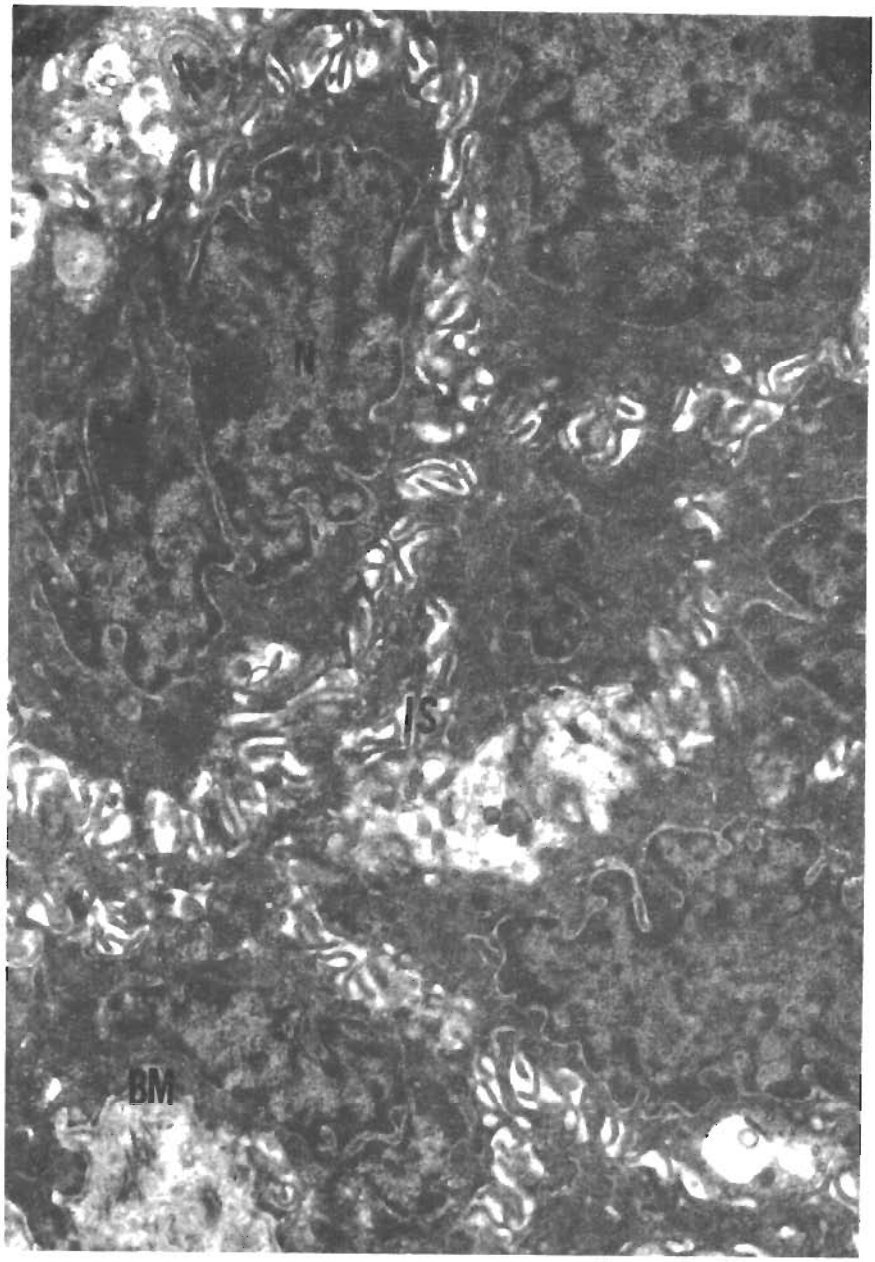

Sample No. 74

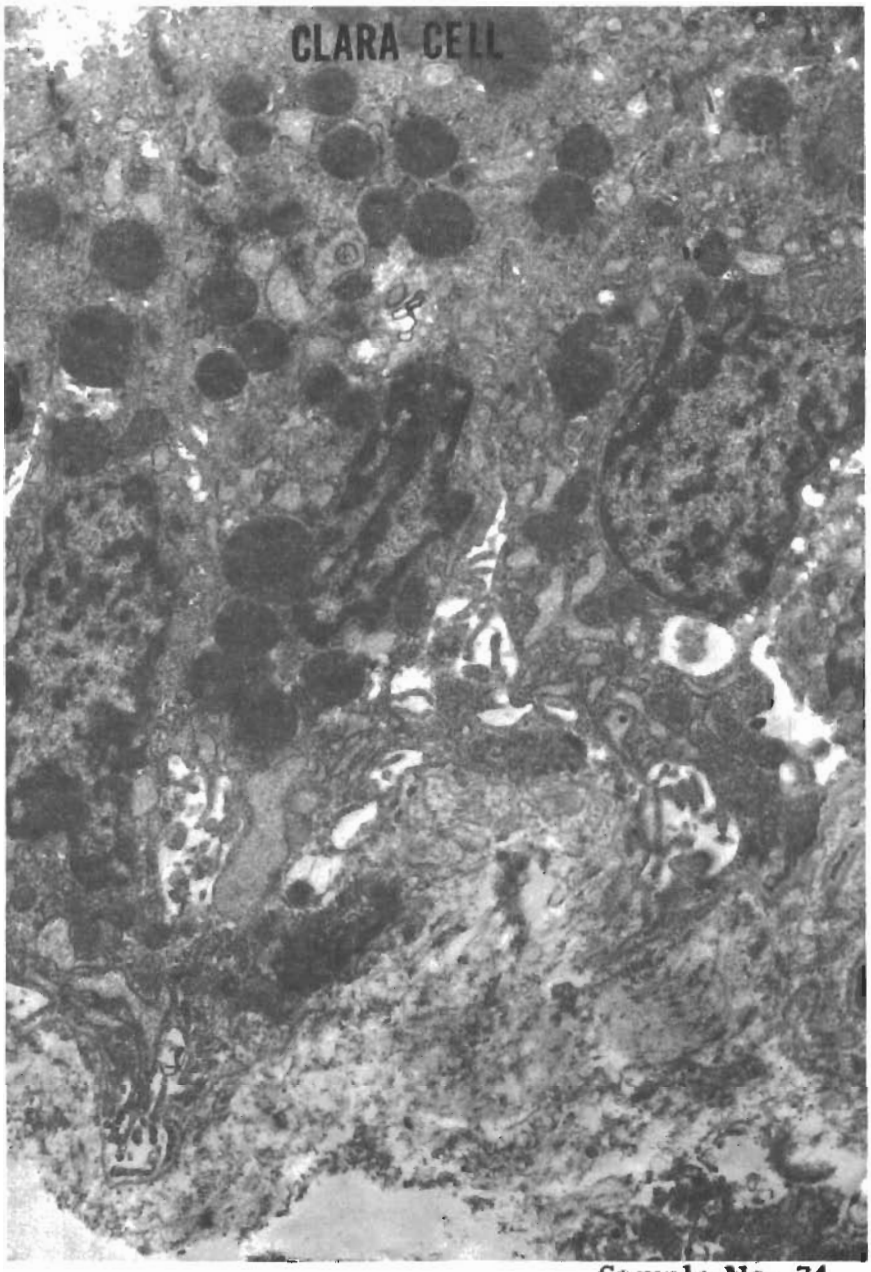

Sample No. 74

Sample No. 74

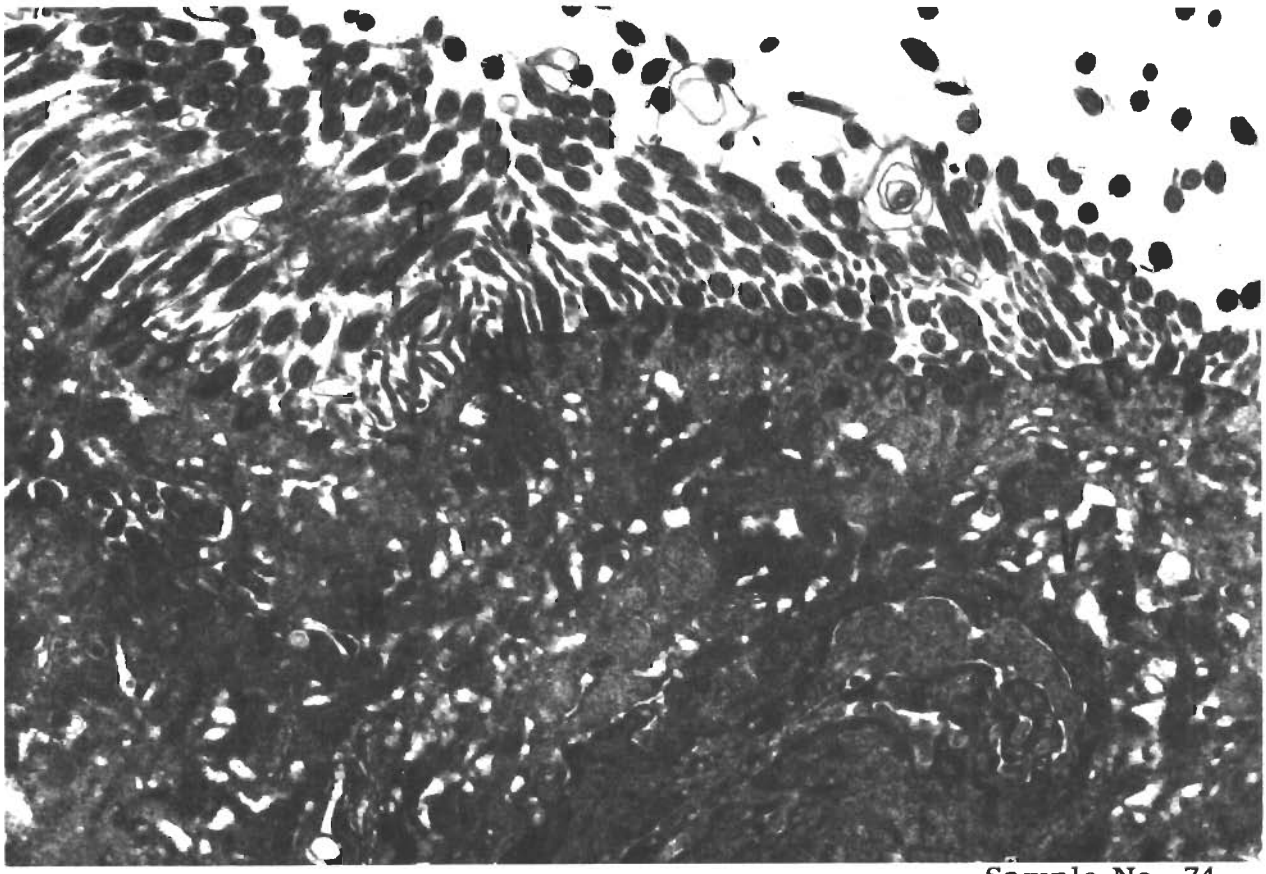

Sample No. 74

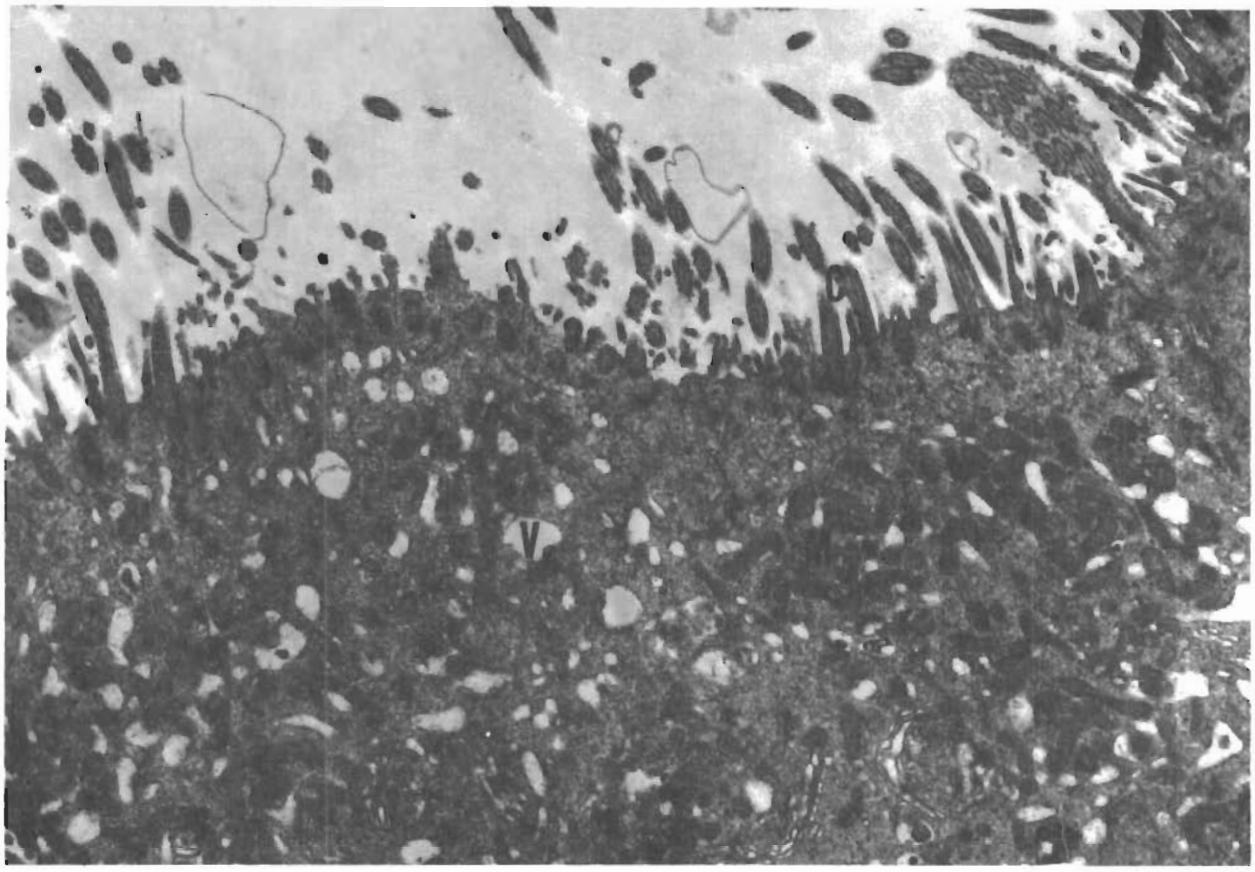

Sample No. 74

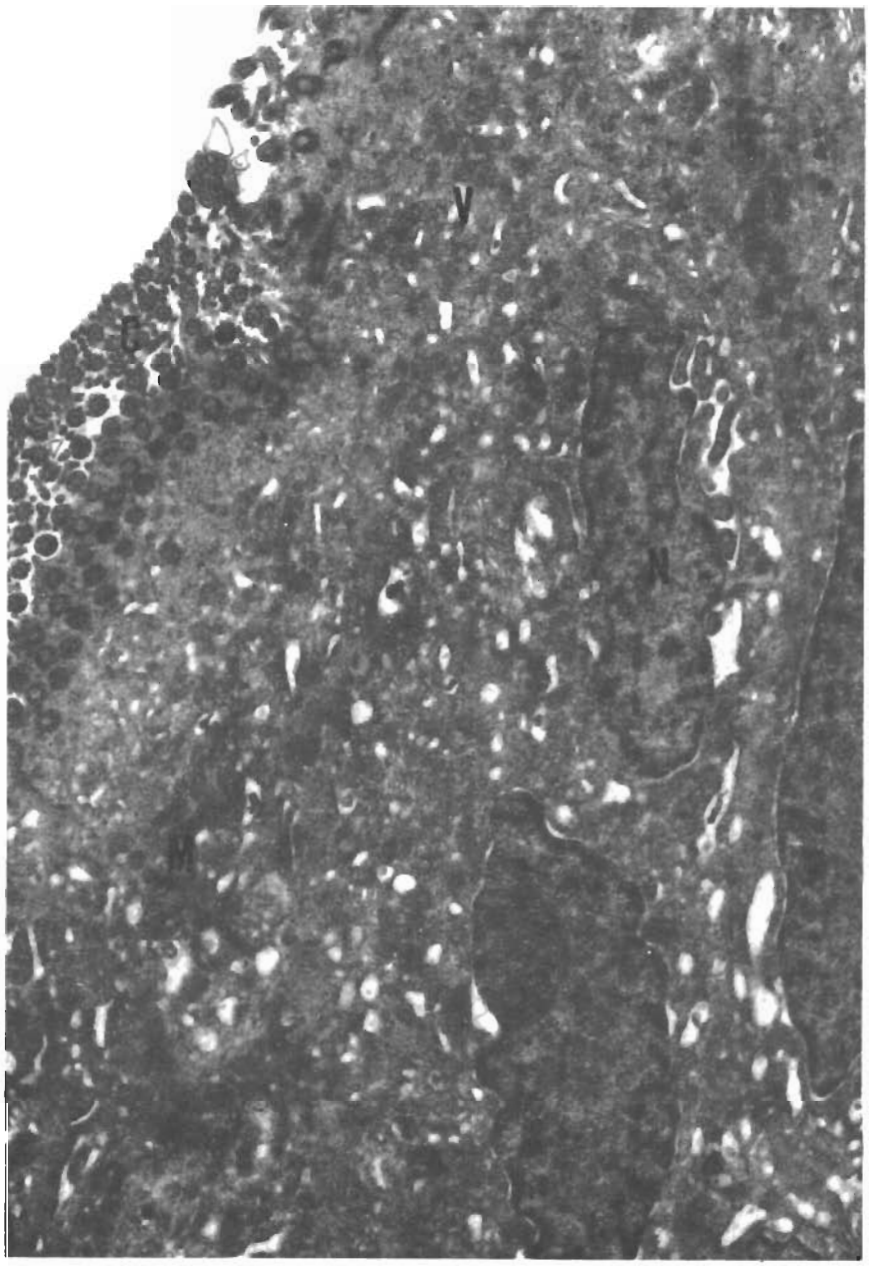

Sample No. 74

Sample No. 101

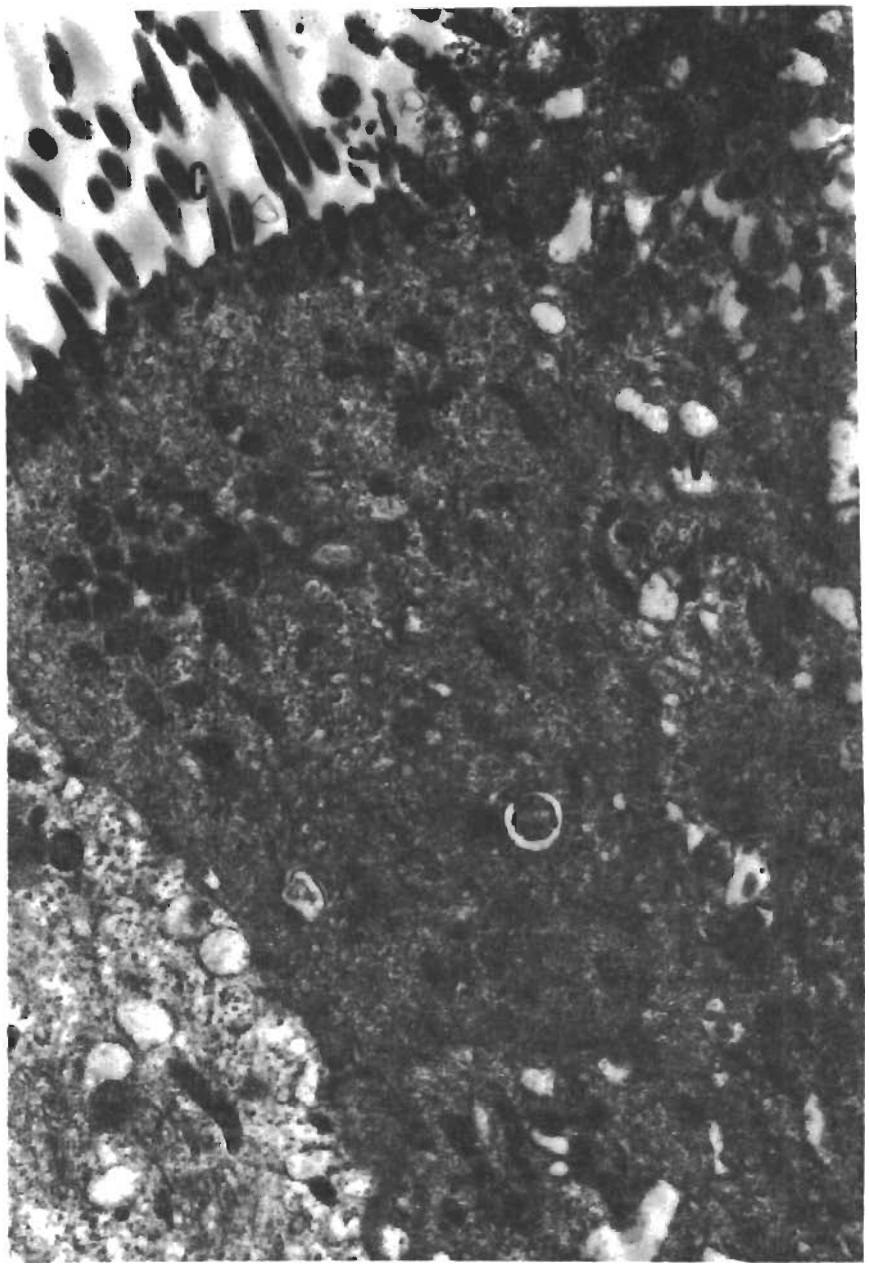

Sample No. 101

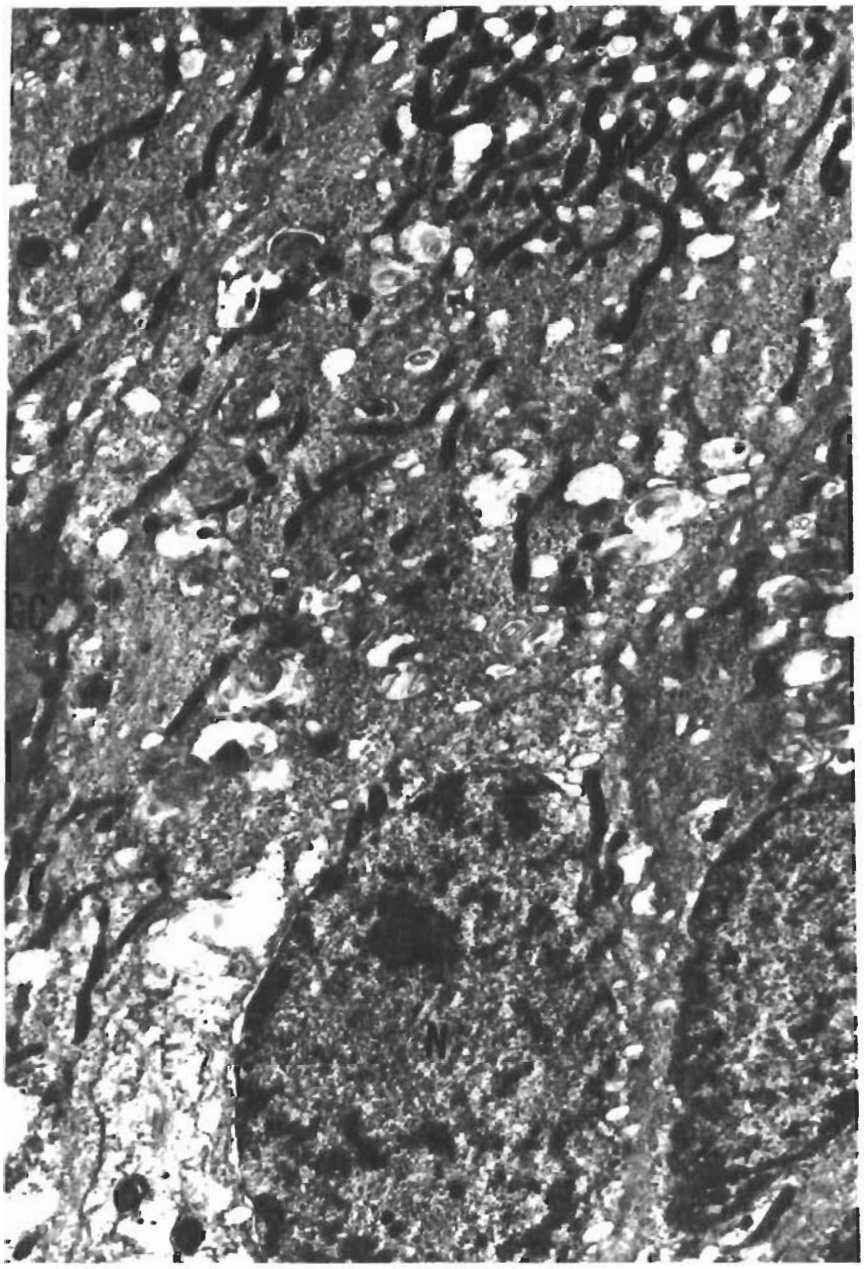

Sample No. 101

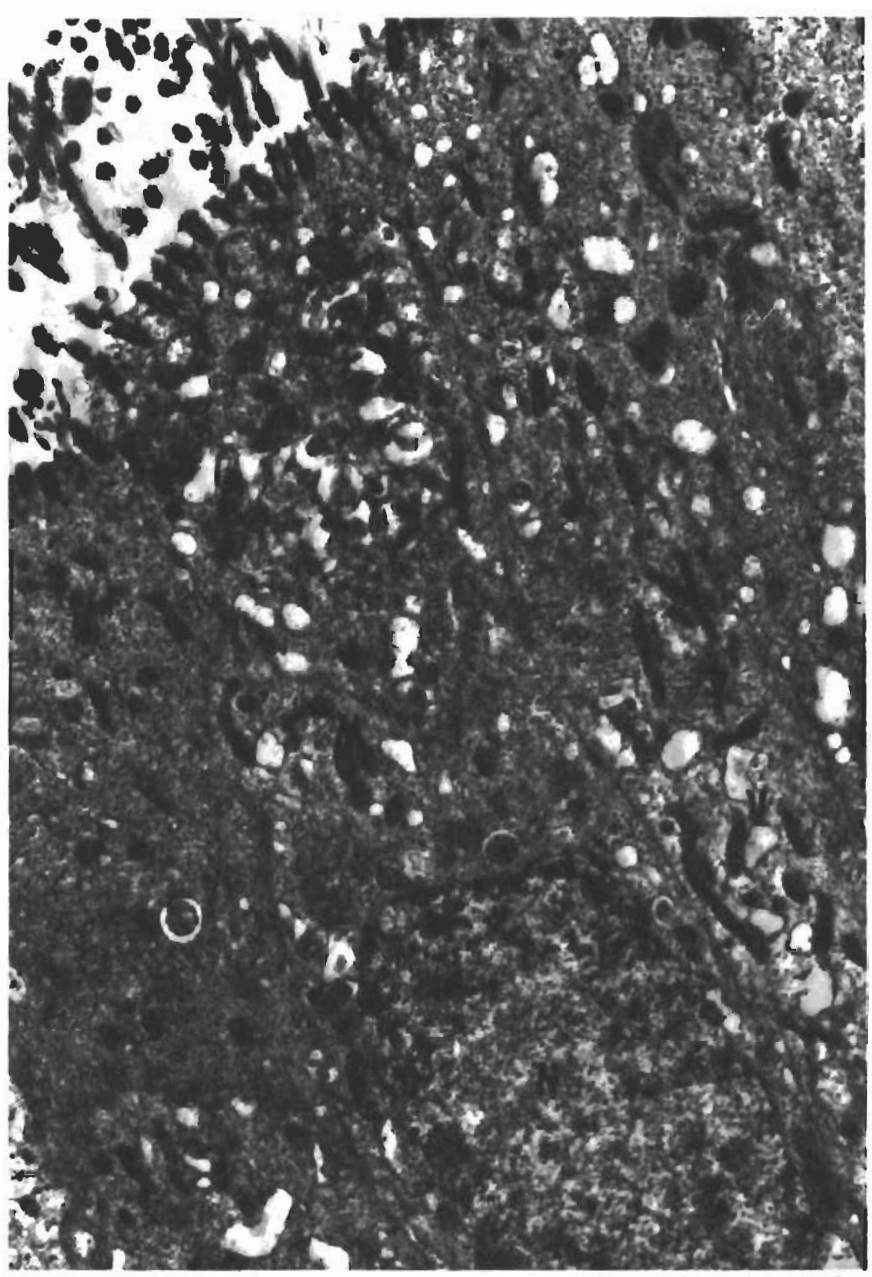

Sample No. 101

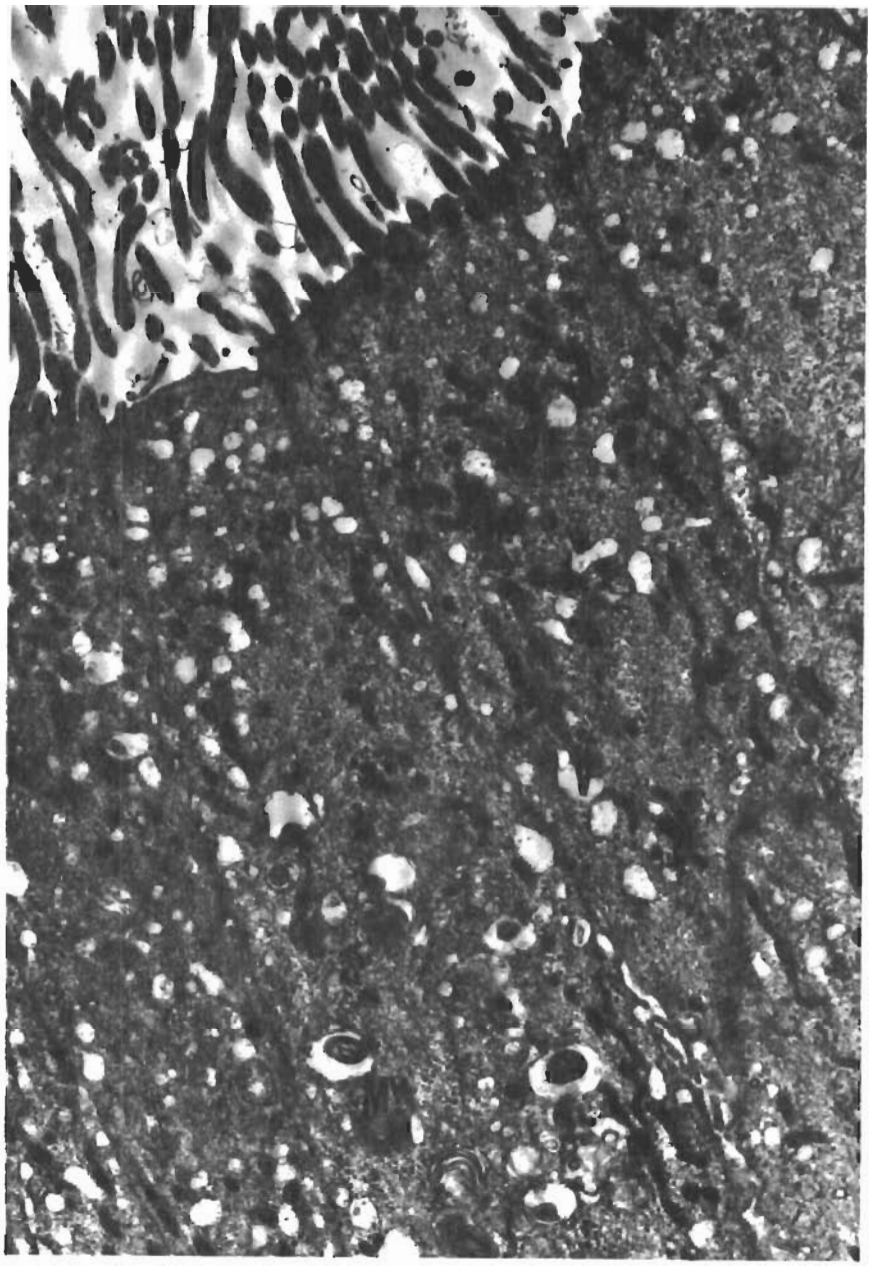

Sample No. 101

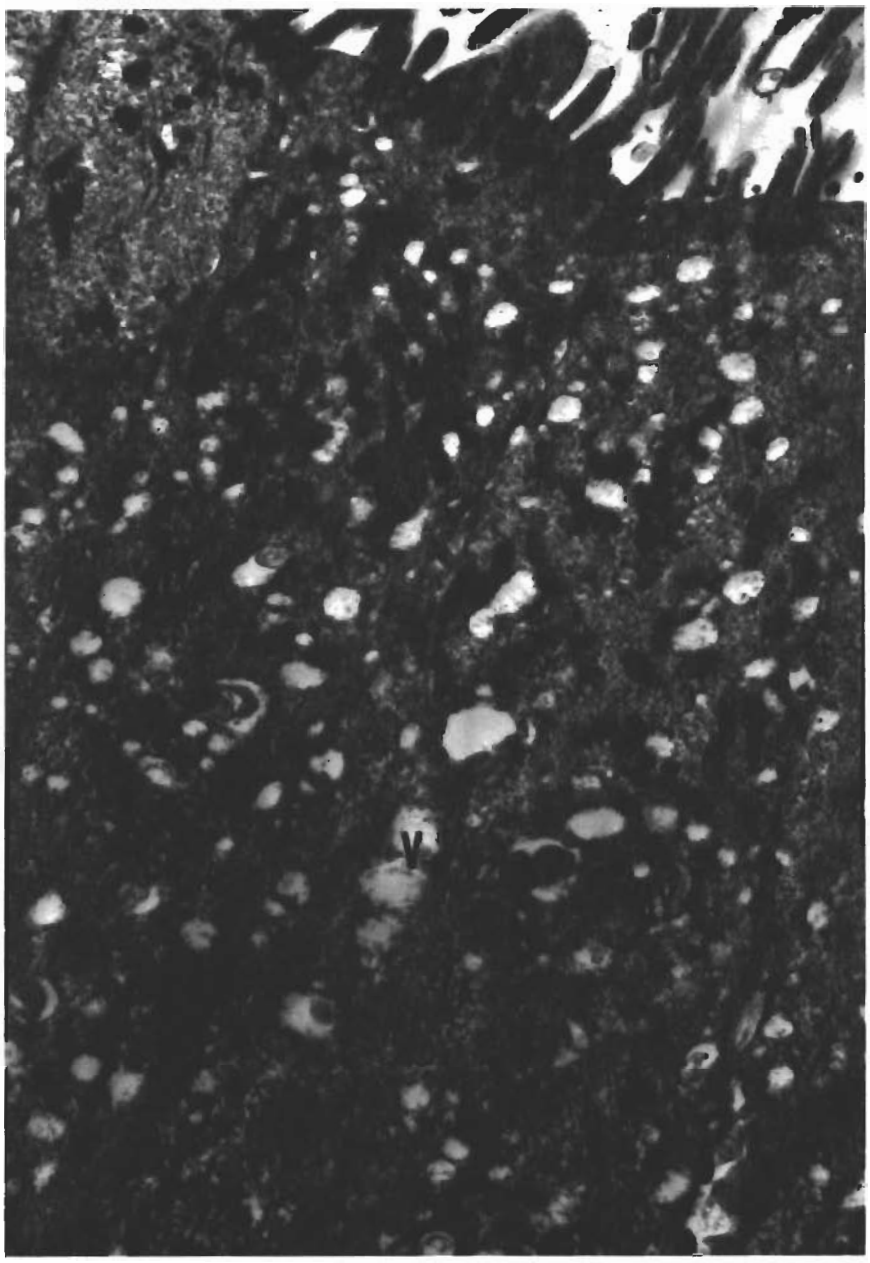

Sample No. 101

SECTION IV
DISCUSSION

In appraising these findings of the limited program, it appears that the results, though not complete, suggest parallel effects and correlated changes at functional, chemical, biochemical, and subcellular levels. In order to establish the response of mammalian respiratory tissue to environmental irritants, these involve proliferation into several disciplines.

Evidence of self-limiting changes in mucociliary response has been established for continuous exposure to pure oxygen at 0.33 atmosphere. The effects with more deleterious irritants, ozone and nitrogen dioxide, have yielded a base against which it has been feasible to demonstrate correlations between mucus velocity and viscosity. Under the same conditions experiments have been performed to characterize the events in terms of total lipid, fatty acid, amino acids, and protein content, and oxidative enzyme activity. Though several studies have advanced only to the point of establishing normal values for the species, the results indicate the existence of changes in energy yielding subcellular reactions that have both morphologic and physical significance in characterizing the work of the cilia in facilitating mucus flow, and in dealing with the effects of irritants in the respiratory tract.

The limitation of the photographic program resulted from the nonavailability of high speed cinematographic apparatus, and the need to apply methodology derived from investigations in lower orders or less complex total organ-tissue systems.

REFERENCES

(1) Albert, R. E. and Arnett, L. C., Clearance of Radioactive Dust from the Human Lung. AMA Arch. Industr. Health, 12, 99 (1955).

(2) Laurenzi, G. A., Guarneri, J. J., Endriga, R. B., and Carey, J. P., Clearance of Bacteria by the Lower Respiratory Tract. Science, 142, 1572 (1963).

(3) Carson, S., Goldhamer, R., and Mackars, A., Deposition and Clearance of Carbon Particles from the Cat Lung. Presented American Industrial Hygiene Association Meeting, May 3, 1967, Chicago, Illinois.

(4) Carson, S., and Goldhamer, R., Mucus Transport int the Respiratory Tract. Presented at the Symposium on Cilia at Duke University Medical Center, Durham, N. C., February 18-19 (1965).

(5) Carson, S., Goldhamer, R., and Weinberg, M. S., Characterization of Physical, Chemical and Biological Properties of Mucuc in the Intact Animal. Presented at the New York Academy of Sciences Conference on Interdisciplinary Investigation of Mucus Protection and Transport, October 30 (1965).

(6) Goldhamer, R. E., Barnett, B., and Carson, S., A New Technique for the Study of Mucus Flow in the Intact Animal. Federation Proc., 23, 406 (1964).

(7) Carson, S, Goldhamer, R. E., and Carpenter, R., Mucus Transport in the Respiratory Tract. Amer. Rev. Resp. Dis., 93, 86 (1966).

(8) Carson, S., Goldhamer, R., Barnett, B., and Weinberg, M., The Rheology of Mucus Flow in Cat Trachea, VI International Congress of Biochemistry, V-D73, 407, (1964).

(9) Goldhamer, R., Carson, S., and Weinberg, M. S., A Method for the Determination of Mucus Transport in the Intact Respiratory Tract. Presented at the Cystic Fibrosis Club Meeting, May. (1965)

(10) Goldhamer, R., Carson, S., and Weinberg, M. S., Studies on Muscocillary System of the Cat. Presented at the Federation of American Sooieties for Experimental Biology Meeting, Atlantic City, April, (1966).

(11) Rhodin, J., Structure of Ciliated Cells, Presented at the Symposium on Cilia at Duke University Medical Center, February 18-19 (1966).

(12) Miller, C. E., and Goldfarb, H., An in vitro Investigation of Ciliated Activity. Transcription of the Society of Rheology, 9, 1, 135 (1965)

(13) Dalhamn, T., Mucous flow and ciliary activity in the trachea of healthy rats and rats exposed to respiratory irritant gases (SO_2, H_3N, HCHO), Acta Physiol. Scand, 36 (1956)

(14) Dalhamn, T., and Rylander, R. Ciliastatic Action of Smoke from Filter-tipped and Non-tipped Cigarettes, Nature (London), 1964, 201, 401.

(15) Battista, S.P., DiNunzio, J., and Kensler, C.J. A Versatile Apparatus for Studying the Effects of Gases, Aerosols, and Drugs on Ciliary Activity in the Non-immersed Trachea, Fed Proc, 1962, 21, 453.

(16) Tremer, H.M., Falk, H.L., and Kotin, P. Effects of Air Pollutants on Ciliated Mucus-Secreting Epithelium. J. National Cancer Institute, 27, 979 (1961).

(17) Food and Drug Research Laboratories, Inc. unpublished data.

(18) Milton, A.S. Personal communication.

(19) DeGroot, L.J. and Dunn, A.D. Biochim Biophys Acta 92, 205 (1964).

(20) Waddell, W.J. J. Lab. Clin. Med. 48, 311 (1956).

Security Classification

DOCUMENT CONTROL DATA - R & D

(Security classification of title, body of abstract and indexing annotation must be entered when the overall report is classified)

1. ORIGINATING ACTIVITY *(Corporate author)*
Food and Drug Research Laboratories, Inc.
Maurice Avenue at 58th Street
Maspeth, New York 11378

2a. REPORT SECURITY CLASSIFICATION
UNCLASSIFIED

2b. GROUP
N/A

3. REPORT TITLE
BIOCHEMICAL DEFENSE MECHANISMS AGAINST PULMONARY IRRITANTS

4. DESCRIPTIVE NOTES *(Type of report and inclusive dates)*
Final Report, 15 July 1966 - 15 July 1967

5. AUTHOR(S) *(First name, middle initial, last name)*
Steven Carson, PhD
Richard E. Goldhamer

6. REPORT DATE
October 1968

7a. TOTAL NO. OF PAGES
130

7b. NO. OF REFS
20

8a. CONTRACT OR GRANT NO.
AF 33(615)-5309

b. PROJECT NO. 7163

c.

d.

9a. ORIGINATOR'S REPORT NUMBER(S)

9b. OTHER REPORT NO(S) *(Any other numbers that may be assigned this report)*
AMRL-TR-67-212

10. DISTRIBUTION STATEMENT
This document has been approved for public release and sale; its distribution is unlimited.

11. SUPPLEMENTARY NOTES
Cosponsored by the Life Sciences Division of the Office of Aerospace Research, Arlington, Virginia 22209.

12. SPONSORING MILITARY ACTIVITY
Aerospace Medical Research Laboratories
Aerospace Medical Div., Air Force Systems Command, Wright-Patterson AFB, CH 45433

13. ABSTRACT
Studies have been performed in which mammalian mucociliary apparatus has been characterized under normal conditions following exposure to three irritant gases, i.e., 100 per cent oxygen, ozone (O_2) and nitrogen dioxide (NO_2). Investigations were made in normal and treated animals providing physical, electrophysiological, biochemical, and morphologic data of effects due to exposure. A method for in vitro microscopic observation of viable cilia and adjacent mucus blanket has been described in terms of ciliary beat and movement of particles embedded in the mucus. In vitro volumetric estimation of mucus thickness was compared to electrical resistance measurements in the attempt to provide an in vivo method to determine mucus depth alterations in treated animals. Polarographic studies of oxygen dependent enzymes were carried out on pooled stripped epithelial tissue of untreated animals and comparison made with tissues exposed to ozone and nitrogen dioxide. Exposure to 100 per cent oxygen caused a significant but selflimiting decrease in mucus velocity and viscosity. Acute exposure to nitrogen dioxide (35 and 75 micrograms per kilogram) caused marked dose dependent changes in velocity and viscosity. Exposure to 0.5 ppm ozone for a 14 day period resulted in general mucostasis and elevated viscosity levels

DD FORM 1 NOV 65 1473

Security Classification

Security Classification

14. KEY WORDS	LINK A		LINK B		LINK C	
	ROLE	WT	ROLE	WT	ROLE	WT
Toxicology						
Pharmocology						
Metabolism						
Biochemistry						
Electron microscopy						
Ciliary rheology						
Ozone						
Nitrogen dioxide						
100% oxygen						
Enzymology						
Mucociliary apparatus						
Cats						
Dogs						
Rabbits						

Security Classification